# RESULTATS

## Introducció als resultats

Els resultats d'aquesta Tesi doctoral s'han dividit en tres capítols. El primer capítol engloba dos articles publicats; el segon, un article enviat; i el tercer, un article publicat. A cada capítol s'ha inclòs un apartat de precedents i un resum de cada article. Quan s'ha considerat necessari s'ha inclòs una breu introducció a la temàtica que es tractarà als articles. També s'ha afegit un annex de Material i Mètodes. Cal esmentar que per tal de donar una visió més global a aquest apartat, els resultats no es presenten en ordre cronològic sinó per blocs conceptuals. Així doncs, l'apartat de Resultats té la següent estructura:

**Capítol I**

**L'increment de ROS degut a una reducció en la funció antioxidant de les selenoproteïnes modula la via de senyalització Ras/MAPK.**

**Article 1**: Morey, M., Serras, F., Baguñà, J., Hafen, E. and Corominas, M. (2001). Modulation of the Ras/MAPK signalling pathway by the redox function of selenoproteins in *Drosophila melanogaster*. *Dev Biol*. 2001 Oct 1;238(1):145-56.

- *La via Ras/MAPK: funcions a l'ull i a l'ala de Drosophila*
- Precedents
- Resum
- Article

**Article 2**: Morey, M., Serras, F. and Corominas, M. (2003). Halving the selenophosphate synthetase gene dose confers hypersensitivity to oxidative stress in *Drosophila melanogaster*. *FEBS Lett*. 2003 Jan 16;534(1-3):111-4.

- Precedents
- Resum
- Article
- Annex: Protocols genètics

    *Protocol d'escissió de l'element P i generació de línies isogèniques.*

    *Protocol d'encreuaments dissenyats per tal de dur a terme l'anàlisi de l'efecte de l'expressió ectòpica del gen selD en motoneurones.*

**Capítol II**

**L'acumulació de ROS degut a una reducció en la funció antioxidant de les selenoproteïnes indueix apoptosis a través de la via Dmp53/Rpr.**

**Article 3**: Morey, M., Corominas, M. and Serras, F. DIAP1 suppresses ROS-induced apoptosis caused by impairment of selenoprotein function in *Drosophila*. Enviat a *J. Cell Sci.*

- *L'apoptosi a Drosophila*
- Precedents
- Resum
- Article

**Capítol III**
**Identificació *in silico* i verificació *in vivo* de selenoproteïnes a *Drosophila***

**Article 4**: Castellano, S., Morozova, N., Morey, M., Berry, M.J., Serras, F., Corominas, M. and Guigó R. (2001). In silico identification of novel selenoproteins in the *Drosophila melanogaster* genome. *EMBO Rep*. 2001 Aug;2(8):697-702.

- Precedents
- Resum
- Aportació personal al treball realitzat
- Article i Material Suplementari

# CAPÍTOL I

## L'increment de ROS degut a una reducció en la funció antioxidant de les selenoproteïnes modula la via de senyalització Ras/MAPK

**Article 1**: Morey, M., Serras, F., Baguñà, J., Hafen, E. and Corominas, M. (2001). Modulation of the Ras/MAPK signalling pathway by the redox function of selenoproteins in *Drosophila melanogaster*. *Dev Biol*. 2001 Oct 1;238(1):145-56.

### *La via Ras/MAPK: funcions a l'ull i a l'ala de Drosophila*

La via Ras/MAPK s'activa en diferents teixits i moments del desenvolupament de *Drosophila* per donar lloc a diversos tipus de senyals com proliferació, diferenciació, supervivència o creixement cel·lular (Schweitzer i Shilo, 1997; Prober i Edgar, 2000; Halfar *et al*., 2001). L'ull i l'ala són dues estructures on una de les funcions de la via Ras/MAPK és la diferenciació dels omatidis i venes, respectivament (Fig. 14).

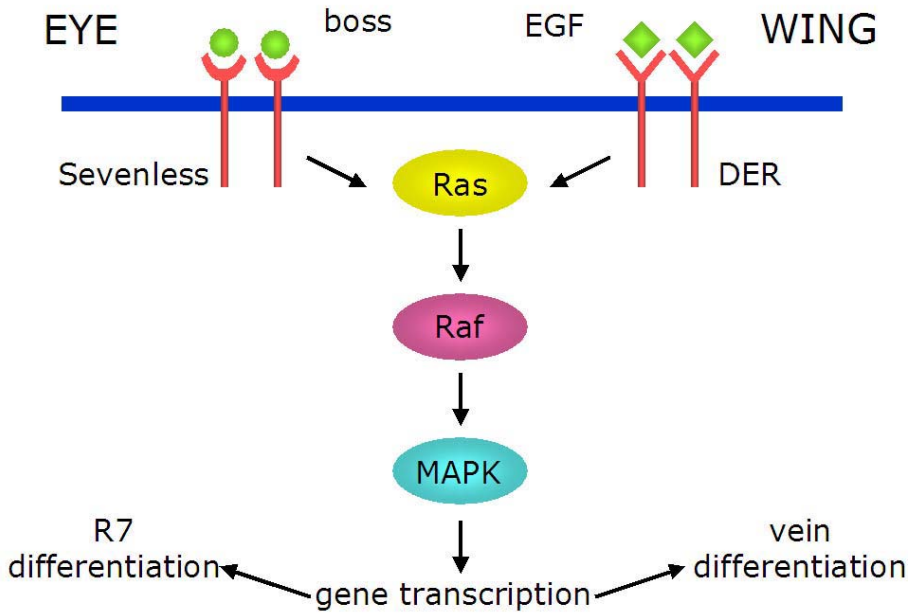


Fig. 14. Funcions de la via Ras/MAPK a l'ull i a l'ala de *Drosophila*.

*L'ull*

L'ull compost de *Drosophila* és una estructura altament organitzada que consta d'aproximadament 800 òrgans fotoreceptors o omatidis disposats de manera hexagonal. Cada omatidi està format per vuit cèl·lules fotoreceptores (R1-R8), quatre *cone cells* o cèl·lules secretores de la lent i diverses cèl·lules pigmentàries. L'ull adult es desenvolupa a partir de la capa epitelial del disc imaginal d'ull. La diferenciació i organització d'aquestes cèl·lules en un patró comença a l'estadi de larva III (Fig. 15). Un dels primers esdeveniments és la formació del solc morfogenètic a la part posterior del disc imaginal, que a mida que es mou cap a la part anterior, activa la diferenciació de les cèl·lules que queden al seu darrera. La primera de totes en diferenciar-se és el fotoreceptor R8 que ho fa

amb un posicionament estereotipat. A partir d'aquí, l'activació reiterativa de la via Ras/MAPK a través del receptor DER (*Drosophila* epidermal growth factor receptor) permet el reclutament seqüencial de les cèl·lules R1-R6. La darrera cèl·lula a diferenciar-se és el fotoreceptor R7 i també ho fa mitjançant l'activació de la cassette Ras/MAPK però a través del receptor Sevenless. L'R7 es situa per sota de l'R8 i la via Ras/MAPK s'engega mitjançant l'activació del receptor Sevenless pel seu lligant Boss, que està anclat a la membrana cel·lular de l'R8. Malgrat en diferents moments de la formació de l'omatidi *sevenless* s'expressa a altres cèl·lules R a part de la propia R7, en condicions normals aquestes altres R mai es diferenciaran com a R7 ja que no tindran accés al lligant. Posterior a la formació del cluster R1-R8, es recluten la resta de cèl·lules de l'omatidi, i ja en estadi de pupa, és refina l'estructura final de l'ull adult eliminant per apoptosi les cèl·lules sobrants que hagin quedat entre omatidi i omatidi (Basler *et al*., 1991; Freeman, 1996).

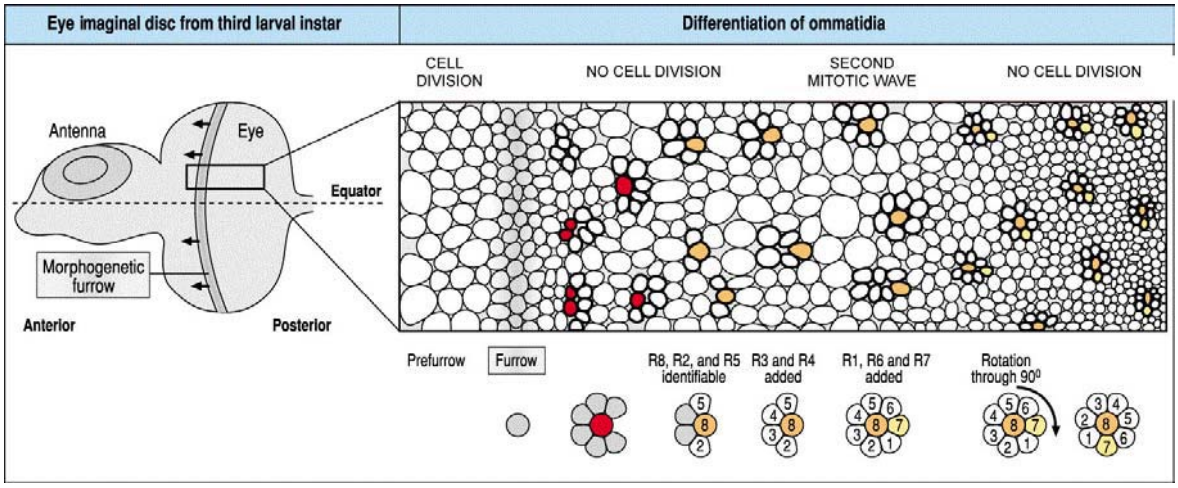


Fig. 15. Etapes de la diferenciació i organització de les cèl·lules fotoreceptores dels ommatidis (adaptat de Wolpert, 2001).

*L'ala*

L'ala de *Drosophila* és una bicapa cel·lular formada per tres components bàsics: les estructures sensorials del marge, les venes i les regions d'intervena. Les venes són esclerotitzacions epidèrmiques que es formen en posicions estereotípiques de l'ala i que engloben tràquees i nervis. La via Ras/MAPK té un paper important en la inducció de les venes durant el desenvolupament del disc imaginal de l'ala i la seva activació és du a terme mitjançant el receptor DER i el seu lligant putatiu Vein (García-Bellido i De Celis, 1992). S'ha postulat que l'activitat de la cassette Ras/MAPK és regulada en l'espai i en el temps durant el desenvolupament de l'ala i que d'aquesta manera té diferents funcions (Fig. 16). Així, durant el període larvari, l'activitat de la via Ras/MAPK es restringeix a les presumptives zones de vena, per tal de que dites regions adquireixen la competència per més tard esdevindre venes. Com a conseqüència de l'activació de la via s'expressen dos gens: *argos* (aos), un inhibidor difusible que previndria de l'activació de la via en les regions d'intervena properes a la presumptiva vena i *rhomboid* que exerciria un *feed back loop* positiu activant encara més la via en la zona de vena. En canvi, en el període pupal, l'activitat de la via Ras/MAPK queda dràsticament disminuïda en la regió de vena permetent la diferenciació de les mateixes per altres vies. Paral·lament, en les regions

d'intervena l'activitat de la cassette Ras/MAPK incrementa, implementant la diferenciació de les cèl·lules d'aquesta regió (Martín-Blanco *et al*., 1999).

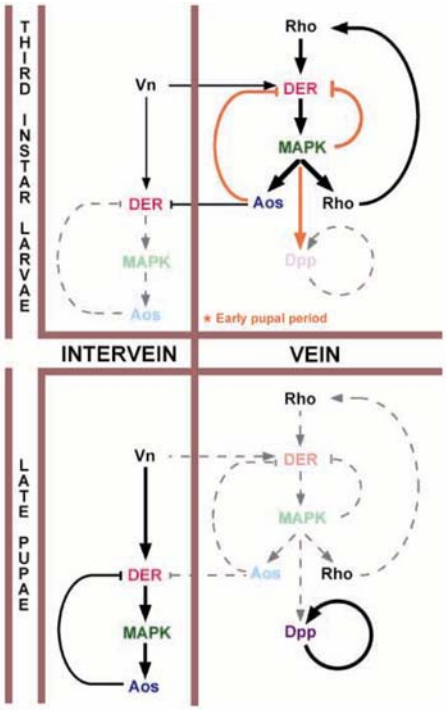


Fig.16. Regulació espaial i temporal de l'activitat de la via Ras/MAPK en el procés de diferenciació de venes (extret de Martín-Blanco et al., 1999).

**Precedents**

El fenotip dels clons de pèrdua de funció de *selD* en l'ala adulta (Alsina *et al*., 1998) eren semblants als descrits per clons de pèrdua de funció de elements de la via de DER/Ras/MAPK en dita estructura (Diaz-Benjumea i Hafen, 1994). Si bé no era el més probable que un enzim com la selenofosfat sintetasa fos un component integral de la via de senyalització Ras/MAPK, es plantejava la possibilitat de que, de manera indirecta si més no, fos capaç de modular la seva activitat. Una manera de fer efectiva aquesta modulació podia ser a traves dels ROS, que s'han vist acumulats a l'homozigot $selD^{ptuf}$ (Alsina *et al*. 1999).

**Resum**

L'estudi del possible paper de *selD* en la modulació de la via de senyalització Ras/MAPK es va dur a terme mitjançant un abordatge genètic. Els fenotips de guany de funció dels components de la cassette Ras/MAPK són sensibles a dosi gènica. Això fa possible la cerca de mutacions que de manera dominat (és a dir, en heterozigosi) modifiquin dits fenotips de guany de funció. D'aquesta manera, s'identifiquen nous components i moduladors de la via en qüestió.

Seguint aquest disseny experimental es va analitzar l'efecte de la mutació $selD^{ptuf}$ en heterozigosi sobre guanys de funció d'elements de la via Ras/MAPK en dos sistemes diferents: l'ull i l'ala de *Drosophila*. En el cas de l'ull ens vàrem centrar en una de les funcions de la via Ras/MAPK en dit teixit: la diferenciació del fotoreceptor R7 que es du a terme quan dita via és activada pel receptor Sevenless. Els guanys de funció d'elements de la via Ras/MAPK expressats sota el promotor de *sevenless* esdevenen en un excés de

cèl·lules R7 en detriment d'altres cèl·lules de l'omatidi, el que externament es tradueix en un ull desorganitzat i rugós. En el cas de l'ala es va examinar la diferenciació de venes que ocorre quan el receptor DER activa la via Ras/MAPK. L'activació constitutiva de la via Ras/MAPK dóna lloc a l'aparició venes ectòpiques. En ambdues situacions es va fer palès que la mutació $selD^{ptuf}$ modula negativament aquesta via ja que suprimeix els fenotips de guany de funció dels diferents elements utilitzats en ambdós sistemes.

L'increment de ROS, presumiblement degut a la reducció en la síntesi de selenoproteïnes a l'heterozigot $selD^{ptuf}$, podia ser responsable de la modulació negativa observada. Per tal de testar aquesta hipòtesi es va cercar una altra manera d'incrementar els ROS i es va utilitzar una mutació en el gen de la catalasa, una proteïna que també està involucrada en el control del balanç redox cel·lular. D'igual manera que $selD^{ptuf}$, la mutació $Cat^{n1}$ suprimeix els fenotips de guany de funció d'elements de la via Ras/MAPK tant a l'ull com a l'ala.

Utilitzant el disseny experimental esmentat al principi d'aquest apartat es van dur a terme experiments amb altres vies de transducció del senyal i cap va resultar ser sensible a l'increment de ROS causat per l'heterozigot $selD^{ptuf}$. Si més no, això suggereix que amb l'aproximació utilitzada, la via Ras/MAPK és la més sensible a una alteració del balanç redox cel·lular.

Developmental Biology 238, 145–155 (2001)
doi:10.1006/dbio.2001.0389, available online at http://www.idealibrary.com on IDEAL®

# Modulation of the Ras/MAPK Signalling Pathway by the Redox Function of Selenoproteins in *Drosophila melanogaster*

**Marta Morey,* Florenci Serras,* Jaume Baguñà,* Ernst Hafen,† and Montserrat Corominas*,1**

*Departament de Genètica, Facultat de Biologia, Universitat de Barcelona, Diagonal 645, 08028 Barcelona, Spain; and †Zoologisches Institut, Universitat Zurich, Winterthurerstrasse 190, Zurich CH-8057, Switzerland

**Modulation of reactive oxygen species (ROS) plays a key role in signal transduction pathways. Selenoproteins act controlling the redox balance of the cell. We have studied how the alteration of the redox balance caused by *patufet* (*selD*$^{puf}$), a null mutation in the *Drosophila melanogaster selenophosphate synthetase 1* (*sps1*) gene, which codes for the SelD enzyme of the selenoprotein biosynthesis, affects the Ras/MAPK signalling pathway. The *selD*$^{puf}$ mutation dominantly suppresses the phenotypes in the eye and the wing caused by hyperactivation of the Ras/MAPK cassette and the activated forms of the Drosophila EGF receptor (DER) and Sevenless (Sev) receptor tyrosine kinases (RTKs), which signal in the eye and wing, respectively. No dominant interaction is observed with sensitized conditions in the Wnt, Notch, Insulin-PI3K, and DPP signalling pathways. Our current hypothesis is that selenoproteins selectively modulate the Ras/MAPK signalling pathway through their antioxidant function. This is further supported by the fact that a selenoprotein-independent increase in ROS caused by the *catalase* amorphic *Cat*$^{n1}$ allele also reduces Ras/MAPK signalling. Here, we present the first evidence for the role of intracelular redox environment in signalling pathways in *Drosophila* as a whole organism.** © 2001 Academic Press

*Key Words:* selenophosphate synthetase; selenoproteins; reactive oxygen species; Ras/MAPK signalling pathway.

## INTRODUCTION

Selenoproteins are characterized by the presence of the amino acid selenocysteine. Incorporation of this amino acid into selenoproteins requires a translational step where UGA, which normally functions as a stop codon, specifies selenocysteine, and the presence of the selenocysteine insertion sequence (SECIS) in the 3′ untranslated region of the selenoprotein mRNA (for reviews see Low and Berry, 1996; Stadtman, 1996). Studies on mutant *Escherichia coli* strains exhibiting defects in selenium metabolism have identified four genes, *selA-selD*, encoding selenocysteine synthase (SelA), a selenocysteine-specific elongation factor (SelB), a selenocysteine-specific tRNA (tRNA$^{Sec}$, *selC* gene product), and selenophosphate synthetase (SelD), all of which are essential for bacterial selenoprotein synthesis (Bock *et al.*, 1991; Bock, 2000). In eukaryotes, the selenocysteine tRNA, the selenocysteine-specific elongation factor (SelB), the SECIS binding protein (SBP2), and two selenophosphate synthetase genes (*sps1* and *sps2*) have so far been identified (Lee *et al.*, 1990; Low *et al.*, 1995; Guimaraes *et al.*, 1996; Persson *et al.*, 1997; Alsina *et al.*, 1998; Zhou *et al.*, 1999; Copeland *et al.*, 2000; Fagegaltier *et al.*, 2000; Hirosawa-Takamori *et al.*, 2000; Tujebajeva *et al.*, 2000). Sps1 and Sps2 differ in the presence of a cysteine codon in the predicted active site of the enzyme in the first while a selenocysteine codon occurs in the latter.

Disruption of the mouse *selenocysteine-tRNA* gene causes early lethality (Bosl *et al.*, 1997). Similarly, the *selD*$^{puf}$ mutation of the *Drosophila melanogaster sps1* gene (*selD*) results in larval lethality (Alsina *et al.*, 1998). These results, together with the conservation of the selenoprotein synthesis machinery between different species, suggest an important role of selenoproteins in cell function. Several selenoproteins have been identified in different organisms, including the eukaryotic glutathione peroxidase and thioredoxin reductase families, iodothyronine deiodinases, or

1 To whom correspondence should be addressed. Fax: +34-93-4110969. E-mail: mcorom@bio.ub.es.

0012-1606/01 $35.00

proteins of unknown function such as selenoprotein P or W (Stadtman, 1996; Burk and Hill, 1999). Most of them appear to have a role as antioxidants suppressing the formation or action of ROS, or catalyzing oxidation-reduction reactions (Stadtman, 1996). Although for many years ROS have been thought of as the unwanted and toxic by-products of living in an aerobic environment, recent evidence suggests that ROS such as superoxide anions and hydrogen peroxide function as intracellular second messengers. Emerging evidence suggests that ROS have an important role in signal transduction (for review see Finkel, 1998).

To explore the possible role of the redox cellular state driven by selenoproteins in the modulation of signalling pathways, we have used the null *selD*$^{mut}$ mutation, which has been shown to block the biosynthesis of selenoproteins (Alsina *et al.*, 1999). It is a recessive mutation causing lethality at third instar stage. Homozygous larvae have extremely reduced and abnormal imaginal discs, showing a completely disorganized epithelium, the cells of which accumulate free radicals and enter apoptosis (Alsina *et al.*, 1998, 1999). In genetic mosaics, homozygous mutant *selD*$^{mut}$ cells show similar phenotypes to those described for loss-of-function mutants of the DER signal transduction pathway. For example, clones are rounded and small, and suppress vein differentiation in both cases (Diaz-Benjumea and Hafen, 1994; Alsina *et al.*, 1998). Although it is unlikely that an enzyme such as selenophosphate synthetase is an integral component of any growth factor signalling pathways, it may play an indirect role, modulating them. Thus, selenoproteins may be instrumental to maintain a certain redox state in the cell necessary for the different activities of the pathway.

We have performed a series of genetic interactions using the eye and wing of *Drosophila melanogaster* as model systems where the Ras/MAPK cassette is activated. The wild-type compound eye of the fly consists of a regular arrangement of ommatidia, each containing an invariant number of cells. Cell fate in the developing eye is determined by the activation of the Ras/MAPK cassette, which is triggered by two RTKs, the DER and Sev, required for the specification of the R1–R6 and R7 photoreceptor cell fate, respectively (Basler *et al.*, 1991; Freeman, 1996). The *Drosophila* wing is also an important model system for analyzing pattern formation in a fully cellularized and proliferating epithelial sheet. Vein differentiation in the adult wing is achieved by the activation of the Ras/MAPK cassette through the DER (Diaz-Benjumea and Garcia-Bellido, 1990; Garcia-Bellido and de Celis, 1992; Sturtevant and Bier, 1995). Herein, we have analyzed gain-of-function mutations of members of the Ras/MAPK signalling pathway and RTKs that trigger their activation in combination with *selD*$^{mut}$ loss-of-function mutation. Furthermore, we have altered the redox balance of the cell in a selenoprotein-independent way using a *catalase* amorphic allele instead of *selD*$^{mut}$. Altogether, the results obtained in this study suggest that the Ras/MAPK pathway is sensitive to the perturbation of the cellular redox balance caused either by the alteration of selenoprotein biosynthesis in the *selD*$^{mut}$ mutant or by *catalase*.

## MATERIALS AND METHODS

### *Drosophila Strains*

*Canton-S* was used as wild-type strain. The *PlacW* insertion lines *l(2)k11320/CyO* (*selD*$^{mut}$ in the text) and *l(2)k07214/CyO* (Torok *et al.*, 1993) were obtained from the Szeged Stock Center. The activated *sevenless* (sev) construct *w*$^{1118}$ *sev*$^{AT}$;*sevS11.5* (Basler *et al.*, 1991), the activated *raf* construct *Raf*$^{gof19}$/*CyO* (Dickson *et al.*, 1996), and the EMS gain-of-function mutation of *rolled* (*MAPK*): D-*raf*$^{CY13}$; *rl*$^{Sem}$ were used. *D-raf*$^{CY13}$;*rl*$^{Sem}$ double mutant flies possess a normal complement of six outer photoreceptor cells and one R7 cell (Brunner *et al.*, 1994). In order to eliminate the *D-raf*$^{CY13}$ allele, present to counteract the weak dominant sterility reported for *rl*$^{Sem}$ heterozygous flies (Lim *et al.*, 1999) and responsible for this wild-type eye phenotype, crosses were designed to score the male +/*Y*;*rl*$^{Sem}$/+ progeny. The activated *ras* construct *e ftz ry/TM3 P{sev-rasV12}* (Fortini *et al.*, 1992) was kindly provided by T. Laverty. The following stocks were also used: *2xsev hsp-rough/CyO* (Basler *et al.*, 1991), sev-wg(III) (Brunner *et al.*, 1997), *yw;GMR-GAL4, UAS-InRwt/CyO* (Huang *et al.*, 1999), *GMR-GAL4, UAS-Dp110 CAAX* (II) (Leevers *et al.*, 1996), and *sevGAL-4*. The *GMR-Rho1*$^{1}$ *GMR-Rho1*$^{1}$/*TM6B* (Hariharan *et al.*, 1995) stock was a gift from J. Settleman. J. Casanova kindly provided the activated *UAS-tkv* stock. For ectopic expression of *selD*, we used *UAS-selD 8.1* transgenic on the third chromosome made by B. Alsina. The *UAS-ΔD-Raf*$^{top}$ construct (Martin-Blanco *et al.*, 1999) and *GAL-4*$^{304}$ insertion line (Brand and Perrimon, 1993) were obtained from E. Martin Blanco. The *GAL-4*$^{304}$ line is expressed in wing discs in late pupal stages (E. Martin Blanco, personal communication). J. Mahaffey kindly provided the *yw*; *Cat*$^{n1}$/*TM3* strain (Mackay and Bewley, 1989; Griswold *et al.*, 1993). The *Elp*$^{S1}$/*CyO* stock and the *Ax*$^{38}$ allele were obtained from the Bloomington Stock Center. Fly cultures were maintained at 25°C using standard medium.

### *Scanning Electron Microscopy and Histology*

To prepare scanning electron microscopy (SEM) samples, flies were dehydrated in 25, 50, 75, 95, and 100% ethanol for 24 h each. To get rid of accumulated debris in the flies' eyes, they were sonicated for 30 s in an ultrasound bath followed by a final change of 100% ethanol. Flies were critical point dried and coated with gold to be examined in a Leica-360 scanning electron microscope.

Eyes to be sectioned were fixed and embedded in Spurr's medium as described previously (Basler and Hafen, 1988). Semithin sections were obtained and stained with methylene blue for light microscopy.

### *Statistical Analysis*

For each genotypic combination, ommatidia from three different eyes were counted. As our data did not accomplish the minimal requirements to do a *t*-test, a chi-square test on contingency tables was performed. The aim was to see if there were significant differences between heterozygotes for the gain-of-function allele and transheterozygotes for the gain-of-function and the *selD*$^{mut}$ mutation for the two parameters studied: normal versus abnormal ommatidia and number of R7 per ommatidium. The program used was STATGRAPHICS Statistical Graphics System Version 7.0.

## RESULTS

### *selD Modulates the Ras/MAPK Signalling Pathway in the Eye*

One approach to identify new components of any given pathway is to search for mutations that dominantly modify the phenotype of another mutation in the same pathway. The rough eye phenotype caused by hyperactivation of components of the Ras pathway is dose sensitive and has been successfully used in dominant modifier screens that led to the identification of essential components in this signalling pathway (Simon *et al.*, 1991; Olivier *et al.*, 1993; Dickson *et al.*, 1996; Karim *et al.*, 1996). Given the similarities of the wing phenotypes caused by homozygous clones for $selD^{mat}$ and for loss-of-function mutations in genes coding for the components of the Ras/MAPK cascade (Diaz-Benjumea and Hafen, 1994; Alsina *et al.*, 1998), we wanted to test whether the alteration of the cellular redox state generated by the loss-of-function mutation $selD^{mat}$ was interfering with the Ras/MAPK signalling pathway in the eye and the wing.

We analyzed whether the removal of one functional copy of the *selD* gene was sufficient to suppress the rough eye phenotype caused by gain-of-function mutations of several members of this signalling cassette: *sevenless* (*sev*), *ras*, *raf*, and *rolled* (*rl*, *MAPK*). Expression of transgenes encoding activated Sev, Ras, or Raf in a subpopulation of ommatidial precursor cells by the *sev* enhancer results in the recruitment of supernumerary R7 photoreceptor cells. The increased number of photoreceptor cells disrupts the regular hexagonal array of the ommatidial units thus leading to an irregular rough eye phenotype. The $rl^{Sem}$ gain-of-function mutation in the *rolled* locus, the structural gene for MAPK, was generated in an EMS screen, and results in a prolonged activation of MAPK also leading to a rough eye phenotype and extra R7-like cells.

To assure that lowering *selD* gene function does not suppress the rough eye phenotype by reducing the expression of the *sev*-enhancer-*hsp*-promoter controlled transgenes, we tested whether the $selD^{mat}$ mutation suppressed an unrelated rough eye phenotype caused by the ectopic expression of the *rough* gene under the control of the same *sev-hsp* enhancer/promoter element (Basler *et al.*, 1990). The ommatidial alteration caused by the overexpression of *rough* is independent of the Ras/MAPK pathway and transforms the presumptive R7 cell into R1–R6 cell fate. $selD^{mat}$ did not suppress the rough eye phenotype associated with the *sev-hsp-rough* (data not shown). We conclude from this that a reduction in functional *selD* product does not alter gene expression from the *sev-hsp* enhancer promoter.

The suppression of the rough eye phenotype caused by activating components of the Sev pathway was analyzed in two ways: the external arrangement of the ommatidial units and by the degree of eye roughness. Eyes were examined by scanning electron microscopy (SEM). To determine whether the degree of roughness of the eyes observed by SEM correlated with the number of extra R7 photoreceptor cells, we analyzed semithin sections and counted the number of normal and abnormal ommatidia per genotype and the number of R7 rhabdomeres per ommatidium.

***sevenless.*** Constitutive activation of Sev in *sevS11.5/+* mutant flies showed a characteristic rough pattern of irregular ommatidia (Fig. 1B). In contrast, the regular arrangement of ommatidia was partially restored in $+/selD^{mat}$; *sevS11.5/+* individuals (Fig. 1C). Sections through the distal part of the eyes of flies carrying one copy of the Sev activated transgene confirmed the highly irregular ommatidial pattern (Fig. 1B). Less than 10% of ommatidia contained a normal set of photoreceptor cells. Many ommatidia contained up to six and seven small in addition to six or seven large rhabdomeres. Sections through haploinsuficient *selD* ($selD^{mat}/+$) eyes in the activated Sev background showed more than 50% wild-type ommatidia (Fig. 1C). The difference between the wild-type and haploinsuficient *selD* dosage in the activated Sev background in the proportion of normal and abnormal ommatidia is highly significant ($P < 0.005$). There was also a significant difference ($P < 0.005$) between both genotypes in the number of R7 rhabdomeres per ommatidium. While only 7.5% of the ommatidia in the activated Sev background contained one R7, 61.2% of the ommatidia haploinsuficient for *selD* in the Sev-activated background contained a single R7 cell (Fig. 2A).

***ras.*** Like Sev, activation of Ras during eye development in *rasV12* flies causes a rough eye phenotype. Adult eye sections revealed that most ommatidia contained two or more supernumerary R7 cells (Fig. 1D). Eye SEM images and semithin sections of *selD* haploinsuficient eyes in the activated Ras background did not show any obvious suppression of the *rasV12* rough eye phenotype (Fig. 1E). The statistical analysis confirmed that the difference between both genotypes for the proportion of normal and abnormal ommatidia, and for the number of R7 rhabdomeres per ommatidium was not significant ($P > 0.05$) (Fig. 2B).

***raf.*** Comparison of the eye SEM images of flies carrying the activated Raf transgene $Raf^{sevW}$ and flies haploinsuficient for *selD* in the activated Raf background showed that the latter presented a more regular ommatidial arrangement (Figs. 1F and 1G). Distal sections through $Raf^{sevW}/+$ eyes revealed a highly irregular ommatidial pattern in which more than 70% of ommatidia had multiple R7-like cells (Figs. 1F and 2C). In distal sections through $Raf^{sevW}/selD^{mat}$ eyes more than 60% of ommatidia had the normal set of photoreceptors (Figs. 1G and 2C). Data from semithin sections showed that there was a significant difference ($P < 0.005$) in the proportion of normal and abnormal ommatidia between both genotypes. There was also a significant difference ($P < 0.005$) between the number of R7 rhabdomeres per ommatidium, which is reflected in the different distribution profiles of these genotypes (Fig. 2C).

***rolled.*** Both $rl^{Sem}/+$ and $rl^{Sem}/selD^{mat}$ eyes displayed the same mild rough phenotype under the SEM (Figs. 1H and 1I). Analysis of sections revealed the presence of three or four R7-like cells in most ommatidia (Fig. 2D). However, an

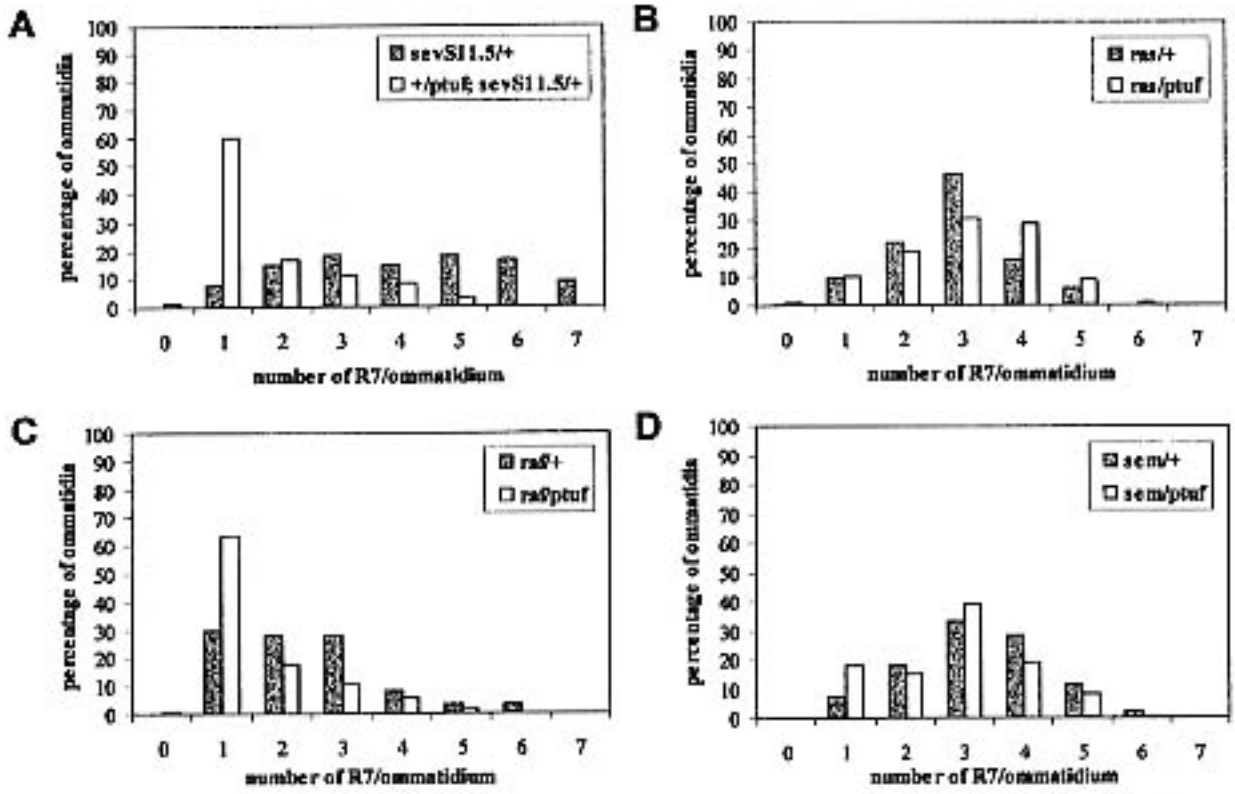


**FIG. 2.** Distribution profiles of the number of R7 rhabdomeres per ommatidium of heterozygous eyes for gain-of-function elements of *sev*, *ras*, *raf*, and *rl*, and for combinations of these elements with the *selD*$^{wuf}$ mutation. Genotypes analyzed are as follows: (A) *sevS11.5/+* and *+/selD*$^{wuf}$ *;sevS11.5/+*, (B) *+/+;+/TM3 P(sev-rasV12)* and *+/selD*$^{wuf}$ *;+/TM3 P(sev-rasV12)*, (C) *Raf* $^{top}$/+ and *Raf* $^{top}$*/selD*$^{wuf}$, and (D) *+/Y;rl*$^{Sem}$/+ and *+/Y;rl*$^{Sem}$*/selD*$^{wuf}$. The X axis stands for the number of R7 rhabdomeres per ommatidium whereas the Y axis stands for percentage of ommatidia. The statistical analysis done on these data show that the number of R7 rhabdomeres per ommatidium distribution profile of *sevS11.5/+* and *+/selD*$^{wuf}$*;sevS11.5/+* are significantly different (A) as well as they are for *Raf* $^{top}$/+ and *Raf* $^{top}$*/selD*$^{wuf}$ genotypes (C) (in both analysis $P < 0.005$). A mild but significant difference ($P < 0.05$) has been detected between the number of R7 rhabdomeres per ommatidium distribution profiles of *+/Y;rl*$^{Sem}$/+ and *+/Y;rl*$^{Sem}$*/selD*$^{wuf}$ (D). No difference has been detected in the case of *+/+;+/TM3 P(sev-rasV12)* and *+/selD*$^{wuf}$ *;+/TM3 P(sev-rasV12)* distribution profiles (B). Note that in the one R7 rhabdomere per ommatidium category of (A), (C), and (D), the absolute difference between the gain-of-function mutant in a *selD*$^{wuf}$ background and the gain-of-function alone decreases: a 52.6% in (A); a 33.3% in (C); a 10.7% in (D) (see Discussion)

increase of 8.4% was found in the percentage of *rl*$^{Sem}$*/selD*$^{wuf}$ (15%) normal ommatidia when compared to the percentage of *the rl*$^{Sem}$/+ ones (6.6%). These numbers pointed to a slightly less severe phenotype of *rl*$^{Sem}$*/selD*$^{wuf}$ compared to *rl*$^{Sem}$/+. Statistical analysis showed that there was a mild but significant difference ($P < 0.05$) between the two genotypes in the proportion of normal and abnormal ommatidia, as well as in the number of R7 rhabdomeres per ommatidium.

Summarizing, Sev, Raf, and MAPK, which are kinases, were modulated by *selD*, but Ras, which is a GTPase, was not. In order to discern whether the suppression of the

(I) *+/Y;rl*$^{Sem}$*/selD*$^{wuf}$. In all scanning electron micrographs, anterior is to the left and dorsal is up. In the presence of one copy of the gain-of-function alleles the adult eye appears rough as compared to wild type (A); i.e., one can no longer see straight rows of ommatidia and the lenses over many of the ommatidia become fused (B, D, F, and H). The rough eye phenotype of the *sev* and *raf* gain-of-function alleles is suppressed by the *selD*$^{wuf}$ mutation in heterozygosis and tangential sections display a closer wild type pattern (compare B with C and F with G). No suppression has been seen for the Ras gain-of-function construct (compare D with E). The statistical analysis of sections reveal that there is a mild suppression of the rough eye phenotype in *+/Y;rl*$^{Sem}$*/selD*$^{wuf}$ though it is not obvious in SEM images and sections (compare H with I).

**TABLE 1**
*selD* Transgene Partially Restores the Activated Sev Phenotype

| Genotypes | Mean of R7 per ommatidium | No. of ommatidia counted |
|---|---|---|
| *+/+;sevS11.5/+* | 4.10 ± s.d. 1.78 | 54 |
| *UAS-selD/selD$^{ptuf}$;sevGAL-4/sevS11.5* | 2.50 ± s.d. 1.01 | 161 |
| *+/selD$^{ptuf}$;sevS11.5/+.* | 1.71 ± s.d. 1.13 | 170 |

rough phenotype depends on the molecular nature of these elements of the Sev pathway, we checked how a different GTPase behaved in combination with *selD$^{ptuf}$* mutation. It has been published that flies carrying two independent copies of the wild-type *Rho1* gene, which encodes for the small-GTPase Rho1, under the expression of the GMR driver display an intermediate rough eye phenotype, which allows for the detection of either enhancement or suppression of eye roughness (Hariharan *et al.*, 1995). No suppression of the rough eye phenotype was observed in *selD$^{ptuf}$/+;GMR-Rho1$^{1}$ GMR-Rho1$^{1}$/+* flies (data not shown).

In order to check the specificity of our observations, we tried to restore the activated Sev phenotype in a *+/selD$^{ptuf}$; sevS11.5/+* background, driving the expression of a *selD* transgene (*UAS-selD*) with a *sevGAL-4* construct. The mean of R7 per ommatidium for each genotype is shown in Table 1. The *selD* transgene was able to partially restore the activated Sev phenotype. The statistical analysis performed on the number of R7 rhabdomeres per ommatidium of these three genotypes showed that their distribution profiles (Fig. 3) were significantly different ($P < 0.005$). This suggests that the ectopic expression of *selD* in an activated Sev and *selD$^{ptuf}$* heterozygous background restores the abnormal Sev phenotype. The fact that just a partial rescue was observed is probably due to the delay in the activation of the *selD* transgene inherent to the GAL4-UAS system. To assure that we were not scoring effects of the overexpression of the *selD* transgene in a *selD$^{ptuf}$* background, we checked if the eyes of these flies presented any alteration that could interfere with the restoration of the characteristic activated Sev rough eye phenotype. Both eye SEM images and sections proved to be wild type (data not shown).

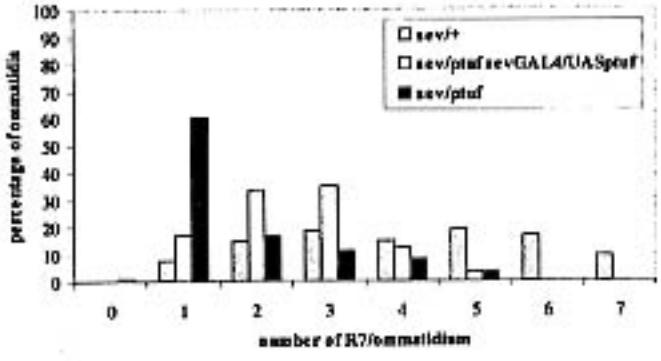


FIG. 3. Distribution profiles of the number of R7 rhabdomeres per ommatidium of the following genotypes: *+/+;sevS11.5/+*, *UAS-selD/selD$^{ptuf}$;sevGAL-4/sevS11.5*, and *+/selD$^{ptuf}$;sevS11.5/+*. The X axis stands for the number of R7 rhabdomeres per ommatidium whereas the Y axis stands for percentage of ommatidia. The comparison between the distribution profiles has shown that there is a significant difference ($P < 0.005$) between them.

Altogether, these results show that lower amounts of functional *selD* gene product suppress the rough eye phenotype caused by the activated forms of Sev and Raf. A mild but statistically significant suppression has also been observed for the *rl$^{Sem}$* eye phenotype. In contrast, no suppression of the *ras* rough eye phenotype has been detected. Moreover, no suppression of eye roughness caused by overexpression of *Rho1*, another GTPase, has been observed. A different *selD* allele, the *PlacW* insertion line *l(2)k07214*, which has the same lethality phase and imaginal disc's morphology as *selD$^{ptuf}$*, behaves in the same way (data not shown).

### *selD Modulates the Ras/MAPK Signalling Pathway in the Wing*

During *Drosophila* development a number of RTKs besides Sevenless activate the highly conserved Ras/MAPK cassette, but each RTK elicits a distinct response. One of the processes in which the DER signalling pathway has been extensively studied is cell fate determination in the *Drosophila* wing. Flies carrying viable combinations of *DER* loss-of-function alleles exhibit a partial loss of wing veins (Clifford and Schupbach, 1989). Overexpression of downstream effectors of DER or gain-of-function alleles results in ectopic wing veins (Brunner *et al.*, 1994; Martin-Blanco, 1998). It has recently been found that the level of DER pathway activity is regulated in time and space during wing development. An early activation of DER signalling is necessary for the acquisition of "vein competence" whereas a later downregulation is necessary to implement vein differentiation. Hence, overexpression of activated Raf in late pupal stages results in vein loss instead of ectopic vein tissue (Martin-Blanco *et al.*, 1999).

To test whether lowering *selD* gene function had an effect on the Ras/MAPK signalling cassette independently of tissue and RTK through which it was activated, we used the wing as a model system. Following the same rationale

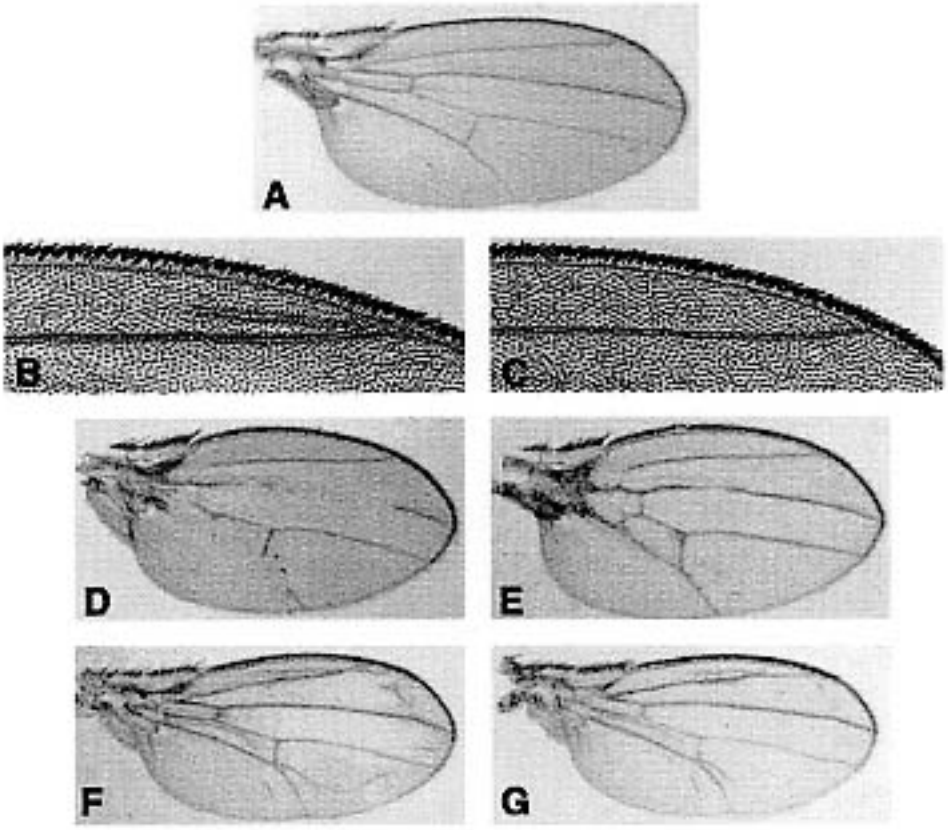


**FIG. 4.** Suppression of the wing phenotypes of gain-of-function elements of the DER pathway by the $selD^{enf}$ mutation. Genotypes are shown as follows: (A) wild type, (B) $Elp^{51}$/+, (C) $Elp^{51}/selD^{enf}$, (D) $UAS\text{-}\Delta D\text{-}Raf^{Y59}/GAL\text{-}4^{sev}$, (E) $+/selD^{enf};UAS\text{-}\Delta D\text{-}Raf^{Y59}/GAL\text{-}4^{sev}$, (F) $+/Y;rl^{Sem}/+$, and (G) $+/Y;rl^{Sem}/selD^{enf}$. The $selD^{enf}$ mutation suppresses the extra vein tissue produced by the gain-of-function allele $Elp^{51}$ (compare B with C). It restores as well the altered venation pattern caused by the overexpression of $UAS\text{-}\Delta D\text{-}Raf^{Y59}$ driven by the $GAL\text{-}4^{sev}$ stock (compare D with E), although the reduced size of these wings is not rescued. No suppression of the wing $rl^{Sem}$ phenotype is seen in $+/Y;rl^{Sem}/selD^{enf}$ wings (compare F with G).

as in the eye, we have analyzed components of this pathway in the wing in combination with $selD^{enf}$ mutation.

***Drosophila EGF receptor (DER).*** We used a gain-of-function allele of *DER*: the $Elp^{51}$/+, which gives rise to ectopic vein tissue in all wings (Fig. 4B). In 66% of $Elp^{51}/selD^{enf}$ wings, the extra vein phenotype was completely reverted and in the remaining 34% the suppression was partial (Fig. 4C).

***raf.*** We used a $UAS\text{-}\Delta D\text{-}Raf^{Y59}$ transgene, which produces a constitutively activated form of Raf, in presence of the $GAL\text{-}4^{sev}$ insertion line. As previously described (Martin-Blanco *et al.*, 1999), flies expressing this transgene had reduced viability (50%) and displayed the following wing phenotypes at 25°C: deletion of the central region of vein L3, total or partial loss of vein L5 and a reduction of the overall wing size (compare Fig. 4D to Fig. 4A). An almost wild-type vein pattern was recovered in $selD^{enf}/+;UAS\text{-}\Delta D\text{-}Raf^{Y59}/GAL\text{-}4^{sev}$ wings (Fig. 4E).

***rolled.*** Besides the rough eye phenotype, the $rl^{Sem}$ gain-of-function mutation produces extra vein tissue, which is seen in $rl^{Sem}/+$ wings (Fig. 4F). The $rl^{Sem}/selD^{enf}$ combination seemed unable to suppress the phenotype displayed by the gain-of-function (Fig. 4G).

Consistent with the results in the eye, *selD* haploinsufiency suppresses the phenotype of the $Elp^{51}$ gain-of-function mutation of *DER* and the activated Raf construct. In contrast, no suppression of the $rl^{Sem}$ wing phenotype has been detected.

### *The Catalase Allele $Cat^{a1}$ Mimics the $selD^{enf}$ Mutation Effects on the Ras/MAPK Signalling Pathway*

Our current hypothesis is that a reduction in SelD product due to $selD^{enf}$ null mutation causes an alteration to the redox balance of the cell, to which the Ras/MAPK signalling pathway is sensitive. To test our hypothesis further, we sought to alter the redox balance by reducing the copy number of another gene whose product is known to participate in its control. Using the same genetic approach out-

lined above, the *catalase* amorphic allele $Cat^{n1}$ (Mackay and Bewley, 1989; Griswold *et al.*, 1993) was used. Indeed, lowering the amount of catalase suppressed the rough eye phenotype of activated Sev and Raf. Both SEM images of $Cat^{n1}/sevS11.5$ and $Raf^{sev/y}/+;Cat^{n1}/+$ eyes showed a rescue of the rough eye phenotype to the same extent as $selD^{enf}$ (compare Fig. 1C to Fig. 5B and Fig. 1G to Fig. 5D). Furthermore, 17% of $Elp^{B1}/+;Cat^{n1}/+$ wings displayed a complete wild-type phenotype and the rest a partial suppression (data not shown). The activated Ras construct was as well tested against the $Cat^{n1}$ allele for a reduction of rough eye phenotype. Again, as with $selD^{enf}$ mutation, the result was no suppression (data not shown). These results show that an independent increase in ROS caused by the *catalase* allele $Cat^{n1}$ has the same effects on the Ras/MAPK signalling pathway as $selD^{enf}$ mutation.

### *Other Pathways Are Not Sensitive to the Change of the Redox Balance Caused by the $selD^{enf}$ Mutation*

The above results suggest that the Ras/MAPK signalling pathway is able to sense changes in the redox balance of the cell. To test whether this sensitivity to the alteration of the redox potential is specific of the Ras/MAPK cassette or a shared feature with other pathways, we analyzed if some of them could be modulated by *selD*.

In order to test whether $selD^{enf}$ would have the same effect on another RTK not directly involved in the activation of the Ras/MAPK cassette, we used the *Drosophila* insulin receptor (InR) of the insulin pathway, shown by several laboratories to regulate growth in *Drosophila* (Bohni *et al.*, 1999). Flies with transheterozygous combinations of hypomorphic mutations in *InR* are smaller than wild type (Chen *et al.*, 1996). In contrast, overexpression of *InR* by the *GMR-GAL4* driver causes enlarged eyes due to an increase in cell number and cell size. This phenotype was not suppressed in a heterozygous $selD^{enf}$ background (Figs. 6B and 6C).

Another element of this pathway is the 1-phosphatidylinositol 3-kinase (Pi3K), which like Raf is also a Ras effector. Although there is ample evidence for the cooperation of Ras-effector pathways in mammalian cells, the genetic characterization of the corresponding pathways in *Drosophila* has not yet provided genetic support for such interactions. Whereas Ras affects cell fate, Pi3K (Dp110) appears to control cell growth during development (for review see Rommel and Hafen, 1998). However, as Pi3K and Raf/MAPK are parallel pathways, and the latter seemingly modulated by *selD*, we attempted to uncover if their possible interaction was based on this modulation. It has been reported that the expression of a constitutively active membrane targeted *Dp110* construct (*Dp110-CAAX*) driven by the GMR-GAL4 insertion line generates enlarged eyes (Leevers *et al.*, 1996). Eye SEM images from flies expressing the *Dp110-CAAX* construct in a heterozygous $selD^{enf}$ background displayed the same phenotype as the control (data not shown).

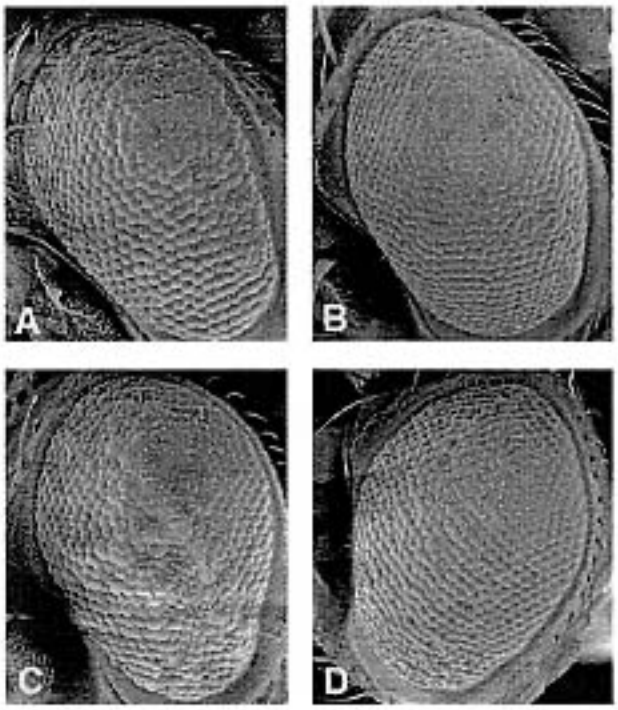


**FIG. 5.** *Catalase* suppresses the rough eye phenotype caused by the *sev* and *raf* gain-of-function alleles. Scanning electron micrographs are shown as follows: (A) *sevS11.5/+*, (B) *sevS11.5/*$Cat^{n1}$, (C) $Raf^{sev/y}/+$, and (D) $Raf^{sev/y}/+;+/Cat^{n1}$. In all pictures, anterior is to the left and dorsal is up. Both *sevS11.5/*$Cat^{n1}$ (B) and $Raf^{sev/y}/+;+/Cat^{n1}$ (D) lack most of the characteristic fused ommatidia seen in their respective controls (A and C).

In addition to the Insulin pathway, we also tested genetic interactions between $selD^{enf}$ and activated components of the Wnt (Wg), the Dpp and the Notch pathways. In the case of the Wnt pathway, it has been described that the eyes of *sev-wg* flies appear normal, except that the interommatidial bristles, normally found at alternating vertices in the eye's hexagonal array, are almost completely missing (Cadigan and Nusse, 1996; Brunner *et al.*, 1997). Though *sev-wg/+* eyes were completely devoid of interommatidial bristles, we also found that ommatidia along the anterior and ventral posterior margin of the eye had lost their array organization. In $selD^{enf}/+;sev\text{-}wg/+$ eyes, we found the same phenotype as in our controls (data not shown). To test the Dpp pathway, a gain-of-function allele of the *Drosophila* type I TGF-$\beta$ receptor family: *thickveins* (*tkv*) was driven under the control of the $GAL\text{-}4^{dpp}$ driver. The *UAS-tkv/GAL-*$4^{dpp}$ wings present extravein tissue surrounding vein L5 severely distorting and thickening it. This phenotype was not reverted in a $selD^{enf}$ heterozygous background (Figs. 6D and 6E). To test the Notch pathway the *Notch* gain-of-function allele $Ax^{2f}$, which in hemizygous condi-

## RESULTS

### *selD Modulates the Ras/MAPK Signalling Pathway in the Eye*

One approach to identify new components of any given pathway is to search for mutations that dominantly modify the phenotype of another mutation in the same pathway. The rough eye phenotype caused by hyperactivation of components of the Ras pathway is dose sensitive and has been successfully used in dominant modifier screens that led to the identification of essential components in this signalling pathway (Simon *et al.*, 1991; Olivier *et al.*, 1993; Dickson *et al.*, 1996; Karim *et al.*, 1996). Given the similarities of the wing phenotypes caused by homozygous clones for $selD^{mat}$ and for loss-of-function mutations in genes coding for the components of the Ras/MAPK cascade (Diaz-Benjumea and Hafen, 1994; Alsina *et al.*, 1998), we wanted to test whether the alteration of the cellular redox state generated by the loss-of-function mutation $selD^{mat}$ was interfering with the Ras/MAPK signalling pathway in the eye and the wing.

We analyzed whether the removal of one functional copy of the *selD* gene was sufficient to suppress the rough eye phenotype caused by gain-of-function mutations of several members of this signalling cassette: *sevenless* (*sev*), *ras*, *raf*, and *rolled* (*rl*, *MAPK*). Expression of transgenes encoding activated Sev, Ras, or Raf in a subpopulation of ommatidial precursor cells by the *sev* enhancer results in the recruitment of supernumerary R7 photoreceptor cells. The increased number of photoreceptor cells disrupts the regular hexagonal array of the ommatidial units thus leading to an irregular rough eye phenotype. The $rl^{Sem}$ gain-of-function mutation in the *rolled* locus, the structural gene for MAPK, was generated in an EMS screen, and results in a prolonged activation of MAPK also leading to a rough eye phenotype and extra R7-like cells.

To assure that lowering *selD* gene function does not suppress the rough eye phenotype by reducing the expression of the *sev*-enhancer-*hsp*-promoter controlled transgenes, we tested whether the $selD^{mat}$ mutation suppressed an unrelated rough eye phenotype caused by the ectopic expression of the *rough* gene under the control of the same *sev-hsp* enhancer/promoter element (Basler *et al.*, 1990). The ommatidial alteration caused by the overexpression of *rough* is independent of the Ras/MAPK pathway and transforms the presumptive R7 cell into R1–R6 cell fate. $selD^{mat}$ did not suppress the rough eye phenotype associated with the *sev-hsp-rough* (data not shown). We conclude from this that a reduction in functional *selD* product does not alter gene expression from the *sev-hsp* enhancer promoter.

The suppression of the rough eye phenotype caused by activating components of the Sev pathway was analyzed in two ways: the external arrangement of the ommatidial units and by the degree of eye roughness. Eyes were examined by scanning electron microscopy (SEM). To determine whether the degree of roughness of the eyes observed by SEM correlated with the number of extra R7 photoreceptor cells, we analyzed semithin sections and counted the number of normal and abnormal ommatidia per genotype and the number of R7 rhabdomeres per ommatidium.

***sevenless.*** Constitutive activation of Sev in *sevS11.5/+* mutant flies showed a characteristic rough pattern of irregular ommatidia (Fig. 1B). In contrast, the regular arrangement of ommatidia was partially restored in $+/selD^{mat}$; *sevS11.5/+* individuals (Fig. 1C). Sections through the distal part of the eyes of flies carrying one copy of the Sev activated transgene confirmed the highly irregular ommatidial pattern (Fig. 1B). Less than 10% of ommatidia contained a normal set of photoreceptor cells. Many ommatidia contained up to six and seven small in addition to six or seven large rhabdomeres. Sections through haploinsuficient *selD* ($selD^{mat}/+$) eyes in the activated Sev background showed more than 50% wild-type ommatidia (Fig. 1C). The difference between the wild-type and haploinsuficient *selD* dosage in the activated Sev background in the proportion of normal and abnormal ommatidia is highly significant ($P < 0.005$). There was also a significant difference ($P < 0.005$) between both genotypes in the number of R7 rhabdomeres per ommatidium. While only 7.5% of the ommatidia in the activated Sev background contained one R7, 61.2% of the ommatidia haploinsuficient for *selD* in the Sev-activated background contained a single R7 cell (Fig. 2A).

***ras.*** Like Sev, activation of Ras during eye development in *rasV12* flies causes a rough eye phenotype. Adult eye sections revealed that most ommatidia contained two or more supernumerary R7 cells (Fig. 1D). Eye SEM images and semithin sections of *selD* haploinsuficient eyes in the activated Ras background did not show any obvious suppression of the *rasV12* rough eye phenotype (Fig. 1E). The statistical analysis confirmed that the difference between both genotypes for the proportion of normal and abnormal ommatidia, and for the number of R7 rhabdomeres per ommatidium was not significant ($P > 0.05$) (Fig. 2B).

***raf.*** Comparison of the eye SEM images of flies carrying the activated Raf transgene $Raf^{sevW}$ and flies haploinsuficient for *selD* in the activated Raf background showed that the latter presented a more regular ommatidial arrangement (Figs. 1F and 1G). Distal sections through $Raf^{sevW}/+$ eyes revealed a highly irregular ommatidial pattern in which more than 70% of ommatidia had multiple R7-like cells (Figs. 1F and 2C). In distal sections through $Raf^{sevW}/selD^{mat}$ eyes more than 60% of ommatidia had the normal set of photoreceptors (Figs. 1G and 2C). Data from semithin sections showed that there was a significant difference ($P < 0.005$) in the proportion of normal and abnormal ommatidia between both genotypes. There was also a significant difference ($P < 0.005$) between the number of R7 rhabdomeres per ommatidium, which is reflected in the different distribution profiles of these genotypes (Fig. 2C).

***rolled.*** Both $rl^{Sem}/+$ and $rl^{Sem}/selD^{mat}$ eyes displayed the same mild rough phenotype under the SEM (Figs. 1H and 1I). Analysis of sections revealed the presence of three or four R7-like cells in most ommatidia (Fig. 2D). However, an

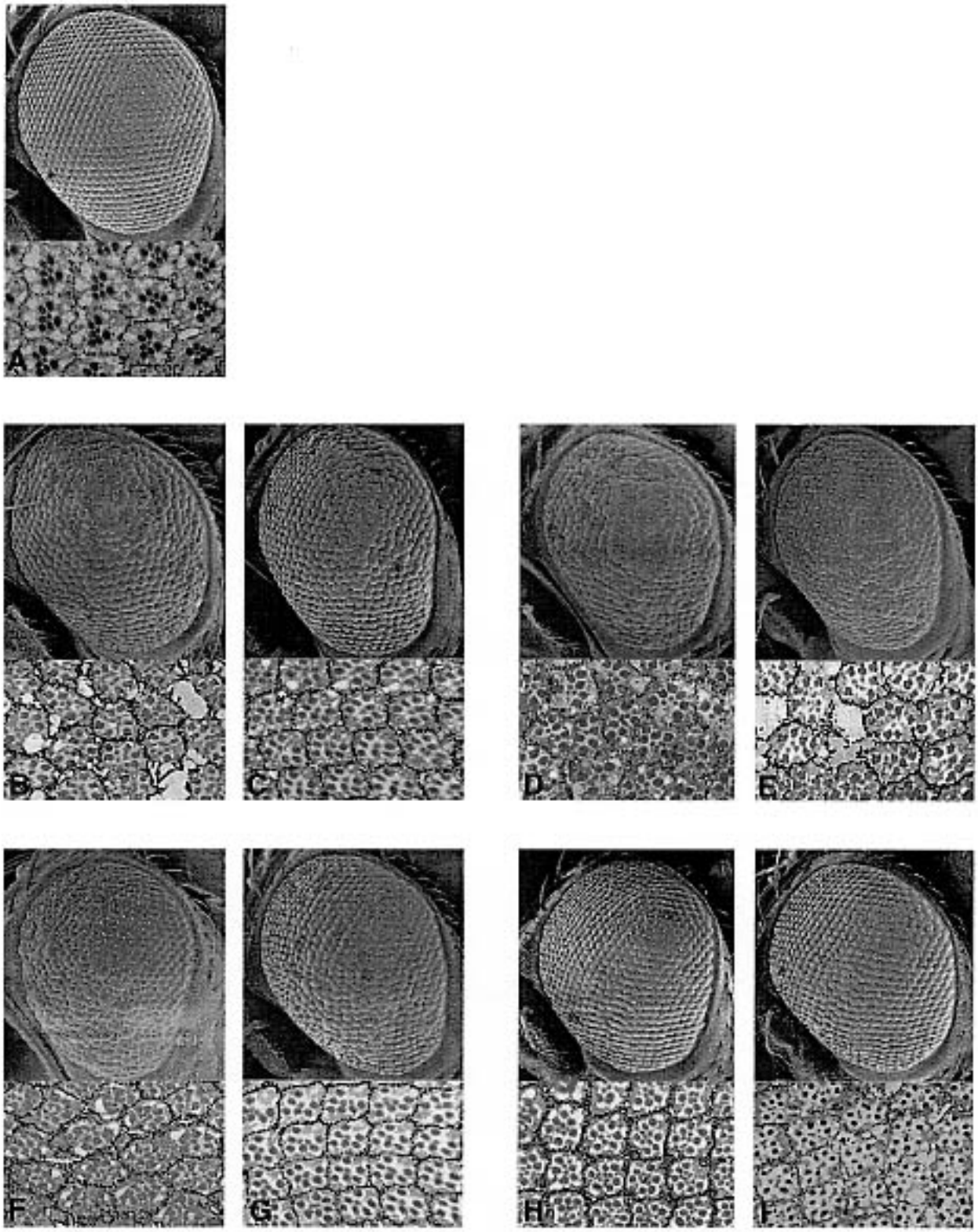


FIG. 1. Suppression of the rough eye phenotype of heterozygous eyes for gain-of-function alleles of the Sev/Ras/MAPK pathway by the *selD*$^{rolf}$ mutation. Scanning electron micrographs and semithin sections are shown as follows: (A) wild type, (B) *sevS11.5/+*, (C) *+/selD*$^{rolf}$; *sevS11.5/+*, (D) *+/+;+/TM3 P{sev-rasV12}*, (E) *+/selD*$^{rolf}$ *;+/TM3 P{sev-rasV12}*, (F) *Raf* $^{sv19}$*/+*, (G) *Raf* $^{sv19}$*/selD*$^{rolf}$ , (H) *+/Y;rl*$^{Sem}$*/+*, and

ment. It has been reported that 3T3 fibroblasts stably transformed with *rasV12*, produce large amounts of ROS superoxide ($O_2-$) by the activation of the NADPH oxidase enzyme, which is triggered by the Rac signalling pathway (Irani *et al.*, 1997). There is evidence that in certain cells MAPK activation in response to growth factors is dependent on the production of ROS (Lo and Cruz, 1995; Sundaresan *et al.*, 1995). Reduction of 50% of *selD* dose might be not enough to alter the initial *ras* rough eye phenotype neither to detect a suppression nor an enhancement. Besides, we have to bear in mind that Ras is a crosstalk point for other signalling pathways (such as PI3K) and that the Raf/MAPK pathway is also activated in a Ras independent way (Hue *et al.*, 1995).

With the exception of *ras*, we have observed a gradient in the strength of the suppression of phenotype from *sev* being the strongest to $rl^{Sem}$ the weakest (Fig. 2, comment in legend). This could be attributed to the differential sensitivity of the particular gain-of-function alleles or to the position in the pathway of the triggering gain-of-function element.

Taking together the eye and wing results, it appears that the *selD* modulation of the Ras/MAPK pathway is independent of tissue and RTK through which this highly conserved signalling cassette is activated. Moreover, the genetic approach used in our experiments has not uncovered any modulation of other signalling pathways by *selD*. Though we can not discard that these modulations may exist, the fact that modulation of the Ras/MAPK pathway has been detected indicates that this pathway is sensitive to the change in the redox balance caused by one-dose reduction of *selD*.

We have previously shown that homozygous $selD^{mut}$ mutants lack selenoproteins and accumulate free radicals (Alsina *et al.*, 1999). Heterozygous $selD^{mut}$ individuals show no sign of impaired Ras/MAPK signalling due to the loss of one dose of *selD*. However, when using activated elements of the Ras/MAPK pathway, the effects of the lack of one dose of *selD* are evident. Therefore, it is tempting to speculate that $selD^{mut}$ in heterozygosis results in an accumulation of ROS due to lower activity of the selenoproteins biosynthesis. This accumulation would be sufficient to impair the Ras/MAPK signalling, suppressing the gain-of-function phenotypes of elements of the pathway. However, our findings are in contrast with the results obtained in tissue culture experiments. It has been observed that ligand stimulation with peptide growth factors acting through RTKs results in an increase in intracellular ROS (Krieger-Brauer and Kather, 1992; Sundaresan *et al.*, 1995; Bae *et al.*, 1997). Moreover, ligand-stimulated ROS generation appears to have a role mediating tyrosine phosphorylation. In addition to that, it has also been shown that extracellular administration of non-lethal concentrations of $H_2O_2$ activates MAPK (Stevenson *et al.*, 1994; Guyton *et al.*, 1996; Kamata *et al.*, 2000). Altogether, these results in tissue culture systems point to activation of the pathway by ROS. In our case, elimination or reduction of selenoprotein function could result in prolonged activity of the signalling pathway (due to the ROS increase caused by $selD^{mut}$) and consequently induce apoptosis. Therefore, one could conclude that the suppression observed in our experiments could be due to cell death of the extra R7s. Loss of any cell of the *sev* equivalence group by apoptosis will result in rough eye phenotype. However, we have instead demonstrated a rescue of the normal ommatidium organisation, which can only be achieved if the number of cells of the ommatidium is not altered. For this reason, we think that apoptosis does not explain the strong suppression observed in our experiments. Rather, our results point to a downregulation of the pathway. The discrepancies found between cell culture and *Drosophila* as a whole organism (i.e., activation versus downregulation of the pathway by ROS respectively) may be due to the inherent differences among the two systems used. A more important difference, however, is that experiments performed in tissue culture study the effect of transient low concentration increases of ROS whereas in our system we are dealing with a gene-dosage dependent constant increase in ROS. To reconcile these discrepancies, we propose that transient increases in ROS could have a physiological function on activation of phosphorylation and thus triggering the Ras/MAPK signalling pathway, whereas a constitutive pathological change in redox potential could activate a defense mechanism blocking the pathway.

We have been using a genetic approach to address a problem that has mainly been tackled biochemically. The heterozygous combinations used in our experiments are viable; therefore, increases in ROS would be very subtle and difficult to detect using conventional methods. What we actually present here is a biological response due to the loss of one dose of either *selD* or *catalase*. Although we did not measure changes in ROS, the read out of our experiments strongly supports that there must be differences in ROS accumulation betweeen the heterozygous and the wild type.

The converse experiments to overexpress SelD and study its effects when in combination with loss-of-function mutations of members of the Ras/MAPK pathway are not feasible due to the nature of SelD. SelD is an enzyme of the biosynthesis pathway of selenocysteine. Overexpressing one component of the pathway does not imply an increase in selenocysteine as other enzymes in the pathway may be limitant; therefore, overexpression of SelD does not imply an increase in selenoproteins. In fact, overexpression experiments done in our laboratory using different GAL-4 drivers gave no visible phenotype.

This is the first example of the role of intracelular redox environment on the Ras/MAPK signalling pathway in a whole organism. The high specificity of our results (i.e., no interaction with other signalling pathways and results confirmed in two different developing tissues: wing and eye) gives strong support to the notion that signalling through the Ras/MAPK pathway is modulated by ROS. Our current hypothesis is that selenoproteins, through an un-

disclosed subset of ROS, modulate the Ras/MAPK signalling pathway. This is consistent with the finding that this pathway is also modulated by *catalase*. A selenoprotein-independent increase of a subset of ROS (i.e., $H_2O_2$) is able to modulate this pathway as well. This observation favors a scenario in which selenoprotein modulation of the Ras/MAPK pathway would be achieved by their control of the redox balance rather than one in which selenoproteins would exert their role directly interacting with one or more elements of this signalling cassette. These results may help to shed light on the role of redox on signalling events under physiological conditions in multicellular organisms.

## ACKNOWLEDGMENTS

We thank J. Casanova, S. Artavanis-Tsakonas, E. Martin-Blanco, J. Gil, and J. Dunlop for insightful discussions and suggestions. We also thank the staff of the Servels Cientifico Tecnics of the U.B. for their help with the SEM and preparation of samples. This work was supported by Grant PB96-1253 (to J.B.) and by a fellowship from CIRIT Generalitat de Catalunya (to M.M.). The experiments reported in this paper were carried out according to the current laws of Spain concerning experimental manipulation.

## REFERENCES

Alsina, B., Corominas, M., Berry, M. J., Baguñà, J., and Serras, F. (1999). Disruption of selenoprotein biosynthesis affects cell proliferation in the imaginal discs and brain of *Drosophila melanogaster*. *J. Cell Sci.* **112**, 2875–2884.

Alsina, B., Serras, F., Baguna, J., and Corominas, M. (1998). patufet, the gene encoding the *Drosophila melanogaster* homologue of selenophosphate synthetase, is involved in imaginal disc morphogenesis. *Mol. Gen. Genet.* **257**, 113–123.

Bae, Y. S., Kang, S. W., Seo, M. S., Baines, I. C., Tekle, E., Chock, P. B., and Rhee, S. G. (1997). Epidermal growth factor (EGF)-induced generation of hydrogen peroxide. Role in EGF receptor-mediated tyrosine phosphorylation. *J. Biol. Chem.* **272**, 217–221.

Basler, K., Christen, B., and Hafen, E. (1991). Ligand-independent activation of the sevenless receptor tyrosine kinase changes the fate of cells in the developing Drosophila eye. *Cell* **64**, 1069–1081.

Basler, K., and Hafen, E. (1988). Control of photoreceptor cell fate by the sevenless protein requires a functional tyrosine kinase domain. *Cell* **54**, 299–311.

Basler, K., Yen, D., Tomlinson, A., and Hafen, E. (1990). Reprogramming cell fate in the developing Drosophila retina: Transformation of R7 cells by ectopic expression of rough. *Genes Dev.* **4**, 728–739.

Bock, A. (2000). Biosynthesis of selenoproteins: An overview. *Biofactors* **11**, 77–78.

Bock, A., Forchhammer, K., Heider, J., and Baron, C. (1991). Selenoprotein synthesis: an expansion of the genetic code. *Trends Biochem. Sci.* **16**, 463–467.

Bohni, R., Riesgo-Escovar, J., Oldham, S., Brogiolo, W., Stocker, H., Andruss, B. F., Beckingham, K., and Hafen, E. (1999). Autonomous control of cell and organ size by CHICO, a Drosophila homolog of vertebrate IRS1–4. *Cell* **97**, 865–875.

Bosl, M. R., Takaku, K., Oshima, M., Nishimura, S., and Taketo, M. M. (1997). Early embryonic lethality caused by targeted disruption of the mouse selenocysteine tRNA gene (Trsp). *Proc. Natl. Acad. Sci. USA* **94**, 5531–5534.

Brand, A. H., and Perrimon, N. (1993). Targeted gene expression as a means of altering cell fates and generating dominant phenotypes. *Development* **118**, 401–415.

Brunner, D., Oellers, N., Szabad, J., Biggs, W. H., Zipursky, S. L., and Hafen, E. (1994). A gain-of-function mutation in Drosophila MAP kinase activates multiple receptor tyrosine kinase signalling pathways. *Cell* **76**, 875–888.

Brunner, E., Peter, O., Schweizer, L., and Basler, K. (1997). pangolin encodes a Lef-1 homologue that acts downstream of Armadillo to transduce the Wingless signal in Drosophila. *Nature* **385**, 829–833.

Burk, R., and Hill, K. E. (1999). Orphan selenoproteins. *BioEssays* **21**, 231–237.

Cadigan, K. M., and Nusse, R. (1996). wingless signalling in the Drosophila eye and embryonic epidermis. *Development* **122**, 2801–2812.

Chen, C., Jack, J., and Garofalo, R. S. (1996). The Drosophila insulin receptor is required for normal growth. *Endocrinology* **137**, 846–856.

Clifford, R. J., and Schupbach, T. (1989). Coordinately and differentially mutable activities of torpedo, the *Drosophila melanogaster* homolog of the vertebrate EGF receptor gene. *Genetics* **123**, 771–787.

Copeland, P. R., Fletcher, J. E., Carlson, B. A., Hatfield, D. L., and Driscoll, D. M. (2000). A novel RNA binding protein, SBP2, is required for the translation of mammalian selenoprotein mRNAs. *EMBO J.* **19**, 306–314.

Diaz-Benjumea, F. J., and Garcia-Bellido, A. (1990). Behaviour of cells mutant for an EGF receptor homologue of Drosophila in genetic mosaics. *Proc. R. Soc. London B Biol. Sci.* **242**, 36–44.

Diaz-Benjumea, F. J., and Hafen, E. (1994). The sevenless signalling cassette mediates Drosophila EGF receptor function during epidermal development. *Development* **120**, 569–578.

Dickson, B. J., van der Straten, A., Dominguez, M. and Hafen, E. (1996). Mutations modulating Raf signalling in Drosophila eye development. *Genetics* **142**, 163–171.

Fagegaltier, D., Hubert, N., Yamada, K., Mizutani, T., Carbon, P., and Krol, A. (2000). Characterization of mSelB, a novel mammalian elongation factor for selenoprotein translation. *EMBO J.* **19**, 4796–4805.

Finkel, T. (1998). Oxygen radicals and signalling. *Curr. Opin. Cell Biol.* **10**, 248–253.

Fortini, M. E., Simon, M. A., and Rubin, G. M. (1992). Signalling by the sevenless protein tyrosine kinase is mimicked by Ras1 activation. *Nature* **355**, 559–561.

Freeman, M. (1996). Reiterative use of the EGF receptor triggers differentiation of all cell types in the Drosophila eye. *Cell* **87**, 651–660.

Garcia-Bellido, A., and de Celis, J. F. (1992). Developmental genetics of the venation pattern of Drosophila. *Annu. Rev. Genet.* **26**, 277–304.

Griswold, C. M., Matthews, A. L., Bewley, K. E., and Mahaffey, J. W. (1993). Molecular characterization and rescue of acatalasemic mutants of *Drosophila melanogaster*. *Genetics* **134**, 781–788.

Guimaraes, M. J., Peterson, D., Vicari, A., Cocks, B. G., Copeland, N. G., Gilbert, D. J., Jenkins, N. A., Ferrick, D. A., Kastelein, R. A., Bazan, J. F., *et al.* (1996). Identification of a novel selD homolog from eukaryotes, bacteria, and archaea: Is there an

autoregulatory mechanism in selenocysteine metabolism? *Proc. Natl. Acad. Sci. USA* **93**, 15086–15091.

Guyton, K. Z., Liu, Y., Gorospe, M., Xu, Q., and Holbrook, N. J. (1996). Activation of mitogen-activated protein kinase by $H_2O_2$. Role in cell survival following oxidant injury. *J. Biol. Chem.* **271**, 4138–4142.

Hariharan, I. K., Hu, K. Q., Asha, H., Quintanilla, A., Ezzell, R. M., and Settleman, J. (1995). Characterization of rho GTPase family homologues in *Drosophila melanogaster*: Overexpressing Rho1 in retinal cells causes a late developmental defect. *EMBO J.* **14**, 292–302.

Hirosawa-Takamori, M., Jäckle, H., and Vorbrüggen, G. (2000). The class 2 selenophosphate synthetase gene of Drosophila contains a functional mammalian-type SECIS. *EMBO Reports* **1**, 441–446.

Huang, H., Potter, C. J., Tao, W., Li, D. M., Brogiolo, W., Hafen, E., Sun, H., and Xu, T. (1999). PTEN affects cell size, cell proliferation and apoptosis during Drosophila eye development. *Development* **126**, 5365–5372.

Hue, X. S., Chou, T. B., Melnick, M. B., and Perrimon, N. (1995). The Torso receptor tyrosine kinase can activate Raf in a Ras-independent way. *Cell* **81**, 63–71.

Irani, K., Xia, Y., Zweier, J. L., Sollott, S. J., Der, C. J., Fearon, E. R., Sundaresan, M., Finkel, T., and Goldschmidt-Clermont, P. J. (1997). Mitogenic signaling mediated by oxidants in Ras-transformed fibroblasts. *Science* **275**, 1649–1652.

Kamata, H., Shibukawa, Y., Oka, S. I., and Hirata, H. (2000). Epidermal growth factor receptor is modulated by redox through multiple mechanisms. Effects of reductants and $H_2O_2$. *Eur. J. Biochem.* **267**, 1933–1944.

Karim, F. D., Chang, H. C., Therrien, M., Wassarman, D. A., Laverty, T., and Rubin, G. M. (1996). A screen for genes that function downstream of Ras1 during Drosophila eye development. *Genetics* **143**, 315–329.

Krieger-Brauer, H. I., and Kather, H. (1992). Human fat cells possess a plasma membrane-bound $H_2O_2$-generating system that is activated by insulin via a mechanism bypassing the receptor kinase. *J. Clin. Invest.* **89**, 1006–1013.

Lee, B. J., Rajagopalan, M., Kim, Y. S., You, K. H., Jacobson, K. B., and Hatfield, D. (1990). Selenocysteine tRNA[Ser]Sec gene is ubiquitous within the animal kingdom. *Mol. Cell. Biol.* **10**, 1940–1949.

Leevers, S. J., Weinkove, D., MacDougall, L. K., Hafen, E., and Waterfield, M. D. (1996). The Drosophila phosphoinositide 3-kinase Dp110 promotes cell growth. *EMBO J.* **15**, 6584–6594.

Lim, Y. M., Nishizawa, K., Nishi, Y., Tsuda, L., Inoue, Y. H., and Nishida, Y. (1999). Genetic analysis of rolled, which encodes a Drosophila mitogen-activated protein kinase. *Genetics* **153**, 763–771.

Lo, Y. Y. C., and Cruz, T. F. (1995). Involvement of reactive oxygen species in cytokine and growth factor induction of c-fos expression in chondrocytes. J. Biol. Chem. **270**, 11727–11730.

Low, S. C., and Berry, M. J. (1996). Knowing when not to stop: Selenocysteine incorporation in eukaryotes. *Trends Biochem. Sci.* **21**, 203–208.

Low, S. C., Harney, J. W., and Berry, M. J. (1995). Cloning and functional characterization of human selenophosphate synthetase, an essential component of selenoprotein synthesis. *J. Biol. Chem.* **270**, 21659–21664.

Mackay, W. J., and Bewley, G. C. (1989). The genetics of catalase in *Drosophila melanogaster*: Isolation and characterization of acatalasemic mutants. *Genetics* **122**, 643–652.

Martin-Blanco, E. (1998). Regulatory control of signal transduction during morphogenesis in Drosophila. *Int. J. Dev. Biol.* **42**, 363–368.

Martin-Blanco, E., Roch, F., Noll, E., Baonza, A., Duffy, J. B., and Perrimon, N. (1999). A temporal switch in DER signalling controls the specification and differentiation of veins and interveins in the Drosophila wing. *Development* **126**, 5739–5747.

Olivier, J. P., Raabe, T., Henkemeyer, M., Dickson, B., Mbamalu, G., Margolis, B., Schlessinger, J., Hafen, E., and Pawson, T. (1993). A Drosophila SH2-SH3 adaptor protein implicated in coupling the sevenless tyrosine kinase to an activator of Ras guanine nucleotide exchange, Sos. *Cell* **73**, 179–191.

Persson, B. C., Bock, A., Jackle, H., and Vorbruggen, G. (1997). SelD homolog from Drosophila lacking selenide-dependent monoselenophosphate synthetase activity. *J. Mol. Biol.* **274**, 174–180.

Rommel, C., and Hafen, E. (1998). Ras—a versatile cellular switch. *Curr. Opin. Genet. Dev.* **8**, 412–418.

Simon, M. A., Bowtell, D. D., Dodson, G. S., Laverty, T. R., and Rubin, G. M. (1991). Ras1 and a putative guanine nucleotide exchange factor perform crucial steps in signalling by the sevenless protein tyrosine kinase. *Cell* **67**, 701–716.

Stadtman, T. C. (1996). Selenocysteine. *Annu. Rev. Biochem.* **65**, 83–100.

Stevenson, M. A., Pollock, S. S., Coleman, C. N., and Calderwood, S. K. (1994). X-irradiation, phorbol esters, and $H_2O_2$ stimulate mitogen-activated protein kinase activity in NIH-3T3 cells through the formation of reactive oxygen intermediates. *Cancer Res.* **54**, 12–15.

Sturtevant, M. A., and Bier, E. (1995). Analysis of the genetic hierarchy guiding wing vein development in Drosophila. *Development* **121**, 785–801.

Sundaresan, M., Yu, Z. X., Ferrans, V. J., Irani, K., and Finkel, T. (1995). Requirement for generation of $H_2O_2$ for platelet-derived growth factor signal transduction. *Science* **270**, 296–299.

Torok, T., Tick, G., Alvarado, M., and Kiss, I. (1993). P-lacW insertional mutagenesis on the second chromosome of *Drosophila melanogaster*: Isolation of lethals with different overgrowth phenotypes. *Genetics* **135**, 71–80.

Tujebajeva, R. M., Copeland, P. R., Xu, X. M., Carlson, B. A., Driscoll, J. W., *et al.* (2000). Decoding apparatus for eukaryotic selenocysteine insertion. *EMBO Reports* **1**, 158–163.

Zhou, X., Park, S. I., Moustafa, M. E., Carlson, B. A., Crain, P. F., Diamond, A. M., Hatfield, D. L., and Lee, B. J. (1999). Selenium metabolism in Drosophila. Characterization of the selenocysteine tRNA population. *J. Biol. Chem.* **274**, 18729–18734.

Received for publication May 17, 2001
Revised July 3, 2001
Accepted July 9, 2001
Published online August 27, 2001

**Article 2**: Morey, M., Serras, F. and Corominas, M. (2003). Halving the selenophosphate synthetase gene dose confers hypersensitivity to oxidative stress in *Drosophila melanogaster*. *FEBS Lett*. 2003 Jan 16;534(1-3):111-4.

**Precendents**

Les larves homozigotes per la mutació $selD^{ptuf}$ no sintetitzen selenoproteïnes i els seus discs imaginals acumulen ROS (Alsina *et al*., 1999). L'heterozigot $selD^{ptuf}$ és aparentment normal i perfectament viable en condicions normals. De totes maneres, és capaç de suprimir els fenotips de guany de funció d'elements de la via Ras/MAPK (Article 1: Morey *et al*., 2001). Per analogia amb els efectes de la mutació en homozigosi, inferíem que la mutació en heretozigosi resultaria en una síntesi de selenoproteïnes menys eficient i per tant en un increment en els nivells de radicals lliures comparat amb una mosca silvestre. El fet que un increment de ROS independent de selenoproteïnes com l'obtingut amb el mutant $Cat^{n1}$ tingués el mateix efecte que $selD^{ptuf}$, reforçava la hipòtesi de l'increment de ROS com a responsable de la modulació de la via Ras/MAPK (Article 1: Morey *et al*., 2001). Tanmateix, no havíem demostrat directament l'acumulació de ROS a l'heterozigot. Ja que dita acumulació és possiblement molt subtil i difícil de mesurar bioquímicament donat que l'heterozigot és normal, es feia necessari demostrar d'alguna altra manera que la síntesi de selenoproteïnes estava disminuïda. Com s'havia descrit que l'expressió ectòpica de SOD humana en motoneurones de *Drosophila* allargava la vida (Parkes et al., 1998), vàrem voler provar quin era l'efecte de l'expressió del gen *selD* en motoneurones.

**Resum**

Si les selenoproteïnes tenen una funció antioxidant i l'heterozigot $selD^{ptuf}$ té la seva síntesis disminuïda, llavors s'esperaria que dites mosques ($selD^{ptuf/+}$) no aguantessin una situació d'estrès oxidatiu de la mateixa manera que unes mosques normals ($selD^{+/+}$). Per tal d'esbrinar si aquesta era la situació, es va sotmetre a l'heterozigot i al seu control a dietes altament oxidatives.

Un aspecte molt important a tenir en compte a l'hora de dur a terme experiments relacionats amb supervivència i longevitat és la necessitat de treballar en un fons genètic equivalent per l'experiment i el control. Amb l'objectiu de comparar l'heterozigot amb el control més adient es va generar una escissió precisa de l'element *P* causant de la mutació $selD^{ptuf}$ i es van dissenyar un seguit d'encreuaments per generar línies isogèniques. Es van realitzar les corbes de vida per l'heterozigot i el control front un panell de diferents concentracions de paraquat i $H_2O_2$, dos agents altament oxidatius afegits al medi de cultiu. En tots dos casos i de manera estadísticament significativa, l'heterozigot sempre presentava una vida mitja més curta que el control. Això ens permet concloure que certament la síntesi de selenoproteïnes està afectada a l'heterozigot i demostrar *in vivo* la funció antioxidant de les selenoproteïnes.

Com ja s'ha esmentat a la Introducció, s'ha postulat que els ROS podrien ser agents causals de l'envelliment. Altres experiments es van dur a terme per a desvelar si la funció antioxidant de les selenoproteïnes és important en el procés de senescència. Es va realitzar una corba de vida per l'heterozigot i el control en condicions normals de dieta i no es va detectar cap diferència en la vida mitja (Fig. 17). Pareix doncs, que l'activitat d'una sola

còpia de *selD* és suficient per a dur una vida normal sempre i quant no es doni una situació d'estrès oxidatiu. També es va realitzar una corba de vida en un fons genètic d'expressió ectòpica de *selD*. L'expressió d'aquest element de la via de síntesis de les selenoproteïnes en motoneurones no allargava la vida mitja. Al contrari, es va observar una reducció respecte al control, que podria ser deguda a l'acumulació de metabòlits intermediaris de Se tòxics.

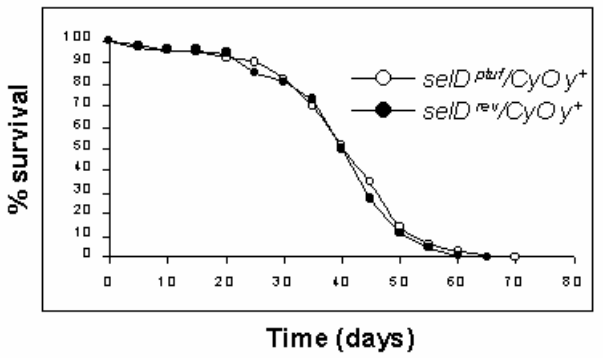


Fig. 17. Les de corbes de vida de l'heterozigot *selD*$^{ptuf}$ i del seu control no són significativament diferents

FEBS 26870 FEBS Letters 534 (2003) 111–114

# Halving the selenophosphate synthetase gene dose confers hypersensitivity to oxidative stress in *Drosophila melanogaster*

Marta Morey, Florenci Serras, Montserrat Corominas*

*Departament de Genètica, Facultat de Biologia, Universitat de Barcelona, Diagonal 645, 08028 Barcelona, Spain*

Received 5 November 2002; revised 29 November 2002; accepted 29 November 2002

First published online 11 December 2002

Edited by Barry Halliwell

**Abstract Several lines of evidence indicate that selenoproteins mainly act as cellular antioxidants. Here, we test this idea comparing the sensitivity to oxidative stress (paraquat and hydrogen peroxide) between wild type and heterozygous flies for the selenophosphate synthetase *selD*$^{ptuf}$ mutation. Whereas under normal laboratory conditions no difference in life span is observed, a significant decrease is seen in heterozygous flies treated with oxidant agents. In contrast, overexpression of the *selD* gene in motoneurons did not extend longevity. Our results strongly suggest that *selD* haploinsufficiency makes heterozygous flies more sensitive to oxidative stress and add further evidence to the role of selenoproteins as cellular antioxidants.**


*Key words:* *selD*$^{ptuf}$; Selenoprotein; Oxidative stress; Life span

## 1. Introduction

Selenium (Se) is an essential dietary micronutrient of fundamental importance to health [1]. Most of the effects of Se are probably mediated by selenoproteins, which have this element covalently incorporated in the form of selenocysteine (Sec), the 21st amino acid. The majority of selenoproteins appear to have a role as antioxidants or catalyze oxidation–reduction reactions [1,2]. As a component of antioxidant enzymes, Se helps to protect cells from the harmful effects of reactive oxygen species (ROS). It is needed for proper function of the immune system, it is required for sperm motility and its deficiency may be linked to adverse mood states [1]. Evidence from prospective studies, intervention trials and studies on animal models has also suggested a strong inverse correlation between selenium intake and cancer incidence [3,4]. Nevertheless, the biological functions of Se are often inferred from epidemiological or cell culture studies pointing at a circumstantial relationship. In this work we have taken a genetic approach to assess the putative relationship between Se metabolism, oxidative stress and life span using the *selD*$^{ptuf}$ mutation of *Drosophila*.

It has been postulated that an increase of macromolecular damage induced by ROS could be the central causal factor promoting the aging process [5]. Studies on oxidative stress and longevity often use molecular-genetic approaches in order to identify specific factors that may influence the rate of aging. The experiments carried out mainly in *Drosophila melanogaster* and *Caenorhabditis elegans* involve transgenic overexpression of antioxidant genes and induction of single loss of function gene mutations, but interpretation of such studies is quite controversial [6–8].

*selD*$^{ptuf}$ is a null mutation affecting the gene encoding selenophosphate synthetase, a key enzyme of the selenoprotein biosynthesis pathway. Homozygous mutants die at third instar larvae and have extremely reduced and abnormal imaginal disks, with cells that accumulate ROS and enter apoptosis [9,10]. No selenoprotein synthesis is observed in those organisms [10]. Heterozygous flies are healthy and viable when kept under normal laboratory conditions. However, a downregulation of the Ras/mitogen-activated protein kinase (MAPK) pathway has been observed in transheterozygous combinations of *selD*$^{ptuf}$ and activated members of this signaling pathway. Because a selenoprotein-independent increase in ROS caused by the catalase null allele *Cat*$^{n1}$ also reduces Ras/MAPK signaling, increases in those free radicals may likely be responsible for this effect [11]. The read-out of our previous experiments strongly suggests that accumulation of ROS should be substantially different between heterozygous and wild type flies. However, changes in ROS might be subtle and biochemically difficult to detect since heterozygous flies are normal-appearing individuals. Therefore, it is necessary to confirm whether haploinsufficiency of *selD*$^{ptuf}$ generates a background of oxidative stress sufficient to alter the efficiency of some cellular events, such as a reduction of the Ras/MAPK activity, without impairing the organism's viability. To that aim we measured the life span of flies on a highly oxidative diet, to test whether heterozygous *selD*$^{ptuf}$ flies are more sensitive than wild type flies. We also overexpressed the *selD* gene specifically in motoneurons to assess the possible effects of increasing *selD* activity in longevity.

## 2. Materials and methods

### 2.1. Drosophila stocks

The *selD*$^{ptuf}$ (*yw*; *l(2)k11320/CyO*) line was obtained from a collection of lethal mutants resulting from *PlacW* insertions on the second chromosome [9,12]. The viable revertant *selD*$^{rev}$, obtained by a precise excision of *PlacW* using the Δ2-3 transposase, was used as a control to minimize differences between genetic backgrounds. The transgenic line *UAS-selD* on chromosome 3 was generated in our laboratory [9] and its expression driven onto motoneurons using the *D42-GAL4* driver on the third chromosome [13] kindly provided by Dr. J.P. Phillips. In all experiments, only males were used because female life span is known to depend upon reproductive history [14]. All experiments were performed at 25°C, in constant humidity and light conditions.

*Corresponding author. Fax: (34)-93-4110969.
*E-mail address:* mcorominas@ub.edu (M. Corominas).

0014-5793/02/$22.00 
doi:10.1016/S0014-5793(02)03790-0

*2.2. Life span measurements*

Adult males (0–48 h old) were maintained in vials (10 flies/vial) containing standard medium. Flies were scored daily for survivorship and transferred to new vials every 3 days. For life span determination we generated isogenic strains for most of the genome of *selD$^{ptuf}$/CyO y$^{+}$* and *selD$^{rev}$/CyO y$^{+}$*. A crossing scheme employing a *w* stock carrying both *CyO* and *TM3* balancers was also devised to produce +/+; *D42-GAL4/UAS-selD* and +/+; *UAS-selD*/+ stocks to minimize variation in genetic background between stocks for the second and third chromosomes. For statistical analysis the mean life span of each strain was calculated as the time (in days) at which survival reached 50% of the starting population. Survival data were analyzed by stratified log rank tests, using the SURVIVAL application of the SPSS10.0 software package.

*2.3. Stress treatments*

Adult males (3–4 days old kept in standard medium) were transferred to vials with 2 ml of special medium containing 1% sucrose, 1.3% low melting agarose and the specified concentration of paraquat (1,1′-dimethyl-4,4′-bipyridinium dichloride) or hydrogen peroxide ($H_2O_2$). To avoid loss of oxidative activity, both substances were added when the temperature of the medium was 45°C. Each vial contained 10 males and survival was scored every day without changing the medium.

## 3. Results

*3.1. Life span determination of selD$^{ptuf}$ heterozygous flies*

Heterozygous *selD$^{ptuf}$* flies develop into normal-appearing perfectly viable adults able to mate and give progeny. They are therefore kept as a regular laboratory strain. To assess the behavior of heterozygous flies regarding viability we determined the life span of *selD$^{ptuf}$* flies as well as that of the *PlacW* revertant, *selD$^{rev}$*, used as a control. As expected, mean life span of flies with one wild type copy of the *selD* gene was not significantly different from control ones. The mean (50% mortality) life span for each genotype was as follows: *selD$^{ptuf}$/CyO y$^{+}$*, 40.00 ± 0.91 days ($n = 319$); *selD$^{rev}$/CyO y$^{+}$*, 38.88 ± 0.67 days ($n = 284$). After performing the log rank test, no significant differences were obtained between *selD$^{ptuf}$* and *selD$^{rev}$* flies ($P = 0.1291$).

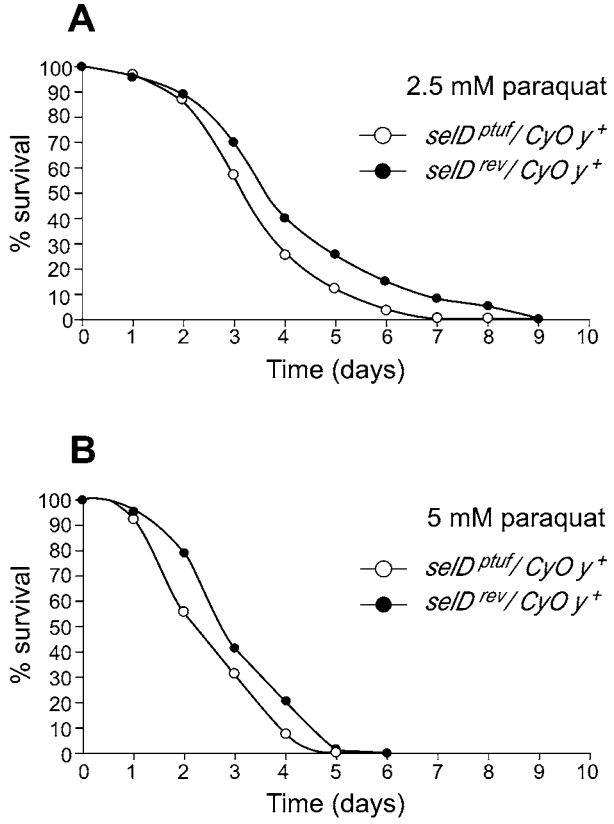


Fig. 1. Effect of different concentrations of paraquat on the longevity of *selD$^{ptuf}$/CyO y$^{+}$* and *selD$^{rev}$/CyO y$^{+}$* flies. *selD$^{ptuf}$* mutant in heterozygous condition is significantly more sensitive to paraquat oxidative treatment compared to its wild type revertant. A: 2.5 mM paraquat, $P = 0.0002$. B: 5 mM paraquat, $P = 0.0010$.

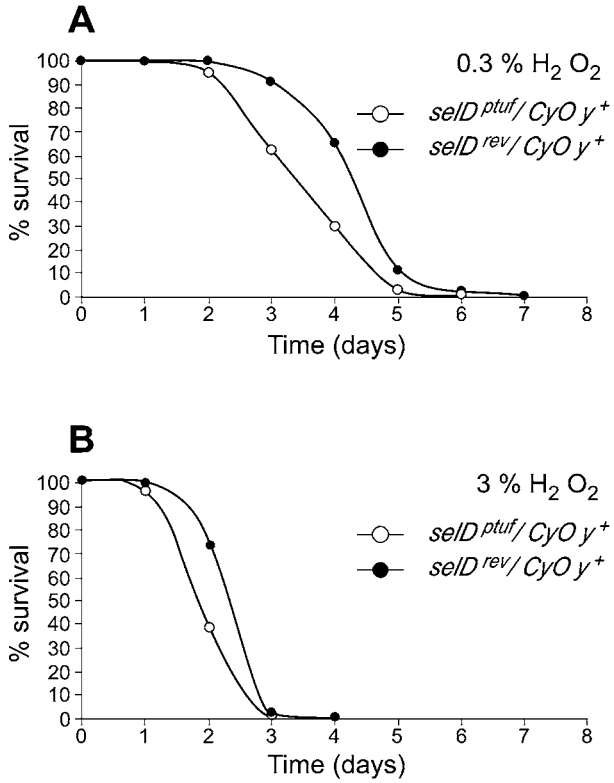


Fig. 2. Effect of different concentrations of hydrogen peroxide on the longevity of *selD$^{ptuf}$/CyO y$^{+}$* and *selD$^{rev}$/CyO y$^{+}$* flies. *selD$^{ptuf}$* mutant in heterozygous condition is significantly more sensitive to $H_2O_2$ oxidative treatment compared to its wild type revertant. A: 0.3% $H_2O_2$, $P < 0.001$. B: 3% $H_2O_2$, $P < 0.001$.

*3.2. Sensitivity to paraquat and hydrogen peroxide toxicity*

The sensitivity of *selD$^{ptuf}$/CyO y$^{+}$* and *selD$^{rev}$/CyO y$^{+}$* to enhanced production of ROS was tested feeding adult *Drosophila* with aqueous paraquat or $H_2O_2$ added to culture medium containing only sucrose as a nutrient. Such treatments likely expose flies to concentrations of ROS above the tolerance level of the fly's endogenous protective mechanisms. To minimize the effects of lower nutrient intake, animals were kept in standard medium for 3–4 days before the start of the experiment. Under these conditions, lack of one functional copy of *selD* conferred hypersensitivity to paraquat (Fig. 1). At 2.5 mM, mean life spans for each genotype were as follows: *selD$^{ptuf}$/CyO y$^{+}$*, 3.88 ± 0.11 days ($n = 150$) and *selD$^{rev}$/CyO y$^{+}$*, 4.55 ± 0.18 days ($n = 110$). At 5 mM, mean life spans were: *selD$^{ptuf}$/CyO y$^{+}$*, 2.91 ± 0.10 days ($n = 110$) and *selD$^{rev}$/CyO y$^{+}$*, 3.43 ± 0.11 days ($n = 100$). After performing the log rank test, the difference between both strains was significant at 2.5 mM ($P = 0.0002$) and 5 mM ($P = 0.0010$) paraquat concentrations. No differences were observed between both strains when lower (1 mM, not reaching the toxicity threshold) or

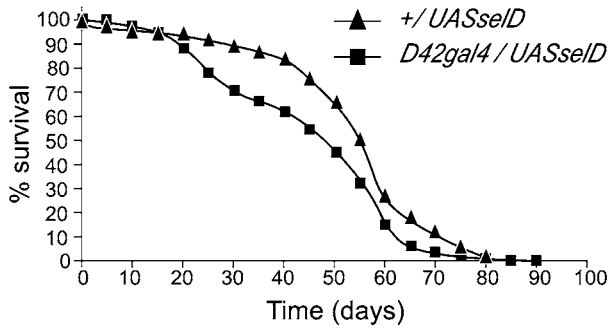


Fig. 3. Longevity determination of flies overexpressing *selD* in motoneurons using the specific driver *D42-GAL4*. Overexpression of *selD* in motoneurons significantly reduces life span compared to the control flies ($P < 0.001$).

higher (10 mM, highly toxic) doses of paraquat were used (data not shown).

A lower resistance of the $selD^{ptuf}$ genotype compared to the $selD^{rev}$ genotype was also observed when flies were exposed to different concentrations of hydrogen peroxide (Fig. 2). At 0.3% $H_2O_2$, mean life spans were: $selD^{ptuf}/CyO$ $y^+$, 3.90 ± 0.08 days ($n = 124$) and $selD^{rev}/CyO$ $y^+$, 4.70 ± 0.09 days ($n = 90$). At 3% concentration mean life spans were: $selD^{ptuf}/CyO$ $y^+$, 2.36 ± 0.05 days ($n = 150$) and $selD^{rev}/CyO$ $y^+$, 2.75 ± 0.05 days ($n = 110$). The difference between $selD^{ptuf}$ and $selD^{rev}$ flies was significant at 0.3% ($P < 0.001$) and 3% ($P < 0.001$) $H_2O_2$ concentrations.

### 3.3. Overexpression of $selD^{ptuf}$ does not extend life span

To determine the effects of *selD* overexpression on longevity, the *D42-GAL4* and *UAS-selD* transgenes were introduced into flies with normal $selD^{+/+}$ genetic background. Increased *selD* activity in motoneurons did not extend life span; on the contrary, it reduced longevity (Fig. 3). Mean life spans and sample sizes for each genotype were: +/+, *UAS-selD*/+, 50.97 ± 0.91 days ($n = 343$) and +/+, *D42-GAL4*/*UAS-selD*, 42.21 ± 0.93 days ($n = 352$). A significant decrease ($P < 0.001$) in life span was observed in flies overexpressing the selenophosphate synthetase compared to control flies.

## 4. Discussion

The main conclusion of our study is that the heterozygous condition of *selD* is more sensitive than wild type to oxidative stress conditions. Heterozygosity may lead to a less efficient biosynthesis of selenoproteins due to a limitation on selenium monophosphate availability. Because selenoproteins are involved in redox balance reactions, it is fair to assume that heterozygous flies have higher rates of ROS accumulation than wild type controls. Therefore, we propose that *selD* heterozygous flies accumulate ROS to levels not enough to impair cell viability, but sufficient to be detected in sensitized genetic backgrounds such as the Ras/MAPK signaling pathway [11]. It has been suggested that synthesis of selenoproteins in *Drosophila* may be driven by a selenophosphate synthetase other than *selD*, selenophosphate synthetase 2 (Sps2) [15,16]. However, the phenotypes observed in $selD^{ptuf}$ mutant animals, the lack of $Se^{75}$-labeled bands in mutant larval extracts [9,10], and the fact that Sps2 is itself a selenoprotein [16] back the key role of *selD* in the pathway.

The beneficial effects of Se on organisms could potentially be divested by a dietary selenium deficiency or impairing its metabolism (i.e. selenoprotein biosynthesis). Recently it has been shown that dietary selenium deficiency shortens while supplementation normalizes *Drosophila* life span [17]. This is consistent with reports on the deleterious effects of low Se intake on several aspects of human and animal health [1,18]. The reduced *selD* activity of heterozygous flies is sufficient for normal life, provided the animals grow in regular yeast-based medium that contains enough Se traces. Le Bourg [6] has suggested that antioxidant enzymes could be mainly considered stress enzymes, which would act as shields if necessary though are not essential for everyday life. Similarly, the haploinsufficiency of *selD* only becomes evident under oxidative stress conditions.

The production of oxidants, together with the ability to respond to oxidative stress, is intricately connected to aging and life span ([19] and references therein). ROS produced during normal metabolism cause damage to macromolecules that, if not repaired, places the organism at risk [5]. Intracellular defense systems that protect cells from ROS-induced damage include glutathione peroxidase (GPX), glutathione reductase (GR), thioredoxin reductase (TrxR), superoxide dismutase (SOD) and catalase (Cat) [20]. *D. melanogaster* flies lack GPX and recently it has been found that the single GR homolog specifies TrxR activity, which compensates for the absence of a true GR system for recycling GSH [21,22]. Although only three selenoproteins have been identified so far in the *Drosophila* genome [17,23] it is not possible at this moment to correlate the antioxidant activity with a particular protein. As the list of selenoproteins is increasing in higher organisms, this might also be the case in *Drosophila*. However, since SOD, Cat and TrxR are normal and functional in the flies used for this study, our results indicate that the burden of ROS metabolism in *Drosophila* is also shared by a defense system that includes selenoproteins.

The effects on longevity of numerous studies overexpressing antioxidant enzymes, such as Cat and SOD, have been controversial because life spans increase in some but not in others [6–8]. Following a report showing extended life span in *Drosophila* expressing human SOD1 in motoneurons [13], we tested the effects of *selD* overexpression in such cells. As expected, because *selD* is just one member of the complex machinery needed to synthesize selenoproteins, higher amounts of *selD* do not extend life span. The reduction observed could be explained by accumulation of toxic intermediaries (maybe selenophosphate) due to *selD* overexpression. Further experiments overexpressing specific *Drosophila* selenoproteins together with elements of the biosynthesis pathway may be a better way to test the contribution of selenoproteins' antioxidant function to prevent aging and extend life span.

*Acknowledgements:* We thank J. Baguñà, L. Serra, H. Tricoire and E. Sanchez-Herreros for insightful discussions and suggestions. This work was supported by Grant PB96-1253 from Dirección General de Investigación Científica y Técnica (DGICYT), by Grant 01/0906 from FIS, Ministerio de Sanidad y Consumo (to M.C.) and by a fellowship from CIRIT, Generalitat de Catalunya (to M.M.). The experiments reported in this paper were carried out according to the current laws of Spain concerning experimental manipulation.

## References

[1] Rayman, M.P. (2000) Lancet 356, 233–241.

[2] Stadtman, T. (1996) Annu. Rev. Biochem. 65, 83–100.
[3] Clark, L.C., Combs, G.F., Turnbull, B.W., Slate, E.H., Chalker, D.K., Chow, J., Davis, L.S., Glover, R.A., Graham, G.F., Gross, E.G., Krongrad, A., Lesher, J.L., Park, H.K., Sanders, B.B., Smith, C.L. and Taylor, J.R. (1996) J. Am. Med. Assoc. 276, 1957–1963.
[4] Ganther, H.E. (1999) Carcinogenesis 20, 1657–1666.
[5] Harman, D. (1956) J. Gerontol. 11, 298–300.
[6] Le Bourg, E. (2001) FEBS Lett. 498, 183–186.
[7] Sohal, R.S. (2002) Free Radic. Biol. Med. 33, 573–574.
[8] Sohal, R.S., Mockett, R.J. and Orr, W.C. (2002) Free Radic. Biol. Med. 33, 575–586.
[9] Alsina, B., Serras, F., Baguñà, J. and Corominas, M. (1998) Mol. Gen. Genet. 257, 113–123.
[10] Alsina, B., Corominas, M., Berry, M.J., Baguñà, J. and Serras, F. (1999) J. Cell Sci. 112, 2875–2884.
[11] Morey, M., Serras, F., Baguñà, J., Hafen, E. and Corominas, M. (2001) Dev. Biol. 238, 145–156.
[12] Török, T., Tick, G., Alvarado, M. and Kiss, I. (1993) Genetics 135, 71–80.
[13] Parkes, T.L., Elia, A.J., Dickinson, D., Hilliker, A.J., Phillips, J.P. and Boulianne, G.L. (1998) Nature Genet. 19, 171–174.
[14] Luckinbill, L.S. and Clare, M.H. (1985) Heredity 55, 9–18.
[15] Persson, B., Böck, A., Jäckle, H. and Vorbruggen, G. (1997) J. Mol. Biol. 274, 174–180.
[16] Hirosawa-Takamori, M., Jäckle, H. and Vorbrüggen, G. (2000) EMBO Rep. 1, 441–446.
[17] Martin-Romero, F.J., Kryukov, G.V., Lobanov, A.V., Carlson, B.A., Lee, B.J., Gladyshev, V.N. and Hatfield, D.L. (2001) J. Biol. Chem. 276, 29798–29804.
[18] McKenzie, R.C., Arthur, J.R. and Beckett, G.J. (2002) Antioxid. Redox Signal. 4, 339–351.
[19] Finkel, T. and Holbrook, N.J. (2000) Nature 408, 239–247.
[20] Halliwell, B. and Gutteridge, J.M. (1999) in: Free Radicals in Biology and Medicine, 3rd edn., Oxford University Press, Oxford.
[21] Kanzok, S.M., Fechner, A., Bauer, H., Ulschmid, J.K., Müller, H.-M., Botella-Munoz, J., Schnewly, S., Schirmer, H. and Becker, K. (2001) Science 291, 634–646.
[22] Missirlis, F., Phillips, J.P. and Jäckle, H. (2001) Curr. Biol. 11, 1272–1277.
[23] Castellano, S., Morozova, N., Morey, M., Berry, M.J., Serras, F., Corominas, M. and Guigó, R. (2001) EMBO Rep. 2, 697–702.

## Annex: Protocols genètics

***Protocol d'escissió de l'element P i generació de línies isogèniques.***

El transposó *PlacW* porta com a marcador d'inserció el gen *white*$^{+}$ (ulls vermells). Quan el transposó s'insereix en mosques mutants pel gen *white* (ulls blancs), els ulls de dites mosques deixaran de ser blancs i passaran a tenir una certa coloració. Així, el color dels ulls pot anar d'un taronja suau a un vermell intens depenent del lloc d'inserció de l'element *P*. A més, aquest element *P* pot mobilitzar-se de nou per l'acció de l'enzim transposasa. L'escissió de l'element *P* es detecta per l'absència de color als ulls de la mosca. Els salts no són sempre perfectes. L'escissió imprecisa pot causar deleccions en el genoma generant d'aquesta manera nous al·lels mutants. Si l'escissió és precisa, el fenotip letal pot revertir-se al fenotip salvatge, i en termes de fons genètic, obtenim una mosca exacta al mutant amb l'excepció de l'element *P*.

Partint de la línia original *yw; l(2)k11320/CyO* es va dur a terme el següent protocol d'escissió del transposó *PlacW* per seleccionar revertents viables que poguéssim utilitzar com a control en els nostres experiments de supervivència i longevitat:

1. Femelles de la línia *yw; l(2)k11320/CyO* es varen encreuar amb mascles portadors de la font de transposasa.
2. De l'encreuament anterior es varen seleccionar mascles portadors de l'element *P* i la font de transposasa (*Δ2-3*). Els gàmetes generats per aquests mascles podran ser de dos tipus: amb l'element *P* escindit de manera precisa o imprecisa. Per tal de detectar els gàmetes que havien sofert una escissió precisa de l'element *P* es varen encreuar dits mascles de nou per la línia original la qual porta l'element *P*.
3. Els mascles descendents de l'encreuament 2 que tenien els ulls vermells (és a dir que un dels seus cromosomes portava l'element *P*) i que no portaven el balancejador *CyO* es varen seleccionar com a escissions precises. El fet de no portar el balancejador *CyO* indica que el cromosoma que hi ha en el seu lloc, en ser viable sobre l'element *P*, ha de ser una escissió precisa del mateix.
   Com cada mascle obtingut venia d'un gàmeta diferent, aquests es varen encreuar de manera individual amb femelles d'una soca balancejadora per tal de generar un estoc de mosques. D'aquesta manera rescatavem el cromosoma on l'element *P* havia estat escindit de manera precisa.
4. Els mascles i femelles de la descendència de l'encreuament 3 portadors del cromosoma revertent sobre el balancejador *y*$^{+}$ *CyO* es varen encreuar entre ells per tal de fer l'estoc final. Donat que el cromosoma revertent és normal, la seva combinació en homozigosi és viable. L'interès d'aquest protocol, en el nostre cas, radicava en obtenir mosques control amb el mateix fons genètic que el mutant heterozigot, i per tant, a cada generació es seleccionaven femelles verges i mascles portadors del balancejador i es creava un nou estoc.

**1.** 20 $\frac{yw}{yw}$ ; $\frac{P(w^+)}{CyO}$ ; $\frac{+}{+}$ x 10 $\frac{yw}{Y}$ ; $\frac{Sp}{CyO}$ ; $\frac{Sb\ \Delta 2\text{-}3}{TM6}$

↓

**2.** 30 $\frac{yw}{Y}$ ; $\frac{P(w^+)}{CyO}$ ; $\frac{Sb\ \Delta 2\text{-}3}{+}$ x 60 $\frac{yw}{yw}$ ; $\frac{P(w^+)}{CyO}$ ; $\frac{+}{+}$

↓

**3.** 1 $\frac{yw}{Y}$ ; $\frac{P(w^+)\ rev}{P(w^+)}$ ; $\frac{+}{+}$ x $\frac{yw}{yw}$ ; $\frac{Sco}{y^+\ CyO}$ ; $\frac{+}{+}$

↓

**4.** $\frac{yw}{Y}$ ; $\frac{P(w^+)\ rev}{y^+\ CyO}$ ; $\frac{+}{+}$ x $\frac{yw}{yw}$ ; $\frac{P(w^+)\ rev}{y^+\ CyO}$ ; $\frac{+}{+}$

↓

$\frac{yw}{Y}$ $\frac{yw}{yw}$ | $\frac{P(w^+)\ rev}{P(w^+)\ rev}$ $\frac{P(w^+)\ rev}{y^+\ CyO}$ | $\frac{+}{+}$

Per als experiments de supervivència i longevitat era molt important que el fons genètic fos el més equivalent possible entre l'heterozigot i el control. Per això, vàrem voler controlar també el balancejador de l'heterozigot per tal que fos el mateix que el del control. Així doncs, vàrem encreuar el mutant heterozigot per la mateixa soca balancejadora utilitzada pel control. Vàrem seleccionar mascles i femelles portadors del balancejador $y^+$ *CyO* i vàrem fer un estoc.

$\frac{yw}{yw}$ ; $\frac{P(w^+)}{CyO}$ ; $\frac{+}{+}$ x $\frac{yw}{Y}$ ; $\frac{Sco}{y^+\ CyO}$ ; $\frac{+}{+}$

$\frac{yw}{yw}$ ; $\frac{P(w^+)}{y^+\ CyO}$ ; $\frac{+}{+}$ x $\frac{yw}{Y}$ ; $\frac{P(w^+)}{y^+\ CyO}$ ; $\frac{+}{+}$

↓

$\frac{yw}{Y}$ $\frac{yw}{yw}$ | $\frac{P(w^+)}{y^+\ CyO}$ | $\frac{+}{+}$

A l'emprar la soca balancejadora *yw; Sco/y*$^{+}$*CyO*, tan en el cas de l'heterozigot com en el cas del control, s'introduïen nous cromosomes X i 3. Per tal d'isogenitzar aquests cromosomes el es va fer el següent: de l'estoc control (*yw; P(w*$^{+}$*)rev/y*$^{+}$*CyO*) es varen seleccionar femelles verges i mascles del genotip adequat i es varen encreuar entre ells. Durant nou generacions, el mínim per assolir consanguinitat dels cromosomes per recombinació (Falconer, 1989), es varen repetir els encreuaments germà-germana. El mateix procés es va seguir amb l'estoc heterozigot (*yw; l(2)k11320/y*$^{+}$*CyO*). Un cop tinguérem el fons genètic equivalent pel control i l'experiment es van dur a terme els experiments de supervivència i longevitat.

***Protocol d'encreuaments dissenyats per tal de dur a terme l'anàlisi de l'efecte de l'expressió ectòpica del gen selD en motoneurones.***

Per tal d'esbrinar l'efecte de l'expressió ectòpica del gen *selD* a motoneurones es va utilitzar el sistema GAL4/UAS (Brand i Perrimon, 1993). Aquest sistema permet l'expressió de gens en el domini d'expressió d'altres gens. Per aconseguir aquesta expressió ectòpica calia disposar de dues línies transgèniques. Una d'elles havia de contenir el gen que codifica per la proteïna GAL4 sota el control del promotor d'un altra gen de *Drosophila*. En el nostre cas, com volíem l'expressió a motoneurones vàrem utilitzar la línia *enhancer trap D42GAL4* (Yeh *et al*., 1995). L'altra línia transgènica contenia el gen *selD* sota el control d'un promotor que conté diverses seqüències d'unió específica UAS per la proteïna GAL4. L'expressió del gen *selD* és silenciosa en absència de GAL4, i en principi, l'expressió de GAL4 no és deletèria per la mosca. Encreuant les dues línies transgèniques s'aconsegueix que els individus que contenen les dues construccions expressin el gen *selD* sota el control de la línia *D42GAL4* a motoneurones.

En aquest experiment també era necessari treballar amb un fons genètic equivalent entre les mosques control (*w/Y; +/+; UASselD/+* i *w/Y; +/+; D42GAL4/+*) i l'experiment (*w/Y; +/+; D42GAL4/UASselD*). Per tal d'assolir aquesta condició es va dissenyar el següent protocol d'encreuaments:

1. En el Departament es disposa d'una soca mutant del gen *white* que ha estat mantinguda durant molts anys en condicions de laboratori. Així era possible que aquella soca fos altament consanguínia, i per tant, convenient per al protocol experimental dissenyat. Dita soca es va encreuar amb un estoc balancejador per tal de d'obtenir mascles portadors d'un cromosoma 2 i un cromosoma 3 de la soca *white*$^{-}$

$$\frac{w}{w} \;;\; \frac{+}{+} \;;\; \frac{+}{+} \quad \text{X} \quad \frac{w}{\text{Y}} \;;\; \frac{If}{CyO} \;;\; \frac{Ly}{TM3}$$

$$\downarrow$$

$$\frac{w}{\text{Y}} \;;\; \frac{+}{CyO} \;;\; \frac{+}{TM3}$$

2. Cada mascle obtingut es va encreuar durant tres dies amb femelles *w; If/CyO; UASselD/TM3* i posteriorment es va encreuar uns altres tres dies més amb femelles *w; If/CyO; D42GAL4/TM3*.
3. De la descendència obtinguda de l'encreuament del mascle per *w; If/CyO; UASselD/TM3* es varen separar les femelles *w; +/CyO; UASselD/TM3* per a utilitzar en un encreuament posterior. Els genotips *w; +/CyO; +/TM3* i *w/Y; +/CyO; UASselD/+* es varen encreuar entre ells per a obtenir mosques control del genotip *w/Y; +/+; UASselD/+* on les dues còpies del cromosoma 2 eren exactament iguals.

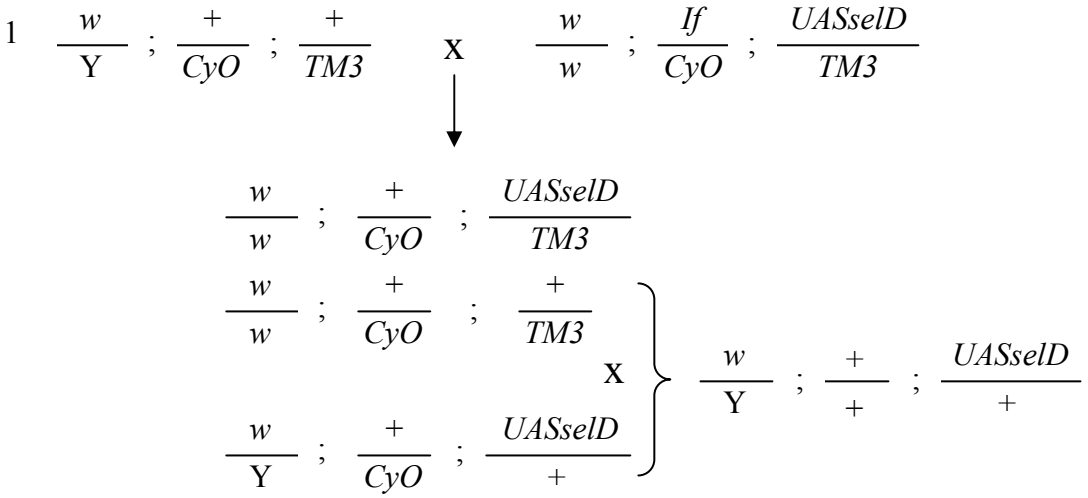


4. De la descendència obtinguda de l'encreuament del mascle per *w; If/CyO; D42GAL4/TM3* es varen separar els mascles *w/Y; +/CyO;D42GAL4/TM3* per a utilitzar en un encreuament posterior. Els genotips *w; +/CyO; +/TM3* i *w/Y; +/CyO; +/D42GAL4* es varen encreuar entre ells per a obtenir mosques control del genotip *w/Y; +/+; D42GAL4/+* on les dues còpies del cromosoma 2 eren exactament iguals, i a més, iguals que les del control *w/Y; +/+; UASselD/+*. Aquests dos controls a més tenien el mateix cromosoma 3.

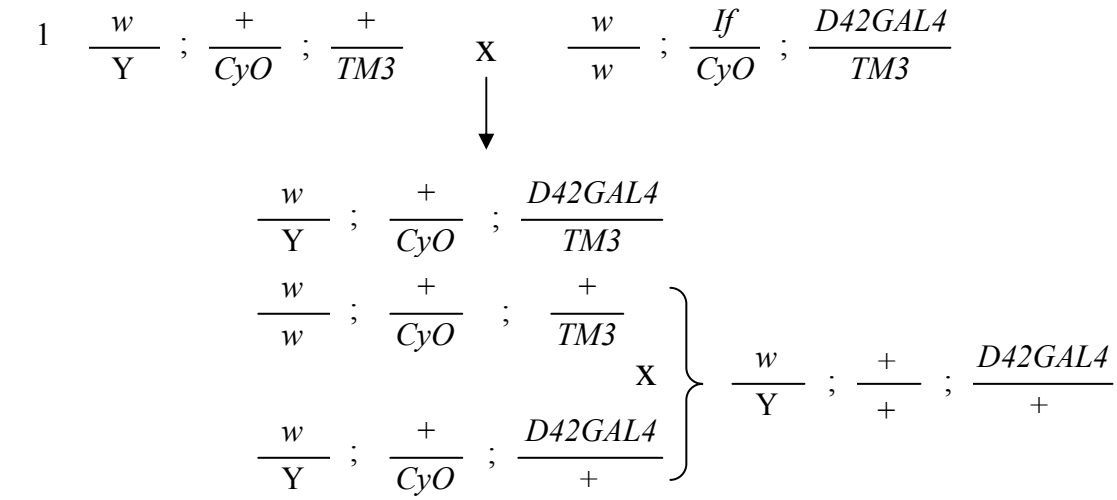


5. Finalment els mascles i femelles separats es varen encreuar i es va seleccionar la descendència portadora tant del transgen *D42GAL4* com del transgen *UASselD*.

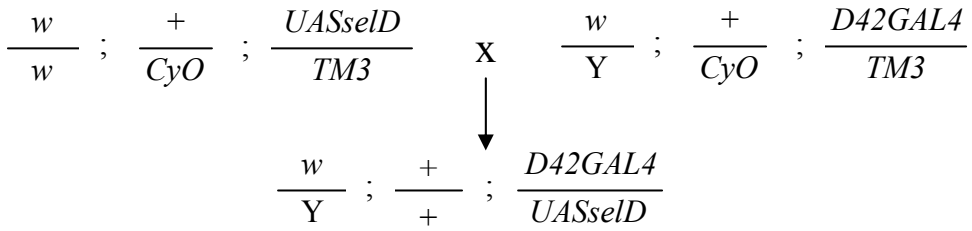


Així, amb aquest seguit d'encreuaments, per cada mascle *w/Y; +/CyO; +/TM3* es varen obtenir mosques control *w/Y; +/+; UASselD/+* i *w/Y; +/+; D42GAL4/+*, i mosques de l'experiment *w/Y; +/+; D42GAL4/UASselD*. En totes elles, el cromosoma salvatge 2 i 3 eren el mateix.

Es varen encreuar al voltant d'uns 40 mascles independents. De 20, després de tots els encreuaments descrits, es varen obtenir mosques dels tres genotips esmentats i aquestes varen ser les mosques utilitzades per a l'estudi de longevitat. Degut a que dels encreuaments per obtenir les mosques control i les mosques de l'experiment s'anaven fent rèpliques, a mida que les mosques del genotip desitjat neixen s'anaven incorporant al protocol de l'experiment de longevitat.

Com s'ha esmentat en començar aquest apartat, en principi, la l'expressió de GAL4 no és deletèria per la mosca. En el cas de la línia *D42GAL4* hem pogut observar que el final de la corba de supervivència el control *D42GAL4* mor abans que el control *UASselD*. Això pareix indicar que una acumulació de GAL4 en motoneurones tindria efectes nocius al llarg del temps.

# CAPÍTOL II

**L'increment de ROS degut a una reducció en la funció antioxidant de les selenoproteïnes indueix apoptosi a través de la via Dmp53/Rpr.**

**Article 3**: Morey, M., Corominas, M. and Serras, F. DIAP1 suppresses ROS-induced apoptosis caused by impairment of selenoprotein function in *Drosophila*. Enviat a *J. Cell Sci.*

### *L'apoptosi a Drosophila*

L'apoptosi o mort cel·lular programada és essencial per a eliminar cèl·lules danyades potencialment perilloses per l'organisme, i és necessària per restringir el nombre de cèl·lules i la mida dels òrgans durant el desenvolupament i la morfogènesi. La importància d'aquest fenomen queda reflectida per la considerable conservació dels elements centrals de la maquinària apoptòtica al llarg de l'evolució des de *Caenorhabditis elegans* fins als mamífers. Alhora, a mida que incrementa la complexitat dels organismes apareixen nous elements i vies per a respondre a diferents tipus d'estímuls apoptòtics. Si més no, les similituds entre l'apoptosi de mamífers i *Drosophila* són moltes (Fig. 18).

Les caspases, una família de cistein proteases, són centrals en la senyalització i execució de l'apoptosi. Les caspases iniciadores oligomeritzen en un apoptosoma i s'autoactiven per proteolisi creuada. Un cop activades inicien una cascada de processament i activació de les caspases efectores, el que desembocarà en la proteòlisi de substrats i la mort cel·lular (Thornberry i Lazebnik, 1998). Dues són les vies d'activació de les caspases descrites a mamífers. La "via intrínseca" s'activa en resposta a estímuls primaris intrínsecs a la cèl·lula. Aquests, poden induir la permeabilització de la membrana mitocondrial externa, mitjançant l'alteració de l'equilibri entre els membres pro- i anti- apoptòtics de la familia Bcl2, alliberant al citosol el factor proapoptòtic mitocondrial citocrom *c* que és un dels components de l'apoptosoma d'aquesta via. També existeix una "via extrínseca" d'apoptosi que respon a les senyals instructives que provenen del context cel·lular. Aquesta mort cel·lular es fa efectiva mitjançant l'activació de la família de receptors de la mort del TNF (Tumor Necrosis Factor). En aquest cas, l'activació de les caspases iniciadores es du a terme per la formació d'un apoptosoma, independent de citocrom *c*, en la regió intracel·lular de dits receptors. Certes evidències que indiquen que hi podria haver *crosstalk* entre les via intrínseca i extrínseca (Green, 2000).

L'activació de caspases per la via intrínseca a *Drosophila* procedeix de la següent manera. L'estímul apoptòtic intracel·lular causa l'alteració de la membrana mitocondrial, possiblement a través de l'acció dels membres pro- i anti- apoptòtics de la familia Bcl2, i es dona l'exposició del citocrom *c* al citosol (Varkey *et al*., 1999). La seva unió a la molècula adaptadora Dark, recluta la caspasa iniciadora facilitant la seva oligomerització i autoactivació. Una vegada activada, aquesta activa les caspases efectores (Dorstyn *et al*., 2002). Com la proteòlisi és irreversible, l'activació de les caspases ha d'estar molt ben regulada. Així, en condicions normals, la proteïna inhibidora de l'apoptosi 1 (DIAP1) inhibeix l'acció de les caspases unint-se directament a elles (Wang *et al*., 1999; Meier *et al*., 2000). Per tal de superar la barrera que imposen els IAPs a l'activació de les caspases,

l'estímul apoptòtic, també activa les proteïnes inductores de l'apoptosi Reaper (Rpr), Head involution defective (Hid) i Grim. Dites proteïnes s'uneixen als DIAPs, alliberant a les caspases i permetent la seva acció (Wang *et al*., 1999; Goyal *et al*., 2000; Wu *et al*., 2001). D'altra banda també ubiquinitzen DIAP1 promovent la seva degradació via proteasoma i inhibeixen la traducció dels seus transcripts (Holley *et al*., 2002; Ryoo *et al*., 2002; Yoo *et al*., 2002). Recentment, també s'han identificat els elements de la via extrínseca a *Drosophila*. Eiger i Wengen són respectivament, el lligand TNF i el seu receptor (Igaki *et al*., 2002; Kanda *et al*., 2002; Moreno *et al*., 2002). A diferència dels mamífers, l'activació de caspases no seria directa per sota del receptor, sino indirecta mitjançant l'activació de la via JNK i depenent de l'apoptosoma citocrom *c*/Dark (Moreno *et al*., 2002). Per tant, des de el punt de vista d'activació de les caspases, seria una via intrínseca.

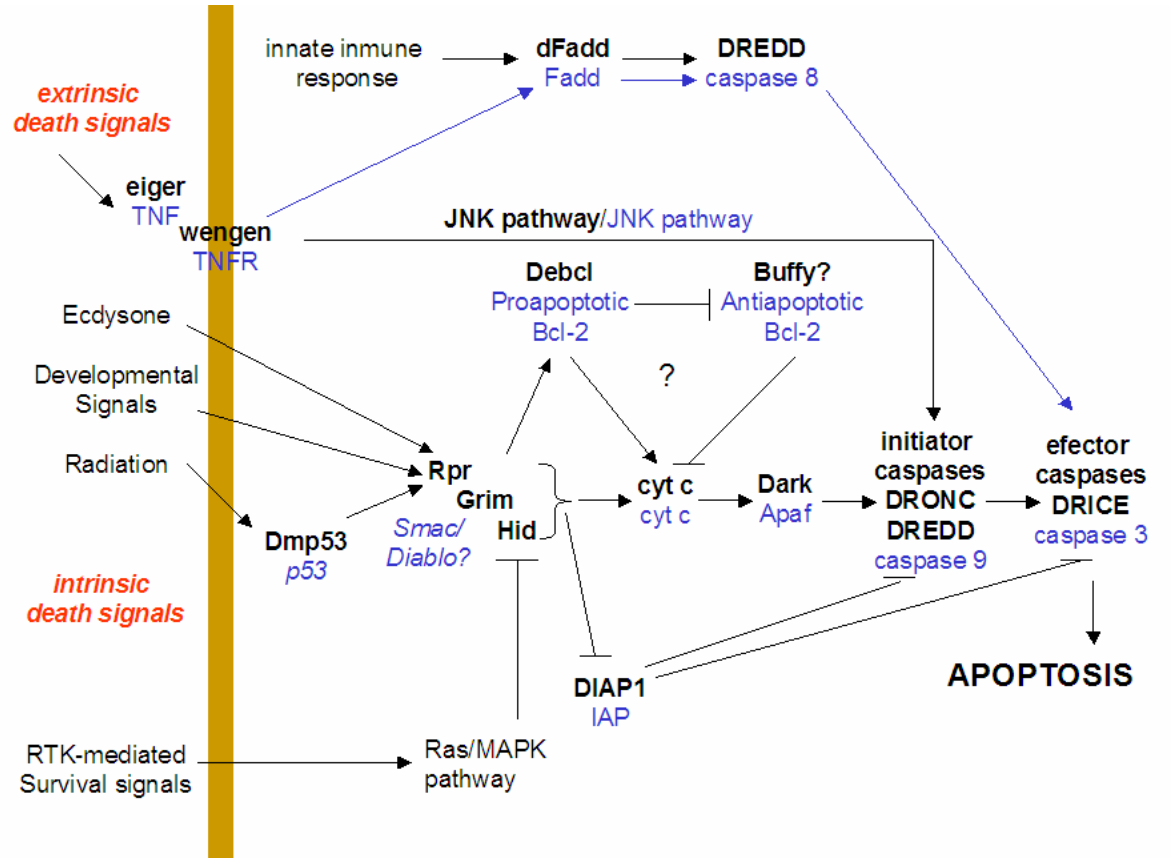


Fig. 18. Comparació de l'apoptosi a mamífers (components en blau) i *Drosophila* (components en negre). Cal destacar que la funció dels elements de la familia Bcl-2 a Drosophila no es coneix tant com a mamífers. La via dels receptors de la mort ha estat recentment identificada a *Drosophila* i de moment sols s'ha demostrat que activa l'apoptosi a través de l'activació de la via JNK, mentre que a mamífers també activa la caspasa 8 que és la caspasa especifica de la via extrínseca (adaptat de Richardson i Kumar, 2002).

Molts treballs han descrit les interaccions entre els diferents components apoptòtics a *Drosophila*, però, malgrat l'esforç, el coneixement de com diferents estímuls apoptòtics cel·lulars convergeixen per activar una mateixa via comú, la via intrínseca, és més reduït. El tres gens inductors de l'apoptosi, *rpr*, *grim* i *hid*, tenen patrons d'expressió diferents. Tant *rpr* com *grim* s'expressen en cèl·lules destinades a morir (White *et al*., 1994). Al

contrari, *hid* s'expressa no sols a cèl·lules que moriran sinó també a cèl·lules que viuran (Grether *et al*., 1995). Això fa pensar que integren diferents senyals apoptòtiques.

Senyals de supervivència regulen l'apoptosi a *Drosophila*, doncs s'ha vist que la l'activitat de la via Ras/MAPK és necessària per a la supervivència cel·lular (Simon *et al*., 1991; Diaz-Benjumea i Hafen, 1994; Freeman 1996; Miller i Cagan 1998; Sawamoto et al 1998; Baker i Yu, 2001; Halfar *et al*., 2001; Bergmann *et al*., 2002). El nexe amb la maquinària apoptòtica s'ha trobat: Hid és un sensor de l'activitat de la via Ras/MAPK. Conseqüentment, en la població de cèl·lules que moriran i que expressen *hid*, la downregulació d'aquesta via incrementa la expressió *hid* i la seva activitat (Bergmann *et al*., 1998; Kurada i White, 1998).

En el cas de *rpr*, la seva expressió s'ha vist associada a mort programada pel desenvolupament durant la metamorfosi i la diferenciació del sistema nerviós (Jiang *et al*., 2000; Peterson *et al*., 2002), però també com a resposta a desenvolupament aberrant i als rajos X (White *et al*., 1994; Nordstrom *et al*., 1996; Brodsky *et al*., 2000). Un element de resposta al dany genotòxic causat per la radiació X s'ha identificat en el promotor de *rpr* i s'ha demostrat que la unió de l'homòleg de p53 a *Drosophila* (Dmp53) activa la transcripció de *rpr* en aquesta situació (Brodsky *et al*., 2000).

**Precedents**

A mamífers, tan la deprivació de factors tròfics com un increment en el nivell de radicals lliures són capaces de causar la mort cel·lular per apoptosi, tanmateix es coneix poc de com aquestes situacions activen la maquinària apoptòtica. L'apoptosi i l'acumulació de radicals lliures són una característica del mutant homozigot $selD^{ptuf}$ (Alsina *et al*., 1998; 1999). També hem demostrat que l'increment del ROS causat per la mutació $selD^{ptuf}$ és el responsable de la modulació negativa de la via Ras/MAPK (Article 1: Morey *et al*., 2001). Una possibilitat és que l'activitat reduïda de la via Ras/MAPK expliqui l'apoptosi observada. Tanmateix, l'acumulació de radicals lliures podria engegar l'apoptosi per altres vies. Així doncs, vàrem voler testar la contribució d'aquestes dues opcions a l'apoptosi observada en el mutant $selD^{ptuf}$.

**Resum**

L'ull de *Drosophila* és un sistema excel·lent per a entendre els mecanismes que coordinadament promouen la supervivència i diferenciació dels omatidis. A més, s'han descrit nombrosos marcadors moleculars per a testar les diferents etapes del procés de diferenciació. La via Ras/MAPK està involucrada tan en la supervivència com en la diferenciació de les cèl·lules de l'omatidi, així doncs, per tal de veure si la reducció en la seva activitat era la responsable de l'apoptosi observada es varen generar clons de cèl·lules mutants $selD^{ptuf}$ a l'ull. L'anàlisi dels clons en l'ull adult i en el disc imaginal va mostrar que la diferenciació i la supervivència estan afectades. A més a més, aquests efectes estan associats a la presència de radicals lliures. Si la modulació negativa de la via Ras/MAPK causada per la mutació $selD^{ptuf}$ fos la responsable de l'apoptosi observada, aquesta hauria de ser activada pel gen proapoptòtic *hid*. Per tant, vàrem testar si la mutació $selD^{ptuf}$ era capaç de modular l'activitat de Hid però els nostres resultats no han mostrat cap interacció

genètica. Sense descartar una possible contribució d'aquesta via a l'apoptosi del mutant *selD*$^{ptuf}$, l'apoptosi semblava ser deguda a l'activació d'una altra via.

El gen proapoptòtic *rpr* era un bon candidat ja que integra diferents tipus de senyals apoptòtiques. Així, es va poder mostrar que aquest gen s'expressa en les cèl·lules mutants *selD*$^{ptuf}$. També s'ha detectat l'acumulació de la proteïna Dmp53, reconegut sensor del dany genotòxic. D'aquesta manera, podem explicar com l'increment de radicals lliures, que poden causar dany al DNA, activa la transcripció de *rpr* ja que s'ha demostrat que aquest té un lloc d'unió de Dmp53 en el seu promotor. Consistent amb que l'activació de *rpr* dona lloc a apoptosi depenent de caspases, hem mostrat la intervenció tant de la caspasa iniciadora DRONC com de la seva efectora DRICE. Alhora, l'expressió ectòpica de l'inhibidor d'apoptosi DIAP1 és capaç de rescatar de manera important la viabilitat del les cèl·lules *selD*$^{ptuf}$. Tot plegat, la presència de radicals lliures, la detecció de Dmp53, l'observació de que DRICE també està involucrada en l'apoptosi causada per l'expressió ectòpica de *Dmp53*, i el rescat observat amb DIAP1, suporten que l'activació de la via depenent de caspases Dmp53/Rpr té una contribució important a l'apoptosi observada en el mutant *selD*$^{ptuf}$.

# *DIAP1* suppresses ROS-induced apoptosis caused by impairment of selenoprotein function in *Drosophila*

Marta Morey, Montserrat Corominas and Florenci Serras
Departament de Genètica, Facultat de Biologia, Universitat de Barcelona,
Diagonal 645, 08028 Barcelona, Spain

**Short title**: DIAP1 suppresses ROS-induced apoptosis
**Keywords**: reaper, p53, DIAP1, selD, selenoprotein, ROS

**Corresponding author**: Florenci Serras.
Departament de Genètica, Facultat de Biologia, Universitat de Barcelona,
Diagonal 645, 08028 Barcelona, Spain
Phone: 34 934037003
FAX: 34 93 4110969
e-mail: fserras@ub.edu

## Summary

The cellular antioxidant defense systems neutralize the cytotoxic byproducts referred to as reactive oxygen species (ROS). Among them, selenoproteins have important antioxidant and detoxification functions. The interference in selenoprotein biosynthesis results in accumulation of ROS and consequently in a toxic intracellular environment. The resulting ROS imbalance can trigger apoptosis to eliminate the deleterious cells. In *Drosophila*, a null mutation in the *selD* gene (homologous to the human *selenophosphate synthetase type 1*) causes an impairment of selenoprotein biosynthesis, ROS burst and lethality. We propose this mutation (known as $selD^{ptuf}$) as a tool to understand the link between ROS accumulation and cell death. To this aim we have analyzed the mechanism by which $selD^{ptuf}$ mutant cells conduct the apoptotic machinery in *Drosophila* imaginal discs. The apoptotic effect of $selD^{ptuf}$ does not require the activity of the Ras/MAPK-dependent pro-apoptotic gene *hid*, but results in stabilization of the tumor suppressor protein Dmp53 and transcription of the *Drosophila* pro-apoptotic gene *reaper* (*rpr*). We also provide genetic evidence that the initiator caspase DRONC is activated and that the effector caspase DRICE is processed to commit $selD^{ptuf}$ mutant cells to death. Moreover, the ectopic expression of the inhibitor of apoptosis DIAP1 rescues the cellular viability of $selD^{ptuf}$ mutant cells. These observations indicate that $selD^{ptuf}$ ROS-induced apoptosis in *Drosophila* is mainly driven by the caspase dependent Dmp53/Rpr pathway.


## Introduction

Apoptosis is an essential cellular process during the morphogenesis of multicellular organisms and its genetic control has become one of the main topics of study for developmental and cell biologists. However, it is not yet well understood how certain processes such as oxidative stress can trigger specific pathways of apoptosis. Aerobic metabolism uses molecular oxygen as a terminal electron acceptor for mitochondrial respiratory energy production. As byproducts of this process reactive oxygen species (ROS) are generated. These are a variety of oxygen metabolites that have either unpaired electrons (i.e. $O_2^-$, $OH\cdot$) or the ability to abstract electrons from other molecules such as hydrogen peroxide Transient fluctuations in ROS serve important regulatory functions, but when present at high and/or sustained levels, they can cause severe damage to DNA, proteins and lipids, which may finally lead to apoptosis (Simon et al., 2000; Curtin et al., 2002).

A number of defense systems have evolved to counteract the persistent state of oxidative siege associated to aerobic life conditions and among them enzymatic intracellular scavengers play an essential role. In this category, selenoproteins, which contain selenium in the form of selenocysteine, are important to control the unwanted ROS as most of them catalyze oxidation-reduction reactions or act as antioxidants (Stadtman, 1996; Rayman, 2000; Hatfield and Gladyshev 2002). We have used a mutation in *Drosophila melanogaster* that perturbs selenoprotein biosynthesis and results in ROS accumulation to understand how a persistent increase in ROS can induce apoptosis (Alsina et al., 1999). *Drosophila* $selD^{ptuf}$ is a recessive mutation affecting a gene encoding for an enzyme involved in selenoprotein biosynthesis: the *selenophosphate synthetase type 1* (*sps1* in humans or *selD* in flies). Homozygous individuals lack selenoproteins and die at

third instar larvae. Consistent with the role of selenoproteins as antioxidants, mutant cells accumulate free radicals and enter apoptosis resulting in extremely reduced and abnormal imaginal discs (Alsina et al, 1998; 1999). Heterozygous *selD*$^{ptuf}$ flies are apparently wild type, however, a downregulation of the Ras/MAPK pathway has been observed in transheterozygous combinations of *selD*$^{ptuf}$ mutant and activated members of this signaling pathway (Morey at al, 2001). This downregulation seems to be a consequence of an increase in ROS levels due to selenoprotein biosynthesis impairment in heterozygous flies (Morey at al., 2001; 2003). Both loss of survival signals and perturbations in the redox balance, among others, are intracellular stimuli that have been shown to trigger apoptosis in mammals (Kroemer and Reed, 2000; Adrain and Martin, 2001). In *Drosophila*, the cell death genes *reaper* (*rpr*), *head involution defective* (*hid*) and *grim* are potent activators of caspase dependent apoptosis (reviewed in Richardson and Kumar 2002). Extensive research has been carried out to uncover how distinct death-inducing stimuli converge to activate a common apoptotic program. Both *rpr* and *grim* are expressed in cells doomed to die (White at al., 1994; Chen et al., 1996). In contrast, *hid* is expressed not only in cells which die, but also in living cells (Grether et al., 1995). Thus, these different expression patterns imply that they integrate different signals regulating apoptosis. Survival signals regulate *Drosophila* apoptosis and several studies have shown the need of Ras/MAPK activity for cell survival in flies (Simon et al., 1991; Diaz-Benjumea and Hafen, 1994; Freeman, 1996; Miller and Cagan 1998; Sawamoto et al., 1998; Halfar et al, 2001). In the subset of *hid*-expressing cells prone to die, downregulation of the Ras/MAPK pathway increases *hid* expression and activity (Bergmann et al. 1998; Kurada and White, 1998). In the case of *rpr*, besides inducing developmentally programmed cell death, it also triggers apoptosis in response to other stimuli such as aberrant development, steroid hormone signaling and X-irradiation (Asano et al., 1996; Nordstrom et al., 1996, Robinow et al., 1997). *rpr* is also a transcriptional target of the *Drosophila* p53 protein, making its expression responsive to genotoxic stress caused by X-irradiation (Brodsky et al., 2000). Because X-irradiation, in addition to direct DNA damage, generates ROS in the aqueous cytoplasm that can also damage DNA, the Dmp53/Rpr pathway is a candidate pathway to be activated in a situation of increased ROS levels such as in the *selD*$^{ptuf}$ mutant.

Herein, we have taken a genetic approach to study how an increase in ROS levels due to a reduction of selenoproteins' antioxidant function triggers apoptosis in *Drosophila* imaginal discs. Our results indicate that *hid* induced apoptosis may not be the major contributor to the apoptosis observed in *selD*$^{ptuf}$ mutant cells and that ROS increase plays an important role in *selD*$^{ptuf}$ apoptosis through the activation of the Dmp53/Rpr pathway. We clearly show that this apoptotic pathway is mediated by DRONC and DRICE caspases and that the inhibitor of apoptosis DIAP1 is able to rescue the viability of *selD*$^{ptuf}$ cells. This work supports the importance of selenoproteins in the maintenance of cellular viability and demonstrates that ROS-induced apoptosis triggered by selenoprotein-depletion is caspase dependent and activated by Dmp53/Rpr function.

# Material and Methods

### *Drosophila* stocks

The *selD*$^{ptuf}$ line (*yw; l(2)k11320/CyO*) was obtained from a collection of lethal mutants resulting from *PlacW* insertions on the second chromosome (Torok et al., 1993; Alsina et al., 1998). The following stocks were used: *yw; Cat*$^{n1}$*/TM3* (Mackay and Bewley, 1989; Griswold et al, 1993); *e ftz ry/TM3 P(sev-rasV12)* (Fortini et al., 1992); *Sco/SM1 P(GMRhid)* (Kurada and White, 1998); *GMRyan*$^{Act}$ on the second chromosome (Rebay and Rubin, 1995); *rprlacZ* on the third chromosome (Nordstrom et al., 1996); *UAS-DIAP1/TM2* (Lisi et al, 2000); *GMR-GAL4 UAS-dronc #80* (*GMR-GAL4 UAS-dronc/CyO; UAS-dronc)* (Quinn et al., 2000); *UAS-Sem* on the third chromosome (Martin-Blanco, 1998); *+; gl-Dmp53/SM6aTM6B* (Ollman et al., 2000; Exelixis Inc.); *hh-GAL4/TM2* (Tanimoto et al., 2000); *2xarm-GAL4/TM3Sb*, *69B-GAL4* on the third chromosome (Bloomington Stock Center).

### Scanning electron microscopy

To prepare scanning electron microscopy (SEM) samples, flies were dehydrated in 25, 50, 75 and 100% ethanol for 24 hours each. Flies were critical point dried and coated with gold to be examined in a Leica-360 scanning electron microscope.

### Generation of mitotic clones

*selD*$^{ptuf}$ clones in the adult eye were generated using the *ey*FLP/FRT technique coupled to a cell lethal mutation (*cl2R11*, Newsome et al., 2000), which kills the twin clone allowing the growth of more mutant tissue. Adults of the genotype *yw eyFLP; FRT42D w+ cl2R11/FRT42D selD*$^{ptuf}$ were examined for mutant clones (two copies of the *mini-w* marker from the *PlacW* insertion in *selD* locus in a *mini-w/ w+* background) in the eye. Histological sections of the eyes were performed as described previously (Basler and Hafen, 1988).

*selD*$^{ptuf}$ mitotic clones in imaginal discs were generated using the *hs*FLP/FRT technique (Xu and Rubin, 1993) in combination with the *Minute* (*M*) technique (Morata and Ripoll, 1975), which gives proliferative advantage to the mutant tissue minimizing perdurance of *selD* product. Larvae of the *yw hsFLP; FRT42D arm-lacZ M/FRT42D selD*$^{ptuf}$ genotype were heat shocked at 60 hours after egg laying (AEL) for 30 minutes at 34$^{o}$C. For *rpr* transcription in *selD*$^{ptuf}$ clones, 60 hours AEL larvae of *yw hsFLP; FRT42D πMyc M/FRT42D selD*$^{ptuf}$*; rpr-lacZ/+* genotype were heat shocked for 1hour at 37$^{o}$C and πMyc was induced as described previously (Xu and Rubin, 1993). In these experiments the homozygous mutant tissue is marked by the absence of β-galactosidase or πMyc staining.

To determine the clonal size in wing discs, clones were induced by 10 minutes heat shock pulse at 34$^{o}$C in *yw hsFLP; FRT42D arm-lacZ/FRT42D selD*$^{ptuf}$*; hh-GAL4/UAS-DIAP1* larvae (4 hours egg collections) at 55 hours AEL and analyzed at 120 hours AEL.

### Inmunohistochemistry

Imaginal discs from third instar larvae were dissected in PBS and fixed for 20min in 4% paraformaldehyde (PFA) at room temperature (for β-galactosidase staining) or PLP (2% PFA, 75mM Lysine; 10mM sodium periodate, 37mM sodium phosphate) at 4ºC (for πMyc

staining). Following permeabilization, overnight incubation was performed with primary antibodies: rabbit anti-β-galactosidase 1:1000 (Cappel), mouse anti-β-galactosidase 1:250 (Promega) or mouse anti-πMyc 1:1000 (Babco) to mark clones, and mouse anti-Boss (Cagan et al., 1992) 1:2000 (a gift from S.L. Zipursky), mouse anti-Elav (Robinow and White, 1988) 1:100 (from DSHB), mouse anti-Dmp53 (Ollmann et al., 2000) 1:250 (Exelisis Inc.), rabbit anti-active DRICE (Dorstyn et al., 2002) 1:1000 (a gift from B. Hay) and mouse anti-FASIII (Brower and Jaffe, 1989) 1:1000 (a gift from D. Brower). Rhodamine Red and FITC conjugated secondary antibodies 1:200 (Jackson ImmunoResearch) were used. YOYO® nuclear marker (1:5000, Molecular Probes, Inc.) was added together with the secondary antibody. Discs were mounted in Slowfade® Light antifade (Molecular Probes, Inc.) and images collected on a Leica TCS 4D confocal laser scanning microscope. Negative controls for these antibodies in *selD$^{ptuf}$* discs and clones were performed in parallel and scanned under the same conditions and showed no staining. All images were processed with Adobe Photoshop 6.0. and ImageJ 1.29v (National Institute of Health, USA).

**TUNEL assay in *selD$^{ptuf}$* clones**

After fixation of *yw hsFLP; FRT42D arm-lacZ M/FRT42D selD$^{ptuf}$* discs, apoptotic cells were detected by labeling the 3'-OH ends of DNA with Chromatide BODIPY® Texas Red-14-dUTP (Molecular Probes, Inc.) for 1 hour 30 minutes at 37$^{o}$C using terminal deoxynucleotidyl transferase (Roche). Primary and secondary antibodies were used to detect clones as described above.

**In vivo detection of ROS in *selD$^{ptuf}$* clones**

Clones to test for accumulation of ROS were generated in *yw hsFPL; FRT42D GFP/FRT42D selD$^{ptuf}$* larvae after heat shock at 48 hours AEL for 30 minutes at 34$^{o}$C. Third instar larvae discs were dissected in Schneider's medium. Staining was performed in medium containing 20μM dihydroethidium (DHE, Molecular Probes, Inc.) for 5 minutes and a series of washes in Schneider's medium were performed protecting the sample from light before mounting in antifade solution. Analysis of the sample with confocal microscopy was done just after mounting.

# Results and Discussion

The *Drosophila* eye development is a paradigm to understand the cellular mechanisms that coordinately promote cell differentiation and survival. During larval development, cell-to-cell interactions in the eye imaginal disc shape the ommatia, the units that form the insect compound eye. The Ras/MAPK pathway controls differentiation and survival of ommatidial cells (Freeman 1996; Halfar et al., 2001), and a wide variety of molecular markers are available to verify these processes. Besides, the role of apoptosis in shaping the eye has been extensively described (Brachmann and Cagan, 2003). We have used the eye imaginal disc as a model to explore how apoptosis is triggered in oxidative stress conditions. We first tested whether *selD$^{ptuf}$* homozygous condition perturbs cell survival and/or normal differentiation in the developing eye. Because the homozygous *selD$^{ptuf}$* individuals are lethal (Alsina et al., 1998; Roch et al., 1998), we have analyzed the mutant condition in genetic mosaics. Clones of *selD$^{ptuf}$* mutant cells were generated in the eye disc

and recovered to adulthood. These clones resulted in scarred tissue with poor ommatidial differentiation (Fig. 1A). Tangential sections revealed that none or very few photoreceptors were present in the mutant area, suggesting that extensive cell death had occurred during the development of the mutant sector (Fig.1B). We also analyzed if recruitment and differentiation of photoreceptor cells was taking place. Although the R8 photoreceptor specific marker Boss revealed that R8 differentiation and spacing occurred properly (data not shown), the recruitment of the following photoreceptors was disrupted as revealed by the pattern of Elav neuronal marker (Fig. 1C). Mutant ommatidia contained less cells than their neighboring wild type heterozygous ones. Besides aberrant ommatidial organization, the epithelial condition of $selD^{ptuf}$ was severely disrupted. As it has been described that disorganization and loss of polarity in epithelial tissues precedes cell death (Tepass et al., 1990), we checked for apoptosis and indeed detected a significant increase in apoptotic cells within $selD^{ptuf}$ clones after TUNEL staining. Interestingly, ectopic apoptotic figures were also observed in the neighboring wild type cells, suggesting a non autonomous effect of $selD^{ptuf}$ mutation (Fig.1D).

We next examined if the impairment of cell differentiation and survival in clones of $selD^{ptuf}$ homozygous mutant cells was associated to a detectable burst of ROS. For that purpose, we used the ROS specific nuclear probe dihydroethidium (DHE). This probe specifically detects superoxide anion ($O_2^-$), a primary oxygen free radical produced by mitochondria rapidly removed by conversion to hydrogen peroxide. Upon an in vivo burst of $O_2^-$, DHE oxidizes to ethidium and incorporates into the nuclear DNA emitting fluorescence (Molecular Probes, Inc.). Certainly, some cells in $selD^{ptuf}$ clones accumulated ROS, as shown by nuclear DHE staining. In addition to that, DHE positive cells were detected in wild type cells adjacent to the clone (Fig. 1E). This could explain the presence of apoptotic cells bordering the clone. ROS are very small molecules that can freely diffuse through cell membranes and after an accumulation in the clone the surrounding heterozygous tissue acts as a sink diluting this accumulation. To confirm that ROS accumulation was the cause and not a consequence of apoptosis, we performed the DHE assay on discs in which apoptosis was ectopically induced by constitutively expression of an inductor of apoptosis (*GMRhid* expressing discs, see below). In those discs no DHE labeling was observed (data not shown) reinforcing the role of ROS in inducing apoptosis.

Because Ras/MAPK downregulation due to ROS increase has been observed in $selD^{ptuf}$ heterozygous conditions (Morey et al., 2001), apoptosis through *hid* could account for cell death in $selD^{ptuf}$ homozygous mutant. To address this question, we checked for enhancement of ectopically expressed *hid* phenotype under the control of the eye-specific *glass* multimer reporter (pGMR, Hay et al., 1994) after removing one copy of *selD*. Flies carrying one copy of *GMRhid* have severely reduced eyes devoid of most normal ommatidial morphology due to massive apoptosis in the eye disc (Fig. 2B; Grether et al., 1995). The reduction of one dose of *selD*, or of *Catalase* (as a selenoprotein independent source of ROS) did not enhance *GMRhid* phenotype (Fig. 2C). Even the combination of $selD^{ptuf}$ and $Cat^{n1}$ mutants in transheterozygosis could not enhance the *GMRhid* phenotype (Fig. 2D), whereas that combination is able to suppress a strong constitutively activated *rasV12* construct (Fig. 2I-J; Fortini et al., 1992). As it is likely that the *GMRhid* phenotype is too strong to detect an enhancement, we generated flies *GMRhid sev-rasV12* to get a

weaker apoptotic phenotype (Fig. 2E; Bergmann et al., 1998; Kurada and White, 1998). Again, neither reduction of one dose of *selD*, nor of *catalase*, enhanced the rough eye phenotype of the *GMRhid sev-rasV12* background (Fig. 2F). In addition, we have performed a genetic interaction with an activated form of *yan* (*GMRyan$^{Act}$*), a negative regulator of the Ras/MAPK pathway. Overexpression of *yan* in the developing eye induces apoptosis (Fig. 2G; Rebay and Rubin, 1995), and increases *hid* mRNA levels (Kurada and White, 1998). *GMRyan$^{Act}$* eyes display a milder phenotype than the *GMRhid* ones, but no enhancement was observed by reduction of one dose of *selD* (Fig. 2H). In addition to that, ectopic expression of a gain of function allele of the MAPK *rolled* locus (*rl$^{sem}$*) under different drivers (*69B-GAL4* and *arm-GAL4*) does not rescue imaginal disc morphology in homozygous mutants at any time during larval development (data not shown). Together these results indicate that the impairment of the Ras/MAPK pathway may not be the main cause of *selD$^{ptuf}$* apoptosis and suggested that other apoptotic inducers could be involved.

Several signaling pathways converge to activate a cell-death program triggered by the pro-apoptotic gene *reaper* (White et al., 1994; Asano et al., 1996; Nordstrom et al., 1996; Brodsky et al., 2000). It is known that in mammals ROS can induce apoptosis (Buttke and Sandstrom, 1994; Simon et al., 2000) thus we tested if the increase in ROS caused by *selD$^{ptuf}$* mutation would trigger apoptosis through *rpr*. Indeed, we found *rpr* transcription in *selD$^{ptuf}$* homozygous discs using a *rpr-lacZ* reporter. Widespread β-galactosidase staining was observed throughout the mutant disc (Fig. 3A). Moreover, *rpr* expression was observed in clones of *selD$^{ptuf}$* homozygous mutant cells in both the wing and eye imaginal discs (Fig. 3B-C). In cell cultures ROS can activate the tumor suppressor protein p53, a sensor of genotoxic stress (Yin et al., 1998; Kitamura et al., 1999; Buschmann et al., 2000). As a transcription factor, one of the critical roles of p53 is to regulate the expression of genes involved in eliminating damaged cells via apoptosis. Activation of *p53* occurs largely through posttranslational mechanisms that enhance its stability and DNA binding activity, making possible the transcription of its targets (Burns and ElDeiry, 1999; Sionov and Haupt, 1999). *Drosophila melanogaster* p53 protein (Dmp53; Brodsky et al., 2000; Jin et al., 2000; Ollman et al., 2000) targets a radiation responsive enhancer at the *rpr* locus (Brodsky et al., 2000). It has been shown that targeted transcription of *rpr* rapidly causes wide spread ectopic apoptosis (White et al., 1996). In fact, overexpression of *Dmp53* in the eye causes apoptosis and gives rise to viable adults that have small rough eyes due to massive apoptosis in the eye disc (Brodsky et al., 2000; Jin et al., 2000; Ollman et al., 2000). Nuclear stabilization of Dmp53, in cells of the eye disc overexpressing *Dmp53* under the *glass*-responsive enhancer elements (*gl*, Moses and Rubin, 1991), can be detected with anti-Dmp53 antibody (Fig. 4A-B; Ollman et al., 2000). Accordingly, we have detected *rpr* transcription in *gl-Dmp53* expressing cells, as shown by double staining of anti-Dmp53 and *rprlacZ* (Fig. 3D). We wondered whether *rpr* transcription observed in *selD$^{ptuf}$* mutant cells was associated to Dmp53. In *selD$^{ptuf}$* homozygous discs, widespread Dmp53 stabilization was detected with anti-Dmp53. This accumulation is characterized by a punctate pattern throughout the whole imaginal disc (Fig. 4C) and localized into the nuclei (Fig. 4D), which is in agreement with the function of p53 as a transcription factor.

In most cases, apoptotic cell death culminates in the activation of the caspase family of cysteine proteases, leading to the orderly dismantling and elimination of the cell. Caspases are central components of the apoptotic machinery induced by the pro-apoptotic genes. The *Drosophila* initiator caspase DRONC (Dorstyn et al., 1999) has been shown to be necessary in *rpr*-induced apoptosis (Hawkins et al., 2000; Meier et al., 2000; Quinn et al., 2000). Likewise, DRONC induces cell death in a dose dependent manner when ectopically expressed in the developing eye under the *GMR* promoter (Meier et al., 2000; Hawkins et al., 2000; Quinn et al., 2000). Adult flies exhibit slightly rough and mottled eyes, due to ablation of photoreceptors and pigment cells (Fig. 5A; Meier et al., 2000). To test the involvement of this caspase in ROS-induced apoptosis, we performed a series of crosses using the $selD^{ptuf}$ mutant as well as a mutation in the *catalase* gene ($Cat^{n1}$) as an example of ROS production in a *selD*-independent mode. Reduction of one dose of *selD* enhanced the mottled-eye phenotype as deduced from the presence of wider areas of *white* tissue (Fig. 5B). The same result was obtained when one dose of *catalase* was removed, reinforcing the idea that an increase in ROS levels might be responsible for $selD^{ptuf}$ apoptosis (Fig. 5C). Moreover, when removing one dose of both *catalase* and *selD* this phenotype became even more severe (Fig. 5D).

DRICE is an effector caspase essential for apoptosis in *Drosophila* cells activated by *rpr* overexpression (Fraser and Evan, 1997; Fraser et al., 1997). It has been shown to physically interact with and to be processed by the initiator caspase DRONC, thus being one of its downstream targets (Meier et al, 2000). We assessed the involvement of DRICE caspase in $selD^{ptuf}$ apoptosis using the processed DRICE-specific antibody (Dorstyn et al., 2002) as a marker for active DRICE. In $selD^{ptuf}$ homozygous mutant imaginal discs we found active DRICE in several cells (Fig. 5E). Accordingly, in $selD^{ptuf}$ clones in the wing and eye imaginal discs we found DRICE in some of the mutant cells (Fig. 5F). Interestingly, we also found non-autonomous labeling of DRICE, as shown by non-mutant cells adjacent to the mutant clone. This observation is in agreement with the previous observation that ROS and apoptotic cells can be also found non-autonomously. Importantly, we have also detected active DRICE in *gl-Dmp53* discs (Fig. 5G), which reinforces the idea that $selD^{ptuf}$ apoptosis is mediated through Dmp53/Rpr caspase dependent pathway.

Since caspases promote and amplify proteolysis cascades, the inhibitor of apoptosis proteins (IAP) provides a critical barrier to impede apoptosis through direct binding and inhibition of caspases (reviewed in Hay, 2000). Thus, apoptotic stimuli could induce cell death through degradation of IAP's. It has been shown that *rpr* can negatively regulate the levels of the *Drosophila IAP1* (*DIAP1*) to trigger apoptosis (Goyal et al., 2000; Holley et al., 2002; Yoo et al., 2002). The inhibition of DRONC and DRICE caspases by DIAP1 has also been extensively demonstrated (Kaiser et al., 1998; Meier et al., 2000; Hawkins et al., 2000; Quinn et al., 2000). To confirm that $selD^{ptuf}$ apoptosis is caspase dependent, we misexpressed the *Drosophila IAP1* (*DIAP1*) to block caspase activity and test for viability rescue. The analysis was performed in the wing imaginal disc since divisions occur throughout the whole disc, whereas in the eye disc the pattern of cell divisions changes along the anterior-posterior axis which renders a statistical analysis difficult. By using *hh-Gal4* as a driver, *DIAP1* can be ectopically expressed in the posterior compartment, and the

anterior compartment can act as a control in the same imaginal disc. We generated twin clones (i.e. wild type control *selD*$^{+}$ clone and *selD*$^{ptuf}$ mutant clone produced in the same recombination event) in both anterior and posterior compartment of these wing discs. We next measured the size of mutant *selD*$^{ptuf}$ clones defined as the ratio of their own area relative to the area of their twin control *selD*$^{+}$ clones and compared the size of mutant clones in the anterior compartment to the size of mutant clones in the posterior compartment. We found that the size of *selD*$^{ptuf}$ mutant clones is almost double in the posterior compartment compared to the size of mutant clones in the anterior compartment (Fig. 6). While the mean area of anterior mutant clones is 34% of the area of their wild type twin clones, the mean area of posterior mutant clones is 58% of the area of their wild type twin clones. Together, ectopic expression of DIAP1 robustly rescues viability to double the size of *selD*$^{ptuf}$ mutant clones, which strongly supports the idea that *selD*$^{ptuf}$ ROS-induced apoptosis is caspase dependent.

The main conclusion of the work presented here is that *selD*$^{ptuf}$ cells generate a ROS oxidative stress that triggers a Dmp53/Rpr mediated apoptosis. The increased levels of ROS, Dmp53 stabilization, *rpr* transcription and activation of caspases that can be inhibited by DIAP1, strongly hint at an important contribution of Dmp53/Rpr caspase pathway in *selD*$^{ptuf}$ apoptosis. However, when a cell is committed to die, several pro-apoptotic molecules may be activated to irreversibly execute an apoptotic program. For example, the Ras/MAPK down-regulation induced by *selD* (Morey et al., 2001) could contribute, in a lesser extend and beyond our detection levels, to apoptosis (Fig. 7). The vast majority of studies about selenoprotein function have been done in either cell culture or *in vitro* whereas the main interest of our work lies on the use of a genetic approach in a whole organism. We propose that the redox-balance, cell scavenging or antioxidant functions of selenoproteins, which are essential for cell viability, will prevent cells from entering the apoptotic program. In pathological conditions, in which the selenoprotein function is altered, the cells will generate an oxidative stress scenario that will cause their own elimination by the Dmp53/Rpr apoptotic machinery.

## Acknowledgements

We would like to thank E. Hafen, K. White, J. Abrams, T. Laverty, H. Richardson, J. Mahaffey, G. Struhl and E. Martín-Blanco for fly stocks. We also thank K. White and I. Patten for critically reading the manuscript. We thank the Developmental Studies Hybridoma Bank, University of Iowa, for providing anti-Elav. *gl-Dmp53* flies and anti-Dmp53 antibody were provided by Exelixis Inc. through their p53 material transfer agreement. This work was supported by grant 01/0906 from FIS, Ministerio de Sanidad y Consumo and BMC2000-076 from Ministerio de Ciencia y Tecnología, Spain. MM is a fellow from CIRIT, Generalitat de Catalunya.

# Figure legends

**Figure 1**. Genetic mosaics of *selD$^{ptuf}$* in the eye. (A) *selD$^{ptuf}$* clones were recovered to adulthood and resulted in aberrant eyes. The mutant area (light red sectors; arrowheads) was scarred and almost no ommatidia differentiated. (B) Tangential sections of *selD$^{ptuf}$* clones revealed no ommatidial cells present in the mutant area. Right half: mutant sector; left half: normal tissue. (C) *selD$^{ptuf}$* homozygous clones in the eye imaginal disc stained with the anti-Elav neuronal cell marker (red) indicated that differentiation of photoreceptors is altered. In the middle panels mutant clones (black) lack e ß-galactosidase staining (green). Right panels: merged images. A confocal section at the normal level of Elav pattern (upper panels) showed no labeling in the *selD$^{ptuf}$* clone; however, deeper in the mutant tissue (lower panels) Elav staining appeared showing abnormal ommatidia (arrows). (D) TUNEL staining (red) in a *selD$^{ptuf}$* clone of an eye imaginal disc. It shows that cells in *selD$^{ptuf}$* clone (dark area lacking β-galactosidase labeling) entered apoptosis. Besides wild type apoptosis along the vicinity of the morphogenetic furrow (arrow), ectopic apoptotic figures were observed in cells adjacent to the clone (arrowhead). (E) *in vivo* detection of ROS with DHE (red) in *selD$^{ptuf}$* clones (dark area lacking GFP labeling) showed DHE labeled cells in the clone and also in cells adjacent to it (arrowheads).

**Figure 2**. Phenotypes resulting from genetic interactions with Hid and the Ras pathway. (A) Wild type eye. (B) GMR*hid*. (C) *GMRhid*/*selD$^{ptuf}$*. (D) *GMRhid/selD$^{ptuf}$*; *Cat$^{n1}$*. (E) *GMRhid; sev-rasV12*. (F) *GMRhid/selD$^{ptuf}$*; *sev-rasV12*. (G) *GMRyan$^{Act}$*. (H) *GMRyan$^{Act}$*/ *selD$^{ptuf}$*. (I) *sev-rasV12*. (J) *selD$^{ptuf}$* ; *sev-rasV12/ Cat$^{n1}$*. Anterior part of the eye to the left.

**Figure 3**. Transcription pattern of *reaper* in *selD$^{ptuf}$* cells. (A) Widespread *rpr* transcription (blue) in a *selD$^{ptuf}$* homozygous mutant imaginal disc where the cell surface was outlined using anti-Fasciclin III antibody (green). (B-C) *rpr* transcription (blue) in *selD$^{ptuf}$* clones (area lacking the green π-Myc labeling) in the wing (B) and the eye (C) disc respectively. (D) Detail of some cells of a *gl-Dmp53* eye disc showing Dmp53 stabilization (red) and *rpr* transcription (blue). Panels on the right correspond to merged images.

**Figure 4.** Dmp53 stabilization in *selD$^{ptuf}$* cells. (A) Detection of Dmp53 (red) in an eye disc overexpressing *Dmp53* under *glass* enhancer sequences. (B) High magnification of nuclear confocal section counterstained with YOYO nuclear marker (green) showed co-localization of Dmp53 (red) into the nuclei. (C) Dmp53 accumulation (red) in a *selD$^{ptuf}$* homozygous mutant imaginal disc stained with YOYO. (D) Zoom of a high magnification focusing two nuclei stained with YOYO nuclear marker (green, middle panel) showed co-localization of Dmp53 (red upper panel) into disrupted *selD$^{ptuf}$* nuclei. Lower panel correspond to merged images.

**Figure 5**. DRONC and DRICE caspases are involved in *selD$^{ptuf}$* apoptosis. (A) Overexpression of DRONC caspase under the control of *GMR-GAL4* driver gives rise to slightly rough and mottled eyes due to ectopic cell death. *white* patches result from the ablation of pigment cells. (B-C) Reduction of one dose of *selD* or *catalase*, respectively, enhanced the mottled eye phenotype. Wider areas of *white* tissue were observed indicating that an increase in ROS levels enhances DRONC apoptotic activity. (D) Combined reduction of *selD* and *catalase* exerted a stronger enhancement of DRONC overexpression

phenotype and few pigmented cells were observed. (E) Active DRICE (red) in a *selD*$^{ptuf}$ homozygous mutant imaginal disc where the cell surface was outlined using anti-Fasciclin III antibody (green). (F) Active DRICE in *selD*$^{ptuf}$ clones (dark area lacking β-galactosidase labeling, green) in the eye disc. Consistent with the finding of non-autonomous apoptosis and ROS, active DRICE was found as well outside the clone. (G) Overexpression of *Dmp53* triggers apoptosis through DRICE caspase as shown by active DRICE (red) present in *gl-Dmp53* discs. In E, F and G lower panels correspond to the respective merged images.

**Figure 6.** Rescue of *selD*$^{ptuf}$ clone size by DIAP1 overexpression. *selD*$^{ptuf}$ clones were induced in the posterior DIAP1 expressing compartment and in the anterior compartment of the wing pouch. Bars represent mean values of the area of *selD*$^{ptuf}$ clones as percentage of the area of their wild-type *selD*$^{+}$ twin clone±s.d., n=number of mutant and wild-type twin clone pairs analyzed in the anterior and posterior compartment. Overexpression of DIAP1 in the posterior compartment almost doubled *selD*$^{ptuf}$ clonal size. Mean area of anterior and posterior *selD*$^{ptuf}$clones, 34% and 58% of their wild type twin clone respectively, were significantly different (*t*-test: $P< 0.001$).

**Figure 7.** A model for ROS-induced apoptosis in cells devoid of selenoproteins. We propose that the increase in ROS due to a reduction in selenoproteins caused by *selD*$^{ptuf}$ mutation will lead to stabilization of Dmp53 and activation of Rpr caspase dependent apoptosis. We can not discard that other pathways such Ras/MAPK downregulation or a ROS-induced caspase independent pathway may have a minor contribution to *selD*$^{ptuf}$ apoptosis.

# References

Adrain, C., and Martin, S.J. (2001). The mitochondrial apoptosome: A killer unleashed by the cytochrome seas. *Trends Biochem. Sci.* 26, 390-397.

Alsina, B., Serras, F., Baguñà, J., and Corominas, M. (1998). *patufet*, the gene encoding the *Drosophila melanogaster* homologue of *selenophosphate synthetase*, is involved in imaginal disc morphogenesis. *Mol. Gen. Gene.t* 257, 113-123.

Alsina, B., Corominas, M., Berry, M. J., Baguñà, J., and Serras, F. (1999). Disruption of selenoprotein biosynthesis affects cell proliferation in the imaginal discs and brain of *Drosophila melanogaster*. *J. Cell Sci.* 112, 2875-2884.

Asano M., Nevins J.R., and Wharton R.P. (1996). Ectopic E2F expression induces S phase and apoptosis in Drosophila imaginal discs. *Genes Dev*. 10(11), 1422-1432.

Basler, K., and Hafen, E. (1988). Control of photoreceptor cell fate by the sevenless protein requires a functional tyrosine kinase domain. *Cell* 54, 299-311.

Bergmann, A., Agapite, J., McCall, K., and Steller, H. (1998). The *Drosophila* gene hid is a direct molecular target of Ras-dependent survival signaling. *Cell* 95, 331-41.
Brachmann, C. B., and Cagan, R. L. (2003). Patterning the fly eye: the role of apoptosis. *Trends Genet.* 19, 91-6.

Brodsky, M. H., Nordstrom, W., Tsang, G., Kwan, E., Rubin, G. M., and Abrams, J. M. (2000). *Drosophila* p53 binds a damage response element at the reaper locus. *Cell* 101, 103-13.

Brower, D. L., and Jaffe, S. M. (1989). Requirement for integrins during *Drosophila* wing development. *Nature* 342, 285-7.

Burns, T. F., and El-Deiry, W. S. (1999). The p53 pathway and apoptosis. *J. Cell Physiol.* 181, 231-9.

Buschmann, T., Yin, Z., Bhoumik, A., and Ronai, Z. (2000). Amino-terminal-derived JNK fragment alters expression and activity of c-Jun, ATF2, and p53 and increases H2O2-induced cell death. *J. Biol. Chem.* 275, 16590-16596.

Buttke, T. M., and Sandstrom, P. A. (1994). Oxidative stress as a mediator of apoptosis. *Immunol Today* 15, 7-10.

Cagan, R. L., Kramer, H., Hart, A. C., and Zipursky, S. L. (1992). The bride of sevenless and sevenless interaction: internalization of a transmembrane ligand. *Cell* 69, 393-399.

Chen, P., Nordstrom, W., Gish, B. and Abrams J.M. (1996). *grim*, a novel cell death gene *in Drosophila*. *Genes Dev*. 10(14):1773-1782.

Curtin, J.F., Donovan, M., and Cotter, T. G. (2002) Regulation and measurement of oxidative stress in apoptosis. *J. Immunological Methods* 265, 49-72.

Diaz-Benjumea FJ, Hafen E. (1994). The *sevenless* signalling cassette mediates *Drosophila* EGF receptor function during epidermal development. *Development* 120, 569-78.

Dorstyn, L., Colussi, P. A., Quinn, L. M., Richardson, H., and Kumar, S. (1999). DRONC, an ecdysone-inducible *Drosophila* caspase. *Proc. Natl. Acad. Sci. U. S. A.* 96, 4307-12.

Dorstyn, L., Read, S., Cakouros, D., Huh, J. R., Hay, B. A., and Kumar, S. (2002). The role of cytochrome c in caspase activation in *Drosophila melanogaster* cells. *J. Cell Biol.* 156, 1089-1098.

Fortini, M. E., Simon, M. A., and Rubin, G. M. (1992). Signalling by the sevenless protein tyrosine kinase is mimicked by Ras1 activation. *Nature* 355, 559-61.

Fraser, A. G., McCarthy, N. J., and Evan, G. I. (1997). drICE is an essential caspase required for apoptotic activity in *Drosophila* cells. *EMBO J.* 16, 6192-6199.

Fraser, A. G., and Evan, G. I. (1997). Identification of a *Drosophila melanogaster* ICE/CED-3-related protease, drICE. *EMBO J.* 16, 2805-2813.

Freeman, M. (1996). Reiterative use of the EGF receptor triggers differentiation of all cell types in the *Drosophila* eye. *Cell* 87, 651-660.

Goyal, L., McCall, K., Agapite, J., Hartwieg, E., and Steller, H. (2000). Induction of apoptosis by *Drosophila reaper*, *hid* and *grim* through inhibition of IAP function. *EMBO J.* 19, 589-597.

Grether, M. E., Abrams, J. M., Agapite, J., White, K., and Steller, H. (1995). The head involution defective gene of *Drosophila melanogaster* functions in programmed cell death. *Genes Dev.* 9, 1694-1708.

Griswold, C. M., Matthews, A. L., Bewley, K. E., and Mahaffey, J. W. (1993). Molecular characterization and rescue of acatalasemic mutants of *Drosophila melanogaster*. *Genetics* 134, 781-788.

Halfar, K., Rommel, C., Stocker, H., and Hafen, E. (2001). Ras controls growth, survival and differentiation in the *Drosophila* eye by different thresholds of MAP kinase activity. *Development* 128, 1687-1696.

Hatfield, D. L., and Gladyshev, V. N. (2002). How selenium has altered our understanding of the genetic code. *Mol. Cell Biol.* 22, 3565-3576.

Hawkins, C. J., Yoo, S. J., Peterson, E. P., Wang, S. L., Vernooy, S. Y., and Hay, B. A. (2000). The *Drosophila* caspase DRONC cleaves following glutamate or aspartate and is regulated by DIAP1, HID, and GRIM. *J. Biol. Chem.* 275, 27084-27093.

Hay, B. A., Wolff, T., and Rubin, G. M. (1994). Expression of baculovirus P35 prevents cell death in *Drosophila*. *Development* 120, 2121-2129.

Hay, B. A. (2000). Understanding IAP function and regulation: a view from *Drosophila*. *Cell Death Differ.* 7, 1045-1056.

Holley, C. L., Olson, M. R., Colon-Ramos, D. A., and Kornbluth, S. (2002). Reaper eliminates IAP proteins through stimulated IAP degradation and generalized translational inhibition. *Nat. Cell. Biol.* 4, 439-444.

Jin, S., Martinek, S., Joo, W. S., Wortman, J. R., Mirkovic, N., Sali, A., Yandell, M. D., Pavletich, N. P., Young, M. W., and Levine, A. J. (2000). Identification and characterization of a p53 homologue in *Drosophila melanogaster*. *Proc. Natl. Acad. Sci. U. S. A.* 97, 7301-6.

Kaiser, W. J., Vucic, D., and Miller, L. K. (1998). The *Drosophila* inhibitor of apoptosis D-IAP1 suppresses cell death induced by the caspase drICE. *FEBS Lett.* 440, 243-8.

Kitamura, Y., Ota, T., Matsuoka, Y., Tooyama, I., Kimura, H., Shimohama, S., Nomura, Y., Gebicke-Haerter, P. J., and Taniguchi, T. (1999). Hydrogen peroxide-induced apoptosis mediated by p53 protein in glial cells. *Glia* 25, 154-164.

Kroemer, G., and Reed, J.C. (2000). Mitochondrial control of cell death. *Nat. Med.* 6, 513-519.

Kurada, P., and White, K. (1998). Ras promotes cell survival in *Drosophila* by downregulating hid expression. *Cell* 95, 319-329.

Lisi, S., Mazzon, I., and White, K. (2000). Diverse domains of THREAD/DIAP1 are required to inhibit apoptosis induced by REAPER and HID in *Drosophila*. *Genetics* 154, 669-678.

Mackay, W. J., and Bewley, G. C. (1989). The genetics of catalase in *Drosophila melanogaster*: isolation and characterization of acatalasemic mutants. *Genetics* 122, 643-652.

Martin-Blanco, E. (1998). Regulatory control of signal transduction during morphogenesis in *Drosophila*. *Int. J. Dev. Biol.* 42, 363-368.

Meier, P., Silke, J., Leevers, S. J., and Evan, G. I. (2000). The *Drosophila* caspase DRONC is regulated by DIAP1. *EMBO J.* 19, 598-611.

Miller DT, Cagan RL. (1998). Local induction of patterning and programmed cell death in the developing *Drosophila* retina. *Development* 125, 2327-2335.

Morata, G., and Ripoll, P. (1975). Minutes: mutants of *Drosophila* autonomously affecting cell division rate. *Dev. Biol.* 42, 211-221.

Morey, M., Serras, F., Baguna, J., Hafen, E., and Corominas, M. (2001). Modulation of the Ras/MAPK signalling pathway by the redox function of selenoproteins in *Drosophila melanogaster*. *Dev. Biol.* 238, 145-156.

Morey, M., Serras, F., and Corominas, M. (2003). Halving the *selenophosphate synthetase* gene dose confers hypersensitivity to oxidative stress in *Drosophila melanogaster*. *FEBS Lett.* 534, 111-114.

Moses, K., and Rubin, G. M. (1991). Glass encodes a site-specific DNA-binding protein that is regulated in response to positional signals in the developing *Drosophila* eye. *Genes Dev*. 5, 583-593.

Newsome, T. P., Asling, B., and Dickson, B. J. (2000). Analysis of *Drosophila* photoreceptor axon guidance in eye-specific mosaics. *Development* 127, 851-860.

Nordstrom, W., Chen, P., Steller, H., and Abrams, J. M. (1996). Activation of the reaper gene during ectopic cell killing in *Drosophila*. *Dev. Biol.* 180, 213-226.

Ollmann, M., Young, L. M., Di Como, C. J., Karim, F., Belvin, M., Robertson, S., Whittaker, K., Demsky, M., Fisher, W. W., Buchman, A., Duyk, G., Friedman, L., Prives, C., and Kopczynski, C. (2000). *Drosophila* p53 is a structural and functional homolog of the tumor suppressor p53. *Cell* 101, 91-101.

Quinn, L. M., Dorstyn, L., Mills, K., Colussi, P. A., Chen, P., Coombe, M., Abrams, J., Kumar, S., and Richardson, H. (2000). An essential role for the caspase dronc in developmentally programmed cell death in *Drosophila*. *J. Biol. Chem.* 275, 40416-40424.

Rayman, M.P. (2000). The importance of selenium to human health. *Lancet* 356 (9225), 233-241.

Rebay, I. and Rubin G.M. (1995). Yan functions as a general inhibitor of differentiation and is negatively regulated by activation of the Ras1/MAPK pathway.
*Cell* 81(6), 857-866.

Richardson, H. and Kumar, S. (2002) Death to flies: *Drosophila* as a model system to study programmed cell death. *J. Immunological Methods* 265, 21-38.

Robinow, S., and White, K. (1988). The locus elav of *Drosophila melanogaster* is expressed in neurons at all developmental stages. *Dev. Biol.* 126, 294-303.

Robinow, S., Draizen, T.A. and Truman, J.W. (1997). Genes that induce apoptosis: transcriptional regulation in identified, doomed neurons of the *Drosophila* CNS.
*Dev. Biol.* 190, 206-213.

Roch, F., Serras, F., Cifuentes, F. J., Corominas, M., Alsina, B., Amoros, M., Lopez-Varea, A., Hernandez, R., Guerra, D., Cavicchi, S., Baguna, J., and Garcia-Bellido, A. (1998). Screening of

larval/pupal P-element induced lethals on the second chromosome in *Drosophila melanogaster*: clonal analysis and morphology of imaginal discs. *Mol. Gen. Genet.* 257, 103-12.

Sawamoto, K., Taguchi, A., Hirota, Y., Yamada, C., Jin, M.H. and Okano, H. (1998). Argos induces programmed cell death in the developing *Drosophila* eye by inhibition of the Ras pathway. *Cell Death Differ*. 5(4), 262-270.

Simon, M.A., Bowtell, D.D., Dodson, G.S., Laverty, T.R. and Rubin, G.M. (1991). Ras1 and a putative guanine nucleotide exchange factor perform crucial steps in signaling by the sevenless protein tyrosine kinase. *Cell* 67(4), 701-716.

Simon, H. U., Haj-Yehia, A., and Levi-Schaffer, F. (2000). Role of reactive oxygen species (ROS) in apoptosis induction. *Apoptosis* 5, 415-418.

Sionov, R. V., and Haupt, Y. (1999). The cellular response to p53: the decision between life and death. *Oncogene* 18, 6145-6157.

Stadtman, T. C. (1996). Selenocysteine. *Annu Rev Biochem* 65, 83-100.

Tanimoto, H., Itoh, S., ten Dijke, P., and Tabata, T. (2000). Hedgehog creates a gradient of DPP activity in Drosophila wing imaginal discs. *Molec. Cell* 5, 59-71.

Tepass, U., Theres, C., and Knust, E. (1990). crumbs encodes an EGF-like protein expressed on apical membranes of *Drosophila* epithelial cells and required for organization of epithelia. *Cell* 61, 787-799.

Torok, T., Tick, G., Alvarado, M., and Kiss, I. (1993). P-lacW insertional mutagenesis on the second chromosome of *Drosophila melanogaster*: isolation of lethals with different overgrowth phenotypes. *Genetics* 135, 71-80.

White, K., Grether, M. E., Abrams, J. M., Young, L., Farrell, K., and Steller, H. (1994). Genetic control of programmed cell death in *Drosophila*. *Science* 264, 677-683.

White, K., Tahaoglu, E., and Steller, H. (1996). Cell killing by the *Drosophila* gene reaper. *Science* 271, 805-7.

Xu, T., and Rubin, G. M. (1993). Analysis of genetic mosaics in developing and adult *Drosophila* tissues. *Development* 117, 1223-1237.

Yin, Y., Terauchi, Y., Solomon, G. G., Aizawa, S., Rangarajan, P. N., Yazaki, Y., Kadowaki, T., and Barrett, J. C. (1998). Involvement of p85 in p53-dependent apoptotic response to oxidative stress. *Nature* 391, 707-710.

Yoo, S. J., Huh, J. R., Muro, I., Yu, H., Wang, L., Wang, S. L., Feldman, R. M., Clem, R. J., Muller, H. A., and Hay, B. A. (2002). Hid, Rpr and Grim negatively regulate DIAP1 levels through distinct mechanisms. *Nat. Cell. Biol.* 4, 416-424.

Fig. 1.

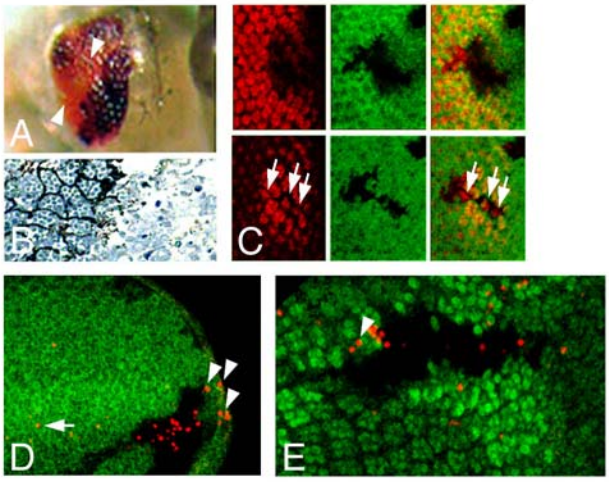

Fig. 2.

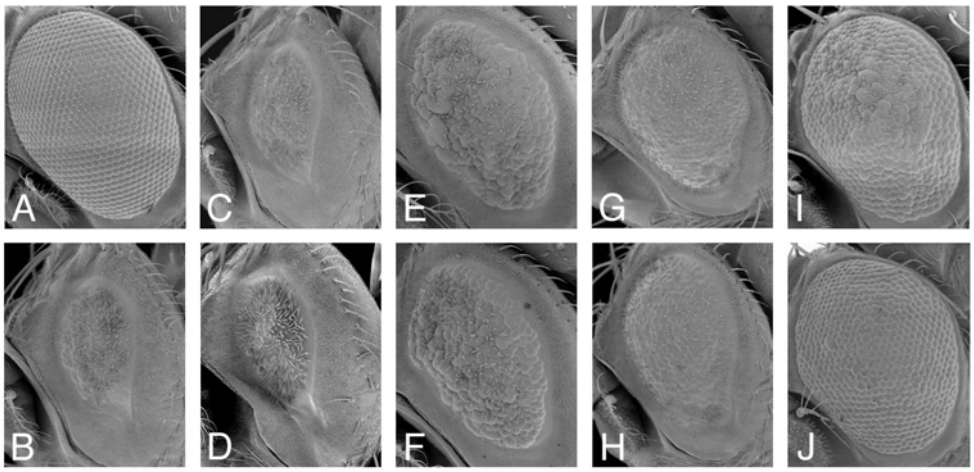

Fig. 3.

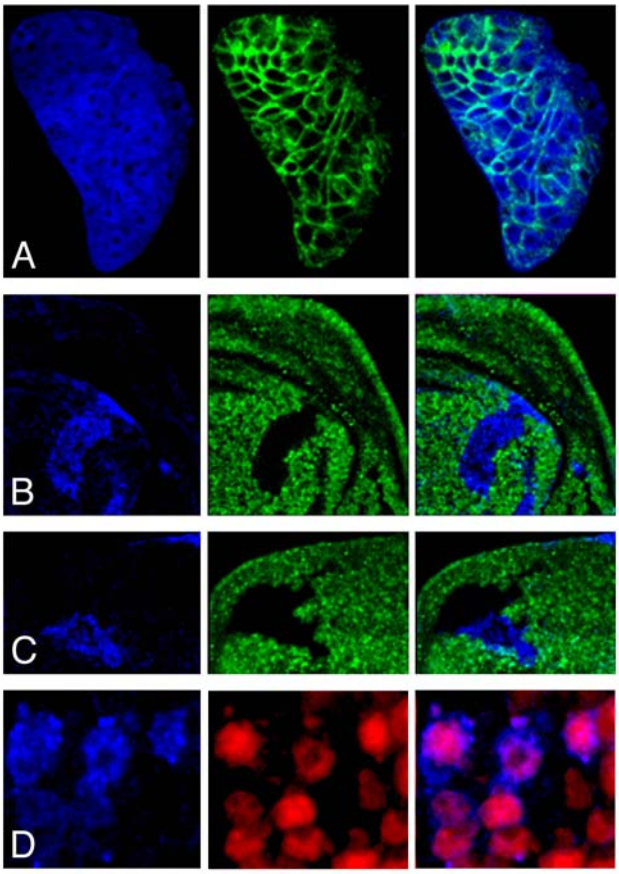

Fig. 4.

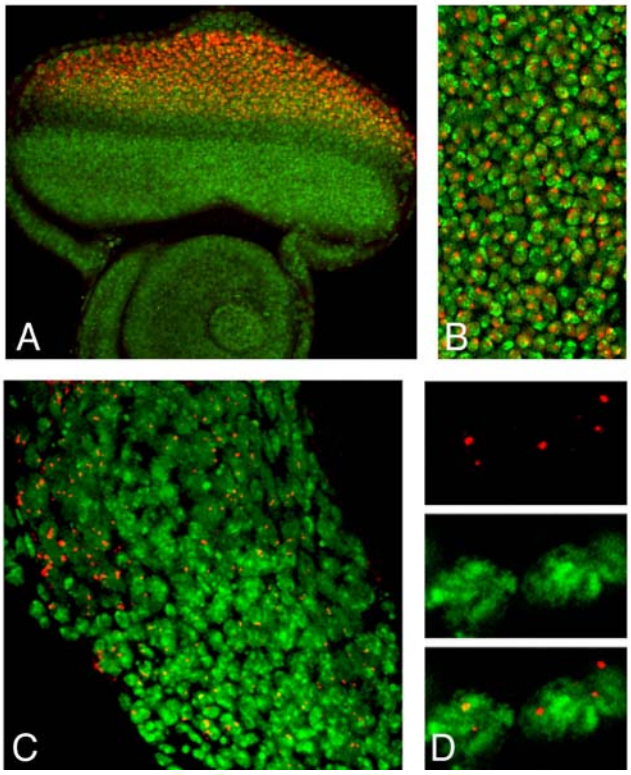

Fig. 5

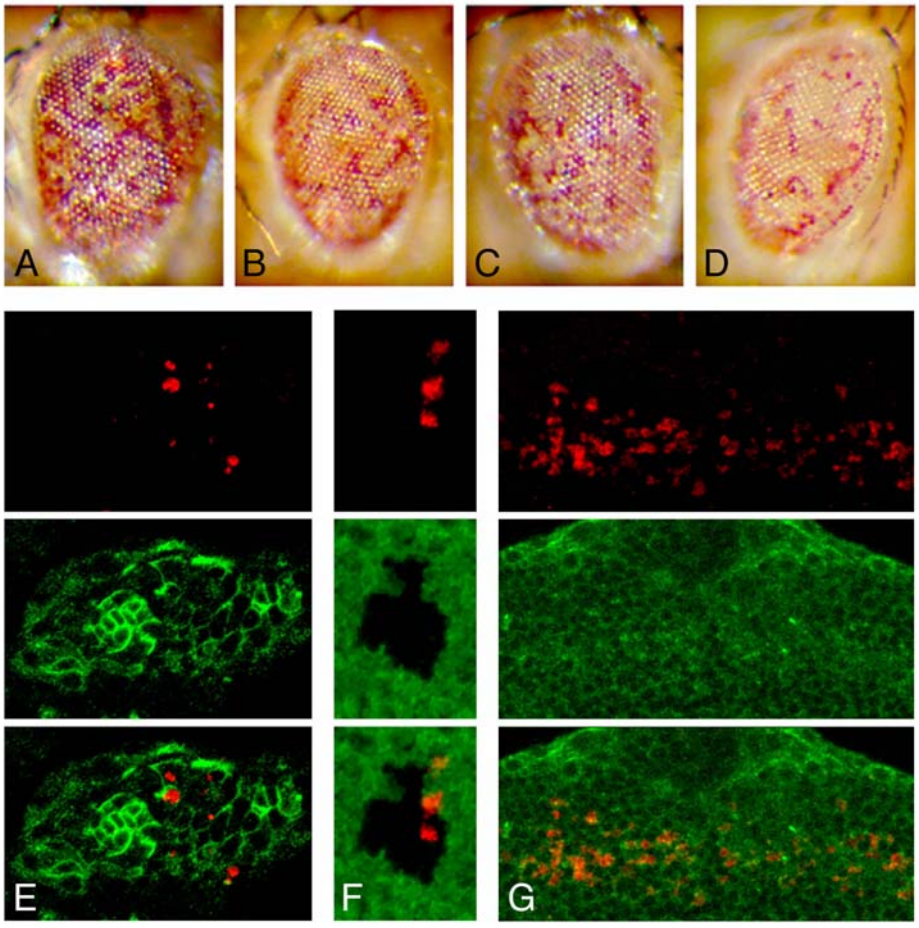

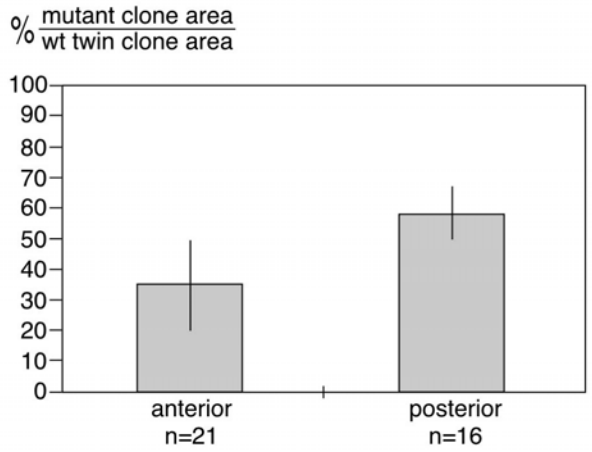
% mutant clone area / wt twin clone area
100
90
80
70
60
50
40
30
20
10
0
anterior
n=21
posterior
n=16

Fig. 7.

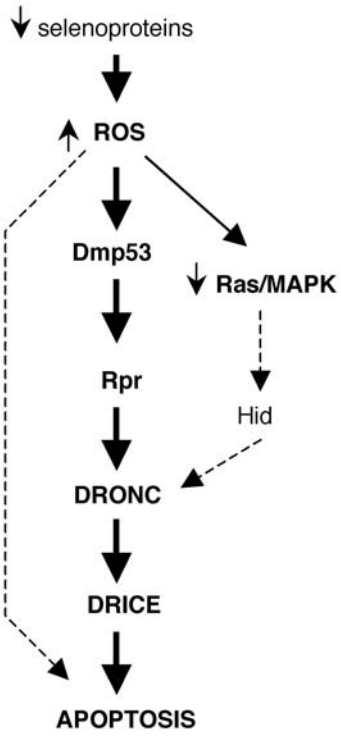
selenoproteins
ROS
Dmp53
Ras/MAPK
Rpr
Hid
DRONC
DRICE
APOPTOSIS

# CAPÍTOL III

## Identificació *in silico* i verificació *in vivo* de selenoproteïnes a *Drosophila*

**Article 4**: Castellano, S., Morozova, N., Morey, M., Berry, M.J., Serras, F., Corominas, M. and Guigó R. (2001). In silico identification of novel selenoproteins in the *Drosophila melanogaster* genome. *EMBO Rep*. 2001 Aug;2(8):697-702.

### Precendents

El fet de que alguns components de la ruta de biosíntesi de les selenoproteïnes havien estat identificats a *Drosophila* (Persson *et al*., 1997; Alsina *et al*., 1998; Zhou *et al*., 1999), l'observació de que proteïnes d'estadis larvaris i pupals incorporaven Se (Robinson i Cooley, 1997; Alsina *et al*., 1999) i els atractius fenotips de la mutació *selD*$^{ptuf}$ (Alsina *et al*., 1998, 1999; Articles 1 i 2: Morey *et al*., 2001; 2003) feien interessant la cerca de selenoproteïnes a *Drosophila*. La recent publicació del genoma de *Drosophila* (Adams *et al*., 2000) predeia l'existència d'uns 13.000 gens, si més no, com els programes existents fins al moment contemplaven el codó TGA com a codó d'*stop*, les selenoproteïnes no estaven ben predites doncs quedaven truncades pel lloc d'incorporació de Sec i no es podien identificar. Així, l'ús del genoma de *Drosophila* per a identificar selenoproteïnes quedava subordinat al desenvolupament de noves estratègies bioinformàtiques i programes de predicció de gens adaptats per reconèixer un codo TGA com a lloc d'incorporació de Sec.

### Resum

Amb l'objectiu d'identificar noves selenoproteïnes en el genoma de *Drosophila* és van seguir els següents passos: (1) es va fer una cerca de SECIS al llarg del genoma i es van filtrar les prediccions més estables termodinàmicament; (2) es va generar un versió modificada del programa d'identificació de gens *geneid* que acceptes codons TGA en pauta de lectura i la presència del SECIS, i es va fer córrer sobre el genoma; (3) un cop seleccionades les prediccions que complien els requisits establerts, es van acceptar les suportades per ESTs; (4) finalment es van obtenir tres prediccions. Una acabava de ser identificada amb lo qual ens servia de control positiu. Les altres dues eren noves proteïnes sense homologia a cap altra proteïna descrita; (5) es va procedir a comprovació funcional de que aquestes dues eren selenoproteïnes mitjançant la incorporació de $^{75}$Se en un sistema heteròleg.

Les dues noves selenoproteïnes identificades a *Drosophila* són anomenades dselG i dselM. Ambdues es troben al cromosoma X i tenen paràlegs amb Cys. El seu patró d'expressió es ubiqu i hi ha un gran component matern en els estadis embrionaris.

### Aportació personal al treball

L'autora d'aquesta Tesi va participar en les reunions de treball dutes a terme amb el grup del Dr. R. Guigó que va dissenyar el programa d'identificació de selenoproteïnes. Va seqüenciar els clons de cDNA de les selenoproteïnes dselG i dselM, a l'hora que realitzar l'estudi del patró d'expressió de les mateixes mitjançant hibridació *in situ whole mount* en diferents estadis del desenvolupament de *Drosophila*. També va realitzar una estada a

Boston amb l'objectiu de dur a terme els experiments d'incorporació de Se radioactiu en el laboratori de la Dra. M.J. Berry i discutir els resultats obtinguts. Finalment, va participar en l'elaboració del manuscrit.

EMBO reports

scientific report

# *In silico* identification of novel selenoproteins in the *Drosophila melanogaster* genome

Sergi Castellano, Nadya Morozova[1], Marta Morey[2], Marla J. Berry[1], Florenci Serras[2], Montserrat Corominas[2] & Roderic Guigó[+]

Grup de Recerca en Informàtica Biomèdica, Institut Municipal d'Investigació Mèdica (IMIM), Universitat Pompeu Fabra, Dr. Aiguader 80, 08003 Barcelona, [2]Departament de Genètica, Universitat de Barcelona, Diagonal 645, 08071 Barcelona, Spain and [1]Thyroid Division, Harvard Institutes of Medicine, 77 Avenue Louis Pasteur, Boston, MA 02115, USA

Received April 4, 2001; revised May 31, 2001; accepted June 6, 2001

**In selenoproteins, incorporation of the amino acid selenocysteine is specified by the UGA codon, usually a stop signal. The alternative decoding of UGA is conferred by an mRNA structure, the SECIS element, located in the 3′-untranslated region of the selenoprotein mRNA. Because of the non-standard use of the UGA codon, current computational gene prediction methods are unable to identify selenoproteins in the sequence of the eukaryotic genomes. Here we describe a method to predict selenoproteins in genomic sequences, which relies on the prediction of SECIS elements in coordination with the prediction of genes in which the strong codon bias characteristic of protein coding regions extends beyond a TGA codon interrupting the open reading frame. We applied the method to the *Drosophila melanogaster* genome, and predicted four potential selenoprotein genes. One of them belongs to a known family of selenoproteins, and we have tested experimentally two other predictions with positive results. Finally, we have characterized the expression pattern of these two novel selenoprotein genes.**

## INTRODUCTION

Selenoproteins are proteins that incorporate the amino acid selenocysteine, a cysteine analog in which a selenium atom is found in place of sulfur. Several components of the selenoprotein synthesis machinery are conserved between different species, suggesting an important role of selenoproteins in cell function (Low and Berry, 1996; Stadman, 1996). Incorporation of selenocysteine into selenoproteins requires an unusual translation step where UGA, normally a stop codon, specifies selenocysteine insertion. Thus, in a single mRNA, UGA can have two contrasting meanings: stop or selenocysteine. The alternative decoding of UGA is conferred by an mRNA secondary/tertiary structure (the selenocysteine insertion sequence, the SECIS element), which is located in eukaryotes in the 3′-untranslated region. SECIS structures are divided into two classes, termed form 1 and form 2, the latter having an additional small stem–loop at the top of the SECIS element. Most selenoproteins contain a single selenocysteine residue per polypeptide chain, but selenoprotein P has as many as 10–12 (Tujebajeva *et al.*, 2000a).

Selenoproteins have been identified in Bacteria, Archaea and Eukarya. Among eukaryotes, selenoproteins appear to be more common in mammals. Thus, 19 selenoproteins have been found to date in mammals (Flohé *et al.*, 2000), but none in the genome of *Saccharomyces cerevisiae*, and only one in the genome of *Caenorhabditis elegans* (Buettner *et al.*, 1999; Gladyshev *et al.*, 1999). Recently, the class 2 selenophosphate synthetase gene (*sps2*)—an enzyme in the pathway of selenoprotein synthesis, and a selenoprotein itself in mammals—has also been shown to be a selenoprotein in *Drosophila melanogaster* (Hirosawa-Takamori *et al.*, 2000). So far, it remains the only selenoprotein identified in this organism and maps to chromosome 2L. However, pupal proteins of 68, 42 and 25 kDa have been reported to incorporate selenium (Robinson and Cooley, 1997), and a major band of 42 kDa has also been observed in protein extracts of larvae labeled with $^{75}$Se (Alsina *et al.*, 1999). In addition, some components of the selenoprotein synthesis machinery have already been identified in the fly (Persson *et al.*, 1997; Alsina *et al.*, 1998; Zhou *et al.*, 1999). Moreover, a mutation in the *sps1* gene (a cysteine homolog of Sps2) leads to larval lethality, increased apoptosis and aberrant imaginal disc morphology (Alsina *et al.*, 1998). These data strongly suggest the existence of as yet

[+]Corresponding author. Tel: +34 93 225 7567; Fax: +34 93 221 3237; E-mail: rguigo@imim.es

unidentified selenoproteins in the *D. melanogaster* genome. The recent availability of the complete DNA sequence of this genome should constitute an invaluable resource for characterizing the *D. melanogaster* selenoproteins.

Prediction of selenoproteins in genomic sequences, however, is particularly difficult. Without exception, computational gene prediction programs rely on the standard stop codons TAA, TAG and TGA to identify open reading frames (ORFs) and predict coding exons, through the determination of suitable splicing sites and the computation of some measure of coding likelihood, usually related to bias in codon usage (see Burge and Karlin, 1998 and Haussler, 1998 for reviews on computational gene finding). Under such an assumption, selenoprotein genes, in which TGA does not necessarily imply termination of translation, will be incorrectly predicted. Indeed, the *D. melanogaster sps2* gene (*dsps2*) is wrongly predicted in the released annotation of the fly genome: >100 amino acids are missing from a 379 amino acids protein. Correct delineation of the exonic structure is singularly important to predict selenoprotein genes. Misprediction of only a single amino acid (the selenocysteine residue) may lead to misidentification of selenoproteins (see Results).

Although searching for potential SECIS elements has proved useful in identifying new selenoproteins in expressed sequence tag (EST) sequences (Kryukov *et al.*, 1999; Lescure *et al.*, 1999), this approach is impractical when applied to genomic sequences, given the high frequency of occurrence of the SECIS pattern (see Results). To reduce the number of false positive predictions, we developed a method that relies on the correlated prediction of SECIS elements and of genes in which the strong codon bias characteristic of protein coding regions extends beyond a TGA codon interrupting the ORF. Indeed, we have found that in selenoproteins the region comprised between the in-frame TGA codon and the stop codon shows codon bias comparable to that found in coding regions, while in non-selenoproteins the region comprised between the stop codon TGA and the next stop codon in-frame shows codon bias comparable to that in non-coding regions (Supplementary data). Therefore, measures of codon bias can be used to distinguish actual selenoproteins from false predictions in SECIS-positive nucleotide sequences

## RESULTS

### Prediction of novel selenoproteins in the *D. melanogaster* genome

The March 24, 2000 release of the *D. melanogaster* genome sequence summing up 115 229 998 bp and containing 13 329 annotated genes was used (Adams *et al.*, 2000). 37 876 potential SECIS elements were found along this sequence using the program PatScan. The minimum free energy of each putative SECIS was measured, and only those fitting an energy stability criteria were considered further. This resulted in 1220 potential SECIS. Along with the sequence, positions of these elements were given to a modified version of the program geneid, which allows for the prediction of genes interrupted by in-frame TGA codons. The restriction was enforced such that genes could not be further than 500 bp upstream from a predicted SECIS. Eleven potential selenoproteins were predicted among a total of 12 194 genes. Seven of them were discarded because the predicted exonic structure was incompatible with the exonic structure of known overlapping genes, contradicted identical EST sequences or was similar to known proteins with functions apparently unrelated to those of selenoproteins. Of the remaining four, one corresponded to the previously identified *D. melanogaster* selenoprotein *dsps2*. For another two, we identified cysteine paralogs within the set of proteins predicted in the *D. melanogaster* genome. No additional evidence was found for the fourth putative selenoprotein, after an exhaustive search against a number of databases of known coding sequences using the BLAST suite of programs (Altschul *et al.*, 1997). In addition, the predicted secondary structure around the selenocysteine residue of this putative selenoprotein is not compatible with the known crystal structure of the bovine glutathione peroxidase, a eukaryotic selenoprotein. This structure appears to be common to most known selenoproteins, including the two other predictions (Supplementary data). We have thus considered this prediction to be a false positive. Incorporation of selenium was subsequently demonstrated for the two other predicted selenoproteins (which we name dselG and dselM), and their expression pattern during development was characterized.

#### *dselG*

dSelG is a 110 aa protein which maps to 10F4-6 of the X chromosome. It differs in only two amino acids from the annotated protein in *D. melanogaster* (CG1844), the in-frame TGA lying only one codon upstream from the stop codon. *dselG* has a cysteine paralog, the *CG1840* gene. They appear in tandem, separated by only 320 bp, and have the same exonic structure sharing 65% identity at the protein level (Figure 1).

#### *dselM*

dSelM is a 249 aa protein which maps to 12A4–6 of the X chromosome. It differs substantially from the protein annotated in *D. melanogaster* (CG11177), the first exon, and a large fraction of the second (in which the in-frame TGA is located) having been missed. *dselM* has two distant paralogs, the *CG13186* and *CG15147* genes (Figure 2).

### $^{75}$Se labeling of the *D. melanogaster* selenoproteins expressed in mammalian cells

$^{75}$Se labeling of HEK cells was undertaken to demonstrate that *GH03581* (*dselG*) and *SD09114* (*dselM*) genes encoded bona fide selenoproteins. In cells transfected with empty vector, the background pattern of endogenously expressed selenoproteins can be seen (Figure 3A, lane 1), including thioredoxin reductases (~55 kDa), glutathione peroxidase (~23 kDa), phospholipid hydroperoxide glutathione peroxidase (~20 kDa), and an ~12–14 kDa triplet. Transfection of the GH03581 expression vector resulted in an increase in labeling in the 12 kDa size range, overlapping the lower band of the endogenous triplet (Figure 3A, lane 2). Transfection of the SD09114 expression vector resulted in appearance of a prominent new band of ~30 kDa (Figure 3A, lane 3), corresponding to the predicted size of SD09114 (~27 kDa). SD09114 protein appears to be a *D. melanogaster*-specific selenoprotein, with no analog in mammalian cells of similar molecular weight.

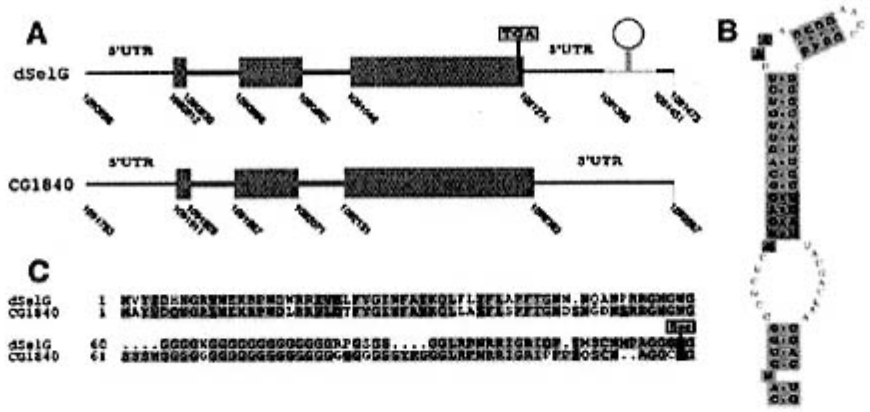


**Fig. 1.** dSelG. (**A**) Gene structure for *dselG* and in-tandem *CG1840* paralog plotted using gff2ps (Abril and Guigó, 2000). Coordinates correspond to the AE002593 (X) scaffold. The extra coding region is shown in red as predicted by geneid and the annotated coding exons are in blue. (**B**) *dselG* form 2 SECIS. (**C**) Alignment of *dSelG* and *CG1840* paralogs using CLUSTAL_W (Thompson *et al.*, 1994).

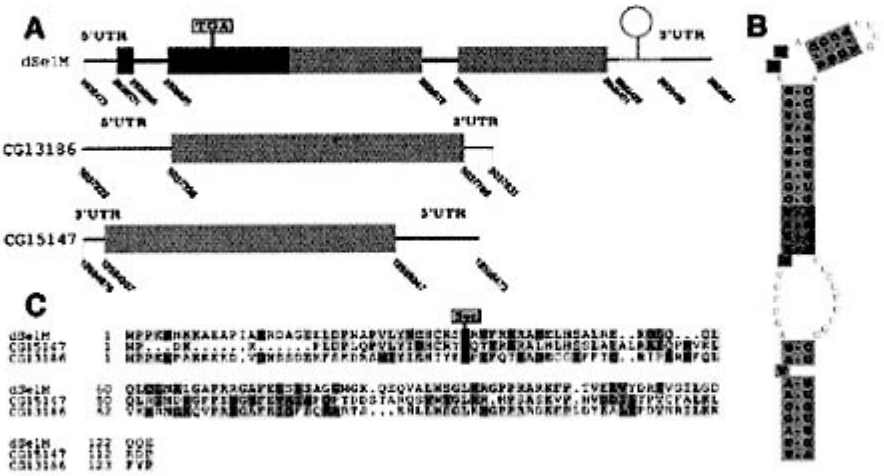


**Fig. 2.** dSelM. (**A**) Gene structure for *dselM* and single exon *CG15147, CG13186* paralogs. Coordinates correspond to the AE002593 (X), AE002690 (2L) and AE002787 (2R) scaffolds, respectively. (**B**) *dselM* form 2 SECIS. (**C**) Alignment of *dSelM* and *CG15147, CG13186* paralogs.

### *In situ* hybridization in embryos, discs and brains

*In situ* hybridization experiments were performed to assess *dselG* and *dselM* mRNA expression patterns. *dselM* mRNA was present in all embryonic stages, especially in the blastoderm stage, suggesting that there is a strong maternal contribution (Figure 4A, C and E). Imaginal discs displayed a ubiquitous *dselM* expression pattern (Figure 4I), and in brain, although the staining was ubiquitous, large cells, probably neuroblasts, were highly stained (Figure 4G). *dselG* expression pattern was analyzed in embryos, and similarly to *dselM*, the mRNA was found ubiquitously in all stages (Figure 4K, M and O). Due to the high similarity at the nucleotide sequence level between *dselG* and the cysteine homolog (64% in the coding fraction), we have to assume that the probe used for the *in situ* hybridization would detect both transcripts, if present.

## DISCUSSION

Most of the functions of selenium involve its incorporation into selenoproteins in the form of selenocysteine. Besides their putative role in regulating the redox state of the cell, selenoproteins seem to possess anticarcinogenic properties, and PHGPx plays a role in reproductive function (Ganther, 1999; Ursini *et al.*, 1999).

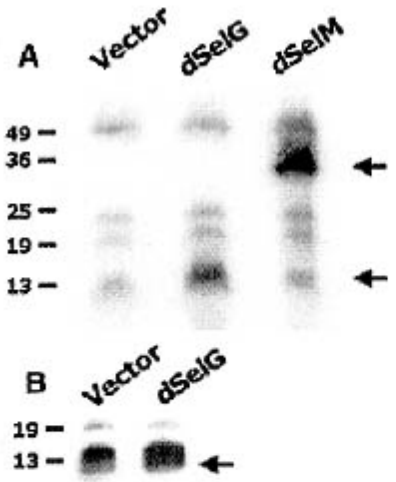


**Fig. 3.** $^{75}$Se-labeling of the *D. melanogaster* selenoproteins expressed in mammalian cells. **(A)** Lane 1: $^{75}$Se-labeling of cells transfected with empty vector. Lane 2: $^{75}$Se-labeling of cells transfected with *dselG*. Lane 3: $^{75}$Se-labeling of cells transfected with *dselM*. **(B)** High magnification of the region corresponding to the *dselG* labeling.

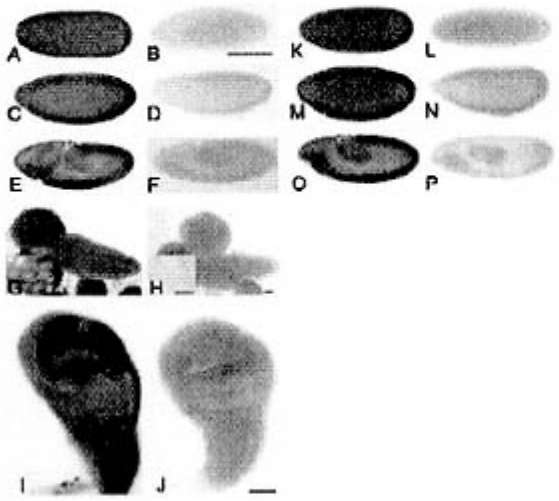


**Fig. 4.** *In situ* hybridization in embryos, imaginal discs and brain. **(A, C and E)** *dselM* expression pattern in sincytial blastoderm, cellular blastoderm and gastrulation embryonic stages, respectively; **(B, D and F)** the corresponding sense controls (scale bar is 50 mm); **(G)** *dselM* expression in brain and neuroblast staining in the inset; **(H)** the brain sense control (scale bar 100 mm, inset scale bar 2.5 mm); **(I)** *dselM* expression in wing disc; **(J)** wing disc sense control (scale bar 50 mm); **(K, M and O)** *dselG* expression pattern in sincytial blastoderm, cellular blastoderm and gastrulation embryonic stages, respectively; **(L, N and P)** are the corresponding sense controls (scale bar is 50 mm).

*Drosophila* provides a convenient tool for investigating selenoprotein function because of the availability of fly genetics and the already existing mutation in the *sps1* gene (Alsina *et al.*, 1998).

Using a novel computational method we have predicted four potential selenoprotein genes in the *D. melanogaster* genome,

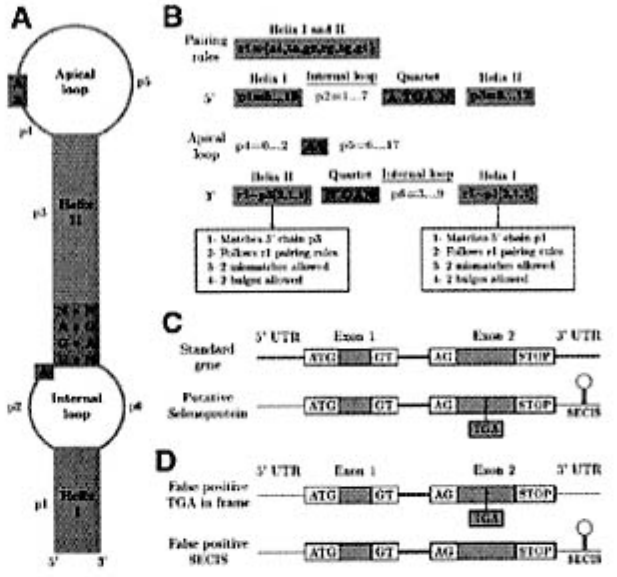


**Fig. 5.** SECIS and gene prediction. **(A)** General form 1 SECIS divided into structural units. Form 2 has an extra short stem–loop in the apical loop. **(B)** PatScan SECIS pattern to search for both form 1 and form 2 SECIS. The extra stem–loop in form 2 is not taken into account when searching. **(C)** The two possible ways of geneid prediction for an ideal two exons gene: as a normal gene or as a selenoprotein gene with a TGA in-frame and a SECIS. Exon defining signals are shown. **(D)** False positive selenoprotein genes with either a TGA in-frame or a SECIS. These partial predictions are not permitted in the gene prediction.

with little human intervention. Three are bona fide selenoproteins: dSps2, already demonstrated as such (Hirosawa-Takamori *et al.*, 2000), and the other two, dSelG and dSelM, shown herein by $^{75}$Se labeling. In addition, cysteine paralogs exist in *D. melanogaster* for these three selenoproteins. While Sps2, a selenophosphate synthetase, belongs to a known family of selenoproteins, dSelG and dSelM are novel selenoproteins, lacking sequence similarity to known proteins. dSelG has a cysteine homolog in *C. elegans* of unknown function, while dSelM appears to belong to a new class of selenoproteins widely distributed across the phylogenetic spectrum: we have found selenocysteine homologs to dSelM in ESTs from zebrafish, human and mouse databases, among other organisms.

It is unclear, however, how complete our characterization of the selenoprotein set in *D. melanogaster* is. Experimental data suggest the existence of a selenoprotein in the 60–70 kDa range (Alsina *et al.*, 1999), for which we have not been able to find a computational prediction. Forcing the SECIS element to occur within 500 bp downstream from the selenoprotein coding region may be too restrictive. Although most mammalian selenoproteins are within this range, longer distances up to >4000 bp are possible. The fly genome is certainly more compact, and while in the human *sps2* the SECIS element is 579 bp downstream from the stop codon, this distance is only 30 bp in *D. melanogaster*. On the other hand, exceptions to the standard eukaryotic SECIS model have recently been reported in *C. elegans*. In this case, a 5′-GUGA motif is present instead of AUGA (Buettner *et al.*, 1999). Therefore, it is possible that additional selenoproteins using an alternative

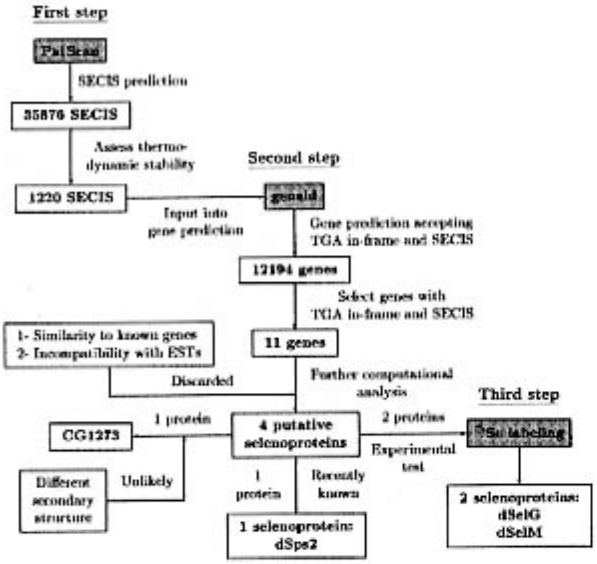


**Fig. 6.** General schema for selenoprotein identification.

SECIS structure exist in the *D. melanogaster* genome. Relaxing the SECIS pattern to capture a more general SECIS structure results in a substantial increase in the number of predicted SECIS elements, which compounds the analysis of the search results. In this regard, the approach presented here could contribute towards systematically exploring alternative SECIS structures.

In summary, we believe that the research described here demonstrates the power of the combined *in silico*, *in vitro* and *in vivo* approaches towards a better understanding of living systems.

## METHODS

**Prediction of selenoproteins in nucleotide sequences.** The method that we have developed is described in detail in the Supplementary data, which can be found at *EMBO reports* Online. A general schema is shown in Figure 6. Broadly, given a query sequence, first we predict SECIS elements using the program PatScan (http://www-unix.mcs.anl.gov/compbio/PatScan/HTML/PatScan.html) (Figure 5A and B). The stability of the predicted SECIS is then assessed using the RNAfold program (Viena RNA package) using the protocol by Kryukov *et al.* (1999). Next, we use a modification of the program geneid (Guigó *et al.*, 1992; Parra *et al.*, 2000) to predict genes that may be interrupted by in-frame TGA codons. Such genes, however, can be predicted only when a putative SECIS, whose position along the genome is input into geneid during gene prediction, exists at the right distance. The modified geneid yields, in the same gene prediction, both standard genes and selenoprotein genes (Figure 5C and D).

**$^{75}$Se labeling.** The pOT2 plasmids containing GH03581 (*dselG*) and SD09114 (*dselM*) cDNA clones were obtained from Research Genetics Inc. and sequenced using the Dye Terminator Cycle Sequencing method. Inserts were subcloned into pUHD10-3 vector via *Eco*RI and *Xba*I sites. Human embryonic kidney cells (HEK-293) were transiently transfected by $CaPO_4$ DNA precipitation method (Tujebajeva *et al.*, 2000b) with either *dselG* or *dselM* expression plasmids and co-transfected with plasmids encoding $tRNA^{Ser[Sec]}$ (Lee *et al.*, 1990) and SECIS-binding protein (SBP2) (Copeland *et al.*, 2000) to increase the efficiency of selenocysteine incorporation (Berry *et al.*, 1994; Tujebajeva *et al.*, 2000b). All transfection experiments were carried out with supplementation of 100 nM sodium selenite to the media. $^{75}$Se as sodium selenite (1000 mCi/mg) was added to media 1 day after transfection, and labeling proceeded for another day. Cells were harvested, sonicated in 0.25 M sucrose in PE buffer (0.1 M potassium phosphate, 1 mM EDTA pH 6.9) and analyzed by polyacrylamide gel electrophoresis, followed by autoradiography.

**Whole-mount *in situ* hybridization.** Embryos collected from a 24-h egg-lay were dechorionated and fixed in 2% formaldehyde and 0.5 M final concentration of EGTA in PBS for 20 min. After precipitation with methanol embryos were kept at –20°C in absolute ethanol. Third-instar wild-type larvae were dissected in PBS and fixed overnight in 4% paraformaldehyde in PBS for 20 min. Further steps before hybridization and hybridization itself were performed as described by Lehner and O'Farrell (1990). Linearized pOT2 vectors containing GH03581 and SD09114 clones were used to generate a riboprobe according to the Boehringer-Mannheim protocol. Embryos and discs were then incubated with 1/2000 anti-DIG conjugated with alkaline phosphatase antibody (Boehringer-Mannheim), preabsorbed against fixed and dissected larvae. Antibody was detected using standard procedures (Boehringer-Mannheim). Embryos were postfixed and posteriorly mounted in DePeX. Discs and brains were dissected and mounted in 87% glycerol.

**Data and software availability.** Sequence data and software can be found at http://www1.imim.es/databases/spdroso2001

**Supplementary data.** Supplementary data are available at *EMBO reports* Online.

## ACKNOWLEDGEMENTS

We wish to thank E. Blanco for his assistance with geneid, and P. Higgs for helpful suggestions. R.G. thanks L.S. Shashidhara for his hospitality at the CCMB (Hyderabad), where part of this manuscript was written. This work was partially supported by grants BIO98-0443-C02-01 and PB96-1253 from 'Plan Nacional de I+D' (Spain). S.C. and M.M. are recipients of predoctoral fellowships from CIRIT, Generalitat de Catalunya.

## REFERENCES

Abril, J.F. and Guigó, R. (2000) gff2ps: visualizing genomic annotations. *Bioinformatics*, **16**, 743–744.

Adams, M.D. *et al.* (2000) The genome sequence of *Drosophila melanogaster*. *Science*, **287**, 2185–2195.

Alsina, B., Serras, F., Baguña, J. and Corominas, M. (1998) Patufet, the gene encoding the *Drosophila melanogaster* homologue of selenophosphate synthetase, is involved in imaginal disc morphogenesis. *Mol. Gen. Genet.*, **257**, 113–123.

Alsina, B., Corominas, M., Berry, M.J., Baguña, J. and Serras, F. (1999) Disruption of selenoprotein biosynthesis affects cell proliferation in the imaginal discs and brain of *Drosophila melanogaster*. *J. Cell Sci.*, **112**, 2875–2884.

Altschul, S.F., Madden, T., Schaffer, A., Zhang, J., Zhang, Z., Miller, W. and Lipman, D. (1997) Gapped BLAST and PSI-BLAST: a new generation of protein database search programs. *Nucleic Acids Res.*, **25**, 3389–3402.

Berry, M.J., Harney, J.W., Ohama, T. and Hatfield, D.L. (1994) Selenocysteine insertion or termination: factors affecting UGA codon fate and complementary anticodon:codon mutations. *Nucleic Acids Res.*, **22**, 3753–3759.

Buettner, C., Harney, J.W. and Berry, M.J. (1999) The *Caenorhabditis elegans* homologue of thioredoxin reductase contains a Selenocysteine Insertion Sequence (SECIS) element that differs from mammalian SECIS elements but directs selenocysteine incorporation. *J. Biol. Chem.*, **274**, 21598–21602.

Burge, C.B. and Karlin, S. (1998) Finding the genes in genomic DNA. *Curr. Opin. Struct. Biol.*, **8**, 346–354.

Copeland, P.R., Fletcher, J.E., Carlson, B.A., Hatfield, D.L. and Driscoll, D.M (2000). A novel RNA binding protein, SBP2, is required for the translation of mammalian selenoprotein mRNAs. *EMBO J.*, **19**, 306–314.

Flohé, L., Andreesen, J.R., Brigelius-Flohé, R., Maiorino, M. and Ursini, F. (2000) Selenium, the element of the moon, in life on Earth. *Life*, **49**, 411–420.

Ganther, H.E., (1999) Selenium metabolism, selenoproteins and mechanisms of cancer prevention: complexities with thioredoxin reductase. *Carcinogenesis*, **20**, 1657–1666.

Gladyshev, V.N., Krause, M., Xu, X.M., Korotkov, K.V., Kryukov, G.V., Sun, Q.A., Lee, B.J., Wooton, J.C. and Hatfield, D.L. (1999) Selenocysteine-containing thioredoxin reductase in *C. elegans*. *Biochem. Biophys. Res. Commun.*, **259**, 244–249.

Guigó, R., Knudsen, S., Drake, N. and Smith, T.F. (1992) Prediction of gene structure. *J. Mol. Biol.*, **226**, 141–157.

Haussler, D. (1998) Computational genefinding. *Trends Biochem. Sci., Supplementary Guide to Bioinformatics*, pp. 12–15.

Hirosawa-Takamori, M., Jäckle, H. and Vorbrüggen, G. (2000) The class 2 selenophosphate synthetase gene of *Drosophila* contains a functional mammalian-type SECIS. *EMBO Rep.*, **1**, 441–446.

Kryukov, G.V., Kryukov, V.M. and Gladyshev, V.N. (1999) New mammalian selenocysteine-containing proteins identified with an algorithm that searches for Selenocysteine Insertion Sequence Elements. *J. Biol. Chem.*, **274**, 33888–33897.

Lee, B.J., Rajagopalan, M., Kim, Y.S., You, K.H., Jacobson, K.B. and Hatfield, D. (1990) Selenocysteine $tRNA^{[Ser]Sec}$ gene is ubiquitous within the animal kingdom. *Mol. Cell. Biol.*, **10**, 1940–1949.

Lehner, C.F. and O'Farrell, P.H. (1990) *Drosophila* cdc2 homologues: a functional homologue is coexpressed with a cognate variant. *EMBO J.*, **9**, 3573–3581.

Lescure, A., Gautheret, D., Carbon, P. and Krol, A. (1999) Novel selenoproteins identified *in silico* and *in vivo* by using a conserved RNA structural motif. *J. Biol. Chem.*, **274**, 38147–38154.

Low, S.C. and Berry, M.J. (1996) Knowing when not to stop: selenocysteine incorporation in eukaryote. *Trends Biochem. Sci.*, **21**, 203–208.

Parra, G., Blanco, E. and Guigó, R. (2000) Geneid in *Drosophila*. *Genome Res.*, **10**, 511–515.

Persson, B.C., Böck, A., Jäckle, H. and Vorbruggen, G. (1997) SelD homologue from *Drosophila* lacking selenide-dependant monoselenophosphate synthetase activity. *J. Mol. Biol.*, **274**, 174–180.

Robinson, D.N. and Cooley, L. (1997) Examination of the function of two kelch proteins generated by stop codon suppression. *Development*, **124**, 1405–1417.

Stadman, T.C. (1996) Selenocysteine. *Annu. Rev. Biochem.*, **65**, 83–100.

Thompson, J.D., Higgins, D.G. and Gibson, T.J. (1994) CLUSTAL_W: improving the sensitivity of progressive sequence alignment through sequence weighting, position-specific gap penalties and weight matrix choice. *Nucleic Acids Res.*, **22**, 4673–4680.

Tujebajeva, R.M., Ransom, D.G., Harney, J.W. and Berry, M.J. (2000a) Expression and characterization of nonmammalian selenoprotein P in the zebrafish, *Danio rerio*. *Genes Cells*, **5**, 897–903.

Tujebajeva, R.M, Copeland, P.R., Xu, X-M., Carlson, B.A., Harney, J.W., Driscoll, D.M., Hatfield, D.L. and Berry, M.J. (2000b) Decoding apparatus for eukaryotic selenocysteine insertion. *EMBO Rep.*, **1**, 158–163.

Ursini, F., Heim, S., Kiess, M., Maiorino, M., Roveri, A., Wissing, J. and Flohé, L. (1999) Dual function of the selenoprotein PHGPx during sperm maturation. *Science*, **285**, 1393–1396.

Zhou, X., Park, S.I., Moustafa, M.E., Carlson, B.A., Crain, F., Diamond, A.M., Hatfield, D.L. and Lee, B.J. (1999) Selenium metabolism in *Drosophila*. Characterization of the selenocysteine tRNA population. *J. Biol. Chem.*, **274**, 18729–18734.

DOI: 10.1093/embo-reports/kve151

Supplementary Data

RESULTS

Search for known selenoproteins in the *D. melanogaster* genome. Sequence similarity searches of all known selenoproteins against the fly genome, and against the proteins predicted in this genome, indicated that four known selenoprotein families do not appear to have a clear *D. melanogaster* homologue (SelW, ID, SelP and SelN), five more have a cysteine homologue in *D. melanogaster* (TR-SelZ, GPx, 15kDa, SelT, and SelR-X), and only one selenophosphate synthetase (Sps2), is also a selenoprotein in *D. melanogaster*.

METHODS

Coding potential. Markov Models of order five are typically used to discriminate coding from non coding regions (Borodowsky and McInich, 1993; Guigó, 1999). In a Markov Model of order five of a nucleotide sequence, the probability of a given nucleotide at a particular position depends on the preceding five nucleotides (hence, the order five). Usually, the probabilities of the Markov Model are estimated separately from sets of coding and non coding sequences. Thus, for each hexamer $h=s_1s_2s_3s_4s_5s_6$, let $E(h)=P(s_6/s_1s_2s_3s_4s_5)$ be the probability in coding sequences of nucleotide $s_6$ given that $s_1s_2s_3s_4s_5$ are the preceding nucleotides, and let I(h) be the same probability in non-coding sequences. Typically, the log-likelihood ratio $L(h)=\log(E(h)/I(h))$ is computed. If $P(s_6/s_1s_2s_3s_4s_5)$ is larger in coding sequences than in non-coding sequences, then L(h) is positive, otherwise it is negative. Then, given a nucleotide sequence S of length l, we compute the coding potential of S as:

(Supplementary equation)

Where $s_{i...j}$ is the subsequence of S from positions i to j. L(S) is the logarithm of the ratio of the probability of S under the coding model (that is, assuming that S is a coding sequence), over the probability of S under the non coding model. L(S) tends to be positive in coding regions, and negative in non coding regions. Actually, L(S) is computed in somehow a more complicated way, since to compute the probability of the Markov chain S, the probability is required of the first five nucleotides in the sequence S (the so-called Initial probabilities I(S), versus the Transition Probabilities E(S)). Moreover, different Markov Models are usually computed for each different reading frame. See Borodovsky and McInich (1993) for details.

We have used Markov Models of order five to compute the coding potential L of the region comprised between the in frame TGA codon and the stop codon in selenoproteins, and of the region comprised between the stop codon TGA, and the next stop codon in frame in non selenoproteins. We hypothesized that the coding potential L will be in general much higher in selenoproteins than in no selenoproteins in this region, and therefore that its value can be used to distinguish between actual selenoproteins and false predictions in SECIS-positive nucleotide sequences. To test this hypothesis, three different sets of non-redundant human mRNAs from the 3' UTR database (Release 12.0, 09/1999, Pesole *et al.*) were extracted: 1) 3001 mRNAs with a UAG or UAA stop codon annotated; 2) 10 annotated selenoproteins; and 3) 1169 mRNAs with a UGA stop codon annotated. The following entries were discarded: partial, non standard, with alternative splicing, pseudogenes, predicted, artificial, viral, mitochondrial, histocompatibility related or with any problem in the CDS.

The resulting sets of sequences can be obtained from http://www1.imim.es/datasets/sp2001

The CDS and 3' UTR of the first set of sequences were used to estimate the previously defined Markov Models of order 5 for coding, E, and non coding, I, sequences, and the resulting log-likelihood ratio, L. Then, the coding potential L was computed in the other two sets. In these L was computed in three separate regions for each mRNA: 1) from the start codon to the first in frame TGA codon (Start-TGA), 2) from this in frame TGA codon to the next in frame stop codon (TGA-Stop); and 3) from this stop codon to the next in frame stop codon (Stop-Stop). Only sequences were further considered for which these regions were at least 30bp long. Results corrected by sequence length are shown in Table I. As hypothesized (and otherwise, expected), the region TGA-Stop shows coding values comparable to those in coding regions for selenoproteins, and to those in non coding regions in non selenoproteins. Therefore, measures of coding potential, such as those used in gene prediction programs, can indeed be used to help distinguishing *bona fide* selenoproteins from false predictions in SECIS-positive sequences.

**Prediction of Selenoproteins in nucleotide sequences.** The method that we have developed relies in the correlated prediction of SECIS elements and of genes in which candidate exons with in frame TGA are allowed. SECIS elements are predicted first, and given as an input to the gene prediction program, which takes them into account to predict gene structures.

Given a query sequence (genomic or cDNA), first of all we predict SECIS elements using the pattern matching program PatScan with the SECIS pattern described below (http://www-unix.mcs.anl.gov/compbio/PatScan/HTML/PatScan.html). Only those predicted SECIS structures showing sufficient thermodynamic stability (as measured by the minimum free energy required to fold the structure) are further considered. Next, a modification (described below) of the program geneid (Guigó *et al.*, 1992; Parra *et al.*, 2000) is used to predict genes along the query sequence. The program is able to predict genes in which exons may be interrupted by in frame TGA codons, as well as standard genes. Together with the query nucleotide sequence, the predicted SECIS elements positions are given as input to the geneid program, so that such genes are only predicted when a suitable SECIS appears upstream of the predicted gene at the appropriate distance. Thus, the coordinate prediction of SECIS and exons with in frame TGA codons decreases enormously the number of these elements that could actually occur in selenoproteins, leading to highly specific predictions of selenoprotein genes in nucleotide sequences (see Results). In what follows, we describe in some more detail the components of our method.

**SECIS prediction.** The program PatScan, which searches protein or nucleotide sequences for instances of a pattern, is used to predict SECIS elements in nucleotide sequence. Eukaryotic SECIS structures fall into two slightly different classes, named forms 1 and 2. Form 2 elements present and additional helix due to base pairing in the apical loop. Thus, form 2 is an extension from form 1. When building a SECIS pattern is enough to model form 1 to be able to retrieve form 2 SECIS, though we may miss some form 2 specificity. In our case, because we favor sensitivity rather than specificity one model is sufficient. An input descriptor of the primary and secondary structure of the SECIS was built from 51 known SECIS (16 form 1 and 35 form 2) from 47 selenoproteins ranging from *Schistosoma mansoni* to human. Figure 5B shows the uniq resulting SECIS pattern. In order to assess the stability of the SECIS structure, the minimum free energy of all matching motifs was calculated with the RNAfold program (Viena RNA package) following the protocol of Kryukov *et al.* (1999). We estimate separately the free energies for Helix I plus internal loop and Helix II plus apical loop regions of the putative SECIS elements (see Figure 5A for SECIS structure). The cutoff parameters estimated by Kryukov *et al*. from 14 human SECIS were slightly changed from -7.4 to -7.5 kcal/mol for Helix I and internal loop, and from -11.0 to -10.0 kcal/mol for Helix II and apical loop. These values excluded the second SECIS of the four SelP proteins in our set of 47 selenoproteins.

**Gene prediction.** geneid is a program to predict protein coding genes in anonymous eukaryotic

sequences designed with a hierarchical structure (see Parra et al., 2000, and the geneid documentation at http://www1.imim.es/geneid for details). Basically, it involves three steps:

**(a) prediction of sites.** In the first step, start, stop codons, and splice sites are predicted and scored along the query sequence. Scores for potential sites are computed using a log-likelihood approach similar---albeit simpler---to the one described earlier. Essentially, given the sequence of a potential site, geneid computes the logarithm of the ratio of the likelihood of the sequence in a real site versus the likelihood of the sequence in a random site.

**(b) prediction of exons.** In the second step, geneid builds all possible exons compatible with the predicted sites. Four types of exons are considered:

1- **First**, an ORF that begins with a start codon and ends with a donor site;

2- **Internal**, an ORF that begins with an acceptor site and ends with a donor site;

3- **Terminal**, an ORF that begins with an acceptor site and ends with a stop codon; and

4- **Single**, an ORF that begins with a start codon and ends with a stop codon. It corresponds to intronless genes

ORFs are defined using the standard stop codons. Exons are scored as the sum of the log-likelihood scores of the exon defining sites, plus the log-likelihood ratio of a Markov model for coding DNA (exactly as the one described earlier) for the exon sequence. The resulting score can be assumed to be a log-likelihood ratio.

**(c) assembly of genes.** From the set of predicted exons, geneid finally assembles the gene structure that maximizes the sum of the scores of the assembled exons. Note that the score of the resulting optimal structure can be assumed to be a log-likelihood ratio itself. geneid can predict multiple genes in both strands in the same query sequence.

When assembling gene structures, geneid can take into account additional information about gene elements along the sequence. This information is provided externally, and may include previous knowledge about coding regions, or predictions obtained by other programs. Is in this way, that predicted SECIS elements can be introduced into the gene predictions.

To be assembled into a gene structure, predicted exons and other genomic elements provided to geneid must conform to a number of user-defined biological constraints, such as frame compatibility, minimum and maximum distance between consecutive elements, and the order in which different genomic elements can be chained. All this rules are stated in the gene model, which is specified externally (see Parra et al., 2000, and the geneid documentation at http://www1.imim.es/geneid for details).

**Prediction of selenoprotein genes.** We have modified slightly geneid in order to include the possibility of predicting selenoproteins. Essentially, the codon TGA has been obviated as a stop codon when building First and Internal exons. When building Terminal exons, or intronless genes (Single exons), both the exons terminating at the codon TGA, and the exons extending beyond this codon to the next stop codon in frame have been considered.

The gene assembly algorithm has been modified to register during gene construction the incorporation of exons interrupted by codons TGA in frame, so that genes containing such exons are only predicted when an appropriate SECIS element is found at the right distance. In this way, the modified version of geneid is able to predict, at the same time, both standard genes and selenoprotein genes.

**Prediction of secondary structure.** The crystal structure of an eukaryotic selenocysteine, the bovine glutathione peroxidase, has been resolved at 0.2 nm resolution (Epp *et al.*, 1983). The catalytic site of this enzyme is characterized by a beta-sheet---turn---alpha-helix structural motif, with the selenocysteine residue lying within the turn. Secondary structure predictions around the selenocysteine residue of most known selenoproteins, obtained using the program Predator (Frishman and Argos, 1997), essentially conformed to this structure (data not shown). The same structure is predicted in dSps2, and dSelM, while dSelG lacked enough sequence context. However, a different structural motif (beta-sheet---turn---beta-sheet with the selenocysteine residue next to the first sheet) is predicted in the case of the fourth potential selenoprotein. We assumed thus, the fourth prediction to be a false positive.

**Prediction of selenoproteins in the sequence of the *D. melanogaster* genome.** geneid was used to scan the *D. melanogaster* genome for potential selenoproteins. The 19 large scaffolds of the genome summing up 115229998bp and with 13329 genes annotated were used (Adams *et al.*, 2000). When using geneid, the restriction was enforced that selenoprotein genes could not be further than 500bp upstream from a predicted SECIS. geneid took about 45 minutes to scan this genome in a Pentium III processor running at 550 MHz. geneid predicted 12,194 genes; this number of genes comes from using the geneid parameters for sensitivity and specificity that achieved the highest accuracy when tested on the *Adh* region (Parra *et al.*, 2000). Because we are interested in properly predicting a small number of genes, the non-standard selenoprotein genes, while keeping false positive to a minimum, accuracy must be the highest possible regardless of the total number of genes predicted. Predicting more genes, therefore, decreases the overall quality.

REFERENCES

Adams,M.D. *et al.* (2000) The genome sequence of *Drosophila melanogaster*. *Science*, 287, 2185-2195.

Frishman,D. and Argos,P. (1997) Seventy-five percent accuracy in protein secondary structure prediction. *Proteins*, 27, 329-335.

Borodovsky,M. and McIninch,J. (1993) GenMark: Parallel gene recognition for both DNA strands. *Comput. Chem.*, 17, 123-134.

Epp,O., Ladenstein,R. and Wendel,A. (1983) The refined structures of the selenoenzyme glutathione peroxidase at 0.2-nm resolution. *Eur. J. Biochem.*, 133, 51.

Guigó,R., Knudsen,S., Drake,N. and Smith,T.F. (1992) Prediction of gene structure.

*J. Mol. Biol.*, 226, 141-157.

Guigó,R. (1999) DNA composition, codon usage and exon prediction. In Bishop, M., editor, *Genetic Databases*, pages 53-80. Academic Press, San Diego, California.

Kryukov,G.V., Kryukov,V.M. and Gladyshev,V.N. (1999) New mammalian selenocysteine-containing proteins identified with an algorithm that searches for Selenocysteine Insertion Sequence Elements. *J. Biol. Chem.*, 274, 33888-33897

Parra,G., Blanco,E. and Guigó,R. (2000) Geneid in *Drosophila*. *Genome Res.*, 10, 511-515.

Pesole,G., Liuni,S., Grillo,G., Ippedico,M., Larissa,A., Makalowski,W. and Saccone,C. (1999) UTRdb: a specialized database of 5' and 3' untranslated regions of eukaryotic mRNAs. *Nucleic Acid. Res*. 1.188-191.

TABLES

Table I. Coding potential in human mRNAs

| | Coding region | TGA-Stop | Stop-Stop |
|---|---|---|---|
| 10 selenoproteins | 10.21 (3.93) | 9.9 (4.6) | -0.16 (3.10) |
| 1169 non selenoproteins | 8.37 (3.90) | -0.83 (4.14) | -2.52 (5.33) |

Selenoprotein mRNAs and human mRNAs with a UGA stop codon. Results corrected by length and normalized to 100. Mean values and standard deviation in brackets are given.